2017

Rehabilitation of Longitudinal Joints in Double-Tee Girder Bridges

Lucas Michael Bohn
South Dakota State University

REHABILITATION OF LONGITUDINAL JOINTS IN DOUBLE-TEE GIRDER BRIDGES

BY

LUCAS MICHAEL BOHN

A thesis in partial fulfillment of the requirements for the

Master of Science

Major in Civil Engineering

South Dakota State University

2017

REHABILITATION OF LONGITUDINAL JOINTS IN DOUBLE-TEE GIRDER BRIDGES

This thesis is approved as a creditable and independent investigation by a candidate for the Master of Engineering degree and is acceptable for meeting the thesis requirements for this degree. Acceptance of this thesis does not imply that the conclusions reached by the candidate are necessarily the conclusions of the major department.

Mostafa Tazarv, Ph.D., P.E.
Thesis Advisor — Date
Civil and Environmental Engineering

Nadim I. Wehbe, Ph.D., P.E.
Thesis Co-Advisor — Date
Civil and Environmental Engineering

Nadim I. Wehbe, Ph.D., P.E.
Department Head — Date
Civil and Environmental Engineering

Kimchel C. Doerner, Ph.D.
Dean, Graduate School — Date

DISCLAIMER

The contents of this report, funded in part through grant(s) from the Federal Highway Administration, reflect the views of the authors who are responsible for the facts and accuracy of the data presented herein. The contents do not necessarily reflect the official views or policies of the South Dakota Department of Transportation, the State Transportation Commission, or the Federal Highway Administration. This report does not constitute a standard, specification, or regulation.

ACKNOWLEDGEMENTS

This study was funded by the South Dakota Department of Transportation (SDDOT) and the Mountain Plains Consortium (MPC) University Transportation Center. Any opinions, findings, and conclusions are those of the author and do not necessarily reflect the views of the funding organizations.

I thank Dr. Tazarv for being my advisor. He provided great advice and assistance throughout the project. I also thank Dr. Wehbe for giving me this project as a master's student. He provided great wisdom and experience to the project. I thank Aaron Breyfogle and all the members of the SDDOT technical panel with their help and guidance.

I thank graduate students Zach Carnahan, Michael Mingo, Ishtiaque Tuhin, Abdullah Hashib, and Abdullah Boudaka for all their help with the project. Special thanks to lab manager, Zach Gutzmer, who assisted with construction, instrumentation, test setup, and testing.

I give special thanks to Jared Gusso of Journey Construction for being a consultant on the project and for performing the rehabilitation on the double-tee test bridge. I give thanks to all third-party members that provided help or donations to the project. This includes: Dominique Corvez, Gaston Doiron, and Paul White of Lafarge North America Inc., Christian Dahl of Headed Reinforcement Corp., In-Steel Wire Products, and Forterra Pipe & Precast.

Finally, I thank all my friends and family who supported me throughout the project. I give special thanks to my parents, Donald and Nancy. They taught me the importance of hard work and education.

TABLE OF CONTENTS

LIST OF ABBREVIATIONS

Abbreviation	**Definition**
AASHTO	American Association of State Highway and Transportation Officials
ABC	Accelerated Bridge Construction
ACI	American Concrete Institute
ADTT	Average Daily Truck Traffic
BRM	Bridge Management Software
DOT	Department of Transportation
FHWA	Federal Highway Administration
ft	Feet
HPC	High Performance Concrete
hrs.	Hours
in.	Inch
kip	1000 pounds
ksi	kip per square inch
LRFD	Load and Resistance Factor Design
LMC	Latex Modified Concrete
LMC-VE	Very Early High Strength Latex Modified Concrete
MAP	Magnesium Ammonium Phosphate Grout
mins.	Minutes
MoDOT	Missouri Department of Transportation
MPC	Mountain Plains Consortium

NCHRP	National Cooperative Highway Research Program
SDDOT	South Dakota Department of Transportation
SD	South Dakota
SDSU	South Dakota State University
UHPC	Ultra-High Performance Concrete
WSDOT	Washington State Department of Transportation
yd.	Yard

LIST OF FIGURES

LIST OF TABLES

ABSTRACT

REHABILITATION OF LONGITUDINAL JOINT IN DOUBLE-TEE GIRDER BRIDGES

LUCAS MICHAEL BOHN

2017

Prefabricated bridge elements have become an essential part of accelerated bridge construction (ABC), which is an emerging technology to expedite bridge construction. Among several bridge girder types, precast double-tee girders are common on county bridges in South Dakota because of the ease of construction, the reduced construction time, and the potentially lower overall cost. However, the longitudinal joints of these bridges are rapidly deteriorating with many needing replacement before the expected 75-year service life. Research was conducted at South Dakota State University (SDSU) to develop, construct, and evaluate the performance of rehabilitation methods on this type of bridge.

Current detailing between adjacent double-tee bridge girders consists of discrete welded steel connections. Wehbe et al. (2016) showed that this longitudinal joint detailing is insufficient for fatigue, service, and strength loading, thereby significantly reducing the lifespan of these type of bridges. Currently, there are more than 700 double-tee girder bridges in South Dakota incorporating this joint detailing.

Twenty joint detailing alternatives for the rehabilitation of the longitudinal joint of double-tee girder bridges were proposed in the present study. Of the 20 alternatives, continuous joint details were selected for further study since they offer minimal durability

issues. Ultra-high performance concrete (UHPC) and latex modified concrete (LMC) were selected as the filler materials because of their improved strength and durability.

Thirteen large-scale beam tests were carried out to investigate the performance of the selected joint rehabilitation details and to select the best for large-scale testing. Subsequently, two joint concepts, "pocket" and "continuous", were developed and analytically investigated using linear finite element analyses to optimize the selected joint detailing.

A full-scale 40-ft long double-tee bridge consisting of two interior girders was constructed using conventional longitudinal joint detailing then initially tested under fatigue loads. Subsequently, the bridge was rehabilitated using the two proposed details, "pocket" joint with UHPC and "continuous" joint with LMC each incorporated on half the length of the bridge. The rehabilitated specimen was first tested under 500,000 cycles of the AASHTO Fatigue II loading followed by an additional 100,000 of the AASHTO Fatigue I load cycles. Stiffness tests were performed to monitor the degradation of the bridge. Finally, the specimen was monotonically tested to failure. No significant damage beyond initial shrinkage cracks in LMC was observed throughout the fatigue testing. In addition, the stiffness of the bridge did not degrade. No damage or yielding of the reinforcement in the joint was observed throughout the strength testing. The rehabilitated bridge met all the AASHTO limit state requirements indicating sufficient performance. Overall, both rehabilitation methods are structurally viable alternatives for rehabilitation of double-tee bridge girders to extend their life for another 75 years. However, only UHPC should be used as filler material. The rehabilitation cost of a double-tee bridge with pocket detailing will be only 30% of the bridge replacement cost.

1. Introduction

1.1 Introduction

Prefabricated bridge elements have become an essential part of accelerated bridge construction (ABC), which is an emerging technology to expedite bridge construction. Among several bridge girder types, precast double-tee girders are common on county bridges in South Dakota because of the ease of construction, the reduced construction time, and the potentially lower overall cost.

The main goal of the study presented in this thesis is to explore different rehabilitation methods for existing prefabricated double-tee girder bridges for the South Dakota Department of Transportation (SDDOT) since the long-term performance of the current longitudinal joint detailing is not adequate. Currently, there are more than 700 bridges in South Dakota that incorporate this type of girder and joint detailing. The focus of this research project is to propose a cost-effective rehabilitation method that offers easy construction, enhanced structural performance, and improved durability for implementation in South Dakota.

1.2 Current Double Tee Joints

The conventional joint detailing currently used for double-tee girders in South Dakota utilizes discrete welded connections spaced every 5 ft along a grouted longitudinal joint

to connect girders. Figure 1-1 shows the current detailing for the double-tee girder bridges.

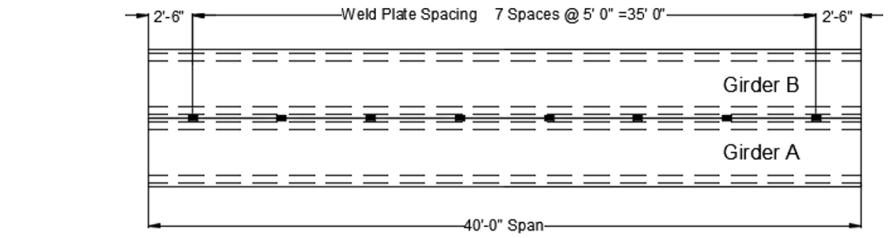

a. Plan View of Conventional Double-Tee Bridge Girder

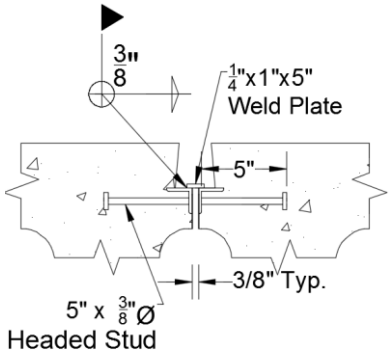

b. Section Detail of Welded Connection

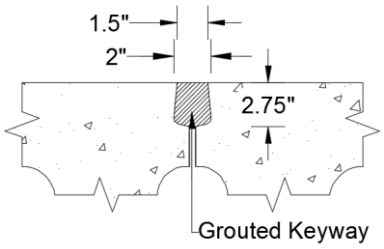

c. Section Detail of Grouted Keyway

Figure 1-1. Conventional Double-tee Girder Longitudinal Joint Detail (Konrad, 2014)

A common problem reoccurring with the existing double tee bridges is the deterioration of the girders longitudinal joints. The inspection of bridges built less than 40 years ago has revealed that there are large cracks along these joints causing reinforcement corrosion and deterioration of the double-tee girders, which can significantly affect the bridges long-term performance. Figure 1-2 illustrates the reflecting cracking of the asphalt overlay, and the spalling and corrosion underneath the longitudinal joint between adjacent double-tee girders. Konrad (2014) studied the behavior of two bridge deck systems under fatigue and static loading conditions (Fig. 1-3) to evaluate the performance of both the current detailing and a new connection. The fatigue test consisted of a loading protocol using a 21-kip load applied at a frequency of

one cycle per second. The fatigue test results for the specimen with the conventional joint detailing were:

- At 19,500 cycles near the midspan, water began seeping through the joint.
- Significant relative deflection between girders causing spalling of the grout occurred at 43,000 cycles
- At 62,000 cycles the welded connection failed near the midspan.
- It was found that the discrete welded connection was inadequate according to the current AASHTO fatigue requirements.

The proposed new joint with overlapping reinforcement in the joint survived more than 100 years of service loads (800,000 fatigue load cycles) without significant stiffness degradation and leakage (Konrad, 2014).

a. Reflective Cracking of Asphalt Overlay

b. Spalling and Corrosion of Underside of Double-tee Girder

Figure 1-2. Visual Observations of Reflective Cracking, Spalling, and Corrosion of Double-tee Girder Bridges (Konrad, 2014)

Figure 1-3. Test Setup for Full-scale Double-tee Girder Testing of Longitudinal Joint (Konrad, 2014)

1.3 Double-Tee Girder Bridges

A database of SD bridges is available through bridge management software (BRM), which includes bridge location, geometry, age, and condition. This software was used to collect information on double-tee girder bridges. It was found that there are currently 761 double-tee girder bridges in SD. Figure 1-4 shows the age of these bridges. Table 1-1 represents the bridges sorted by year the bridge was built and expected year that the bridge will fail using the experimental data reported by Konrad (2014). The number of cycles to fail the welds in the conventional connection under 21-kip fatigue loading was 62,000. Beckemeyer and McPeak (1995) provided average daily truck traffic (ADTT) values for three road types in SD with different traffic volumes: low (15), medium (50),

and high (200). Eq. 1-1 was developed to predict the expected failure year for SD double-tee girder bridges incorporating the conventional connection performance data.

$$Expected\ \ Failure\ (yrs.) = \frac{62{,}000}{ADTT * 365} \qquad \text{Eq. 1-1}$$

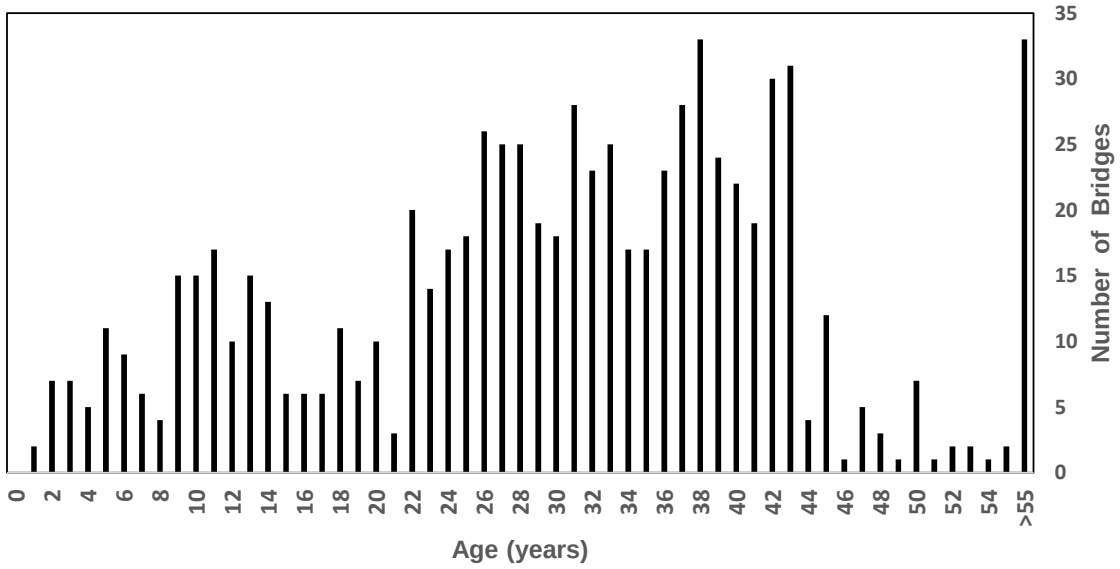

Figure 1-4. South Dakota Double-tee Girder Bridges Age Distribution

Table 1-1. South Dakota's Double-tee Bridges

Year	Age (Yrs.)	No. of Bridges	Expected Failure with[1] Truck Traffic			Year	Age (Yrs.)	No. of Bridges	Expected Failure with Truck Traffic		
			Low[2]	Med.[3]	High[4]				Low[1]	Med.[2]	High[3]
1900 - 1959	>55	33	X[5]	X	X	1988	27	25	X	X	X
1960	55	2	X	X	X	1989	26	26	X	X	X
1961	54	1	X	X	X	1990	25	18	X	X	X
1962	53	2	X	X	X	1991	24	17	X	X	X
1963	52	2	X	X	X	1992	23	14	X	X	X
1964	51	1	X	X	X	1993	22	20	X	X	X
1965	50	7	X	X	X	1994	21	3	X	X	X
1966	49	1	X	X	X	1995	20	10	X	X	X
1967	48	3	X	X	X	1996	19	7	X	X	X
1968	47	5	X	X	X	1997	18	11	X	X	X
1969	46	1	X	X	X	1998	17	6	X	X	X
1970	45	12	X	X	X	1999	16	6	X	X	X
1971	44	4	X	X	X	2000	15	6	X	X	X
1972	43	31	X	X	X	2001	14	13	X	X	X
1973	42	30	X	X	X	2002	13	15	X	X	X
1974	41	19	X	X	X	2003	12	10	X	X	X
1975	40	22	X	X	X	2004	11	17	X	X	X
1976	39	24	X	X	X	2005	10	15		X	X
1977	38	33	X	X	X	2006	9	15		X	X
1978	37	28	X	X	X	2007	8	4		X	X
1979	36	23	X	X	X	2008	7	6		X	X
1980	35	17	X	X	X	2009	6	9		X	X
1981	34	17	X	X	X	2010	5	11		X	X
1982	33	25	X	X	X	2011	4	5		X	X
1983	32	23	X	X	X	2012	3	7		X	X
1984	31	28	X	X	X	2013	2	7			X
1985	30	18	X	X	X	2014	1	2			X
1986	29	19	X	X	X	2015	0	0			
1987	28	25	X	X	X	**Total**		**761**			

[1] The expected failure is based on the welded steel connection failing at 62,000 cycles per 21-kip fatigue test (Konrad, 2014).

[2] Low – based on average daily truck traffic of 15 trucks/day

[3] Med. – based on average daily truck traffic of 50 trucks/day

[4] High – based on average daily truck traffic of 200 trucks/day

[5] X indicates that the steel longitudinal joint connections will fail

1.4 Problem Statement

There are currently more than 700 double-tee girder bridges in SD with the conventional joint detailing. Based on the results of the previous research, bridges incorporating the current double-tee girder longitudinal joint detailing may be deteriorating with the lifespan being much shorter than the expected 75 years. A potential cost-effective rehabilitation method to upgrade the existing bridges is desirable. Therefore, a study is needed to identify potential rehabilitation alternatives and assess the construction feasibility, structural performance, and durability of those alternatives for implementation in South Dakota.

1.5 Objectives and Scopes

1. Review and evaluate rehabilitation methods for longitudinal joints on double-tee girder bridges.
    a. Conduct literature review of current rehabilitation methods at state and national level.
    b. Consult with SDDOT and bridge construction companies in South Dakota.
    c. Submit rehabilitation methods to technical panel for discussion.
2. Test longitudinal joint rehabilitation designs for the existing double-tee for fatigue, service, and strength loads.
    a. Construct full-scale bridge girders with conventional connection and rehabilitate the specimen using the selected details.
    b. Instrument and collect data needed for assessment of long-term performance and the strength of the test specimens.

   c. Test the specimens under fatigue and strength loads at the Lohr Structures Laboratory at South Dakota State University.

3. Recommend a longitudinal joint rehabilitation method for existing double-tee girder bridges in South Dakota based on the performance and cost-effectiveness of the selected alternatives.
   a. Access the constructability, cost, and structural performance of the alternatives.
   b. Compare the results with those measured in the previous research project (SD2013-01).
4. Develop a guideline to facilitate the field implementation of proposed rehabilitation methods.

2. Literature Review

2.1 Introduction

Accelerated bridge construction (ABC), a new paradigm in the US, has gained substantial momentum because of its many advantages such as shorter onsite construction time and less traffic impact. ABC has been practiced for superstructures mainly by precasting the girders. Nevertheless, recent studies have shown the feasibility of precast decks, which must be connected to the adjacent deck though continuous and pocketed joints. Continuous joints consist of a keyway with lap-splicing of the reinforcement that can be hooped, headed, or straight bars. The keyway is filled with several different filler materials. The dowel bar retrofit method consists of saw-cutting a small slot and inserting a dowel bar and back filling the slot with a filler material.

Studies have shown that the performance of connections between precast bridge girders and decks depends on the joint detailing, closure material, and reinforcement. This section presents a summary of the literature review carried out on the superstructure connections.

2.2 Continuous Joints

The Texas DOT frequently uses double-tee girders on many of the state medium span bridges where construction speed is a concern. Jones (2001) conducted a study to investigate the feasibility of different double-tee flange joints to adjacent girders under

distributed wheel loads. Reflective cracking along the joint was the DOT's concern. The connection detailing used in Texas in 2001 consisted of discrete welded connections anchored into the concrete with a headed stud every 5 ft. Two longitudinal connections (Fig. 2-1) were recommended, a "simple" connection detail, and "continuous" connection detail.

- The "simple" detail consisted of 0.5-in. steel plates anchored in the precast concrete and connected by a 1-in. diameter bar welded to the steel plates spaced every 5 feet. The narrow shear key was grouted from the top of the welded connection.
- The "continuous" detail extended the reinforcing out of the double-tee into the joint between adjacent girders and shear key was grouted.

However, the "simple" connection detail was determined to be the most cost-effective alternative. After selection, the "simple" detail was tested for static and fatigue loading. Vehicle loads of 16 kips to a peak of 24 kips were applied to the specimen for a total of 1.5 million cycles. Overall, no signs of failure and degradation were observed.

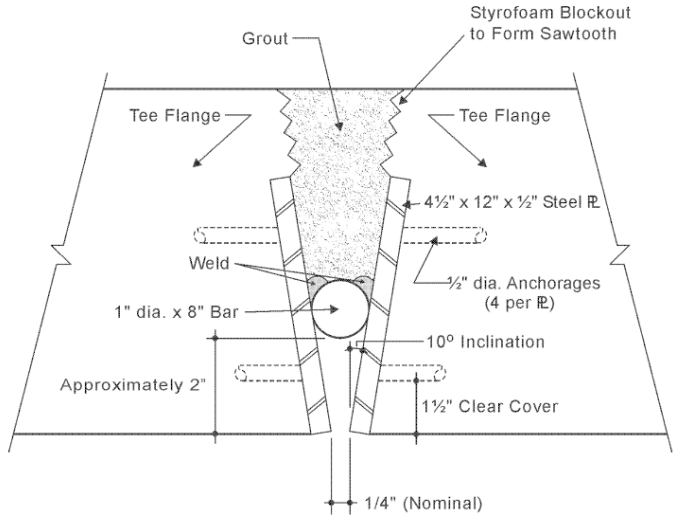

a. "Simple" Detail

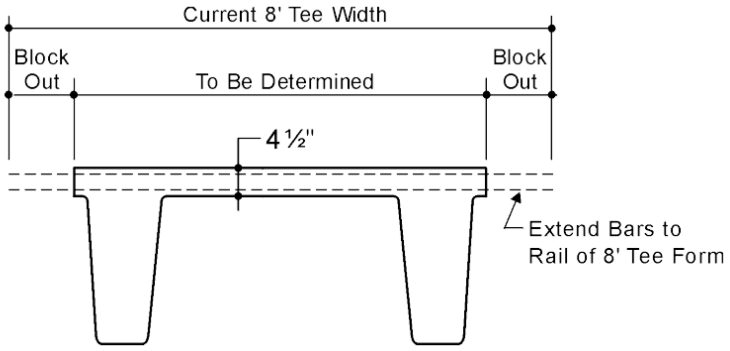

b. "Continuous" Detail

Figure 2-1. Recommended Longitudinal Joint Detailing (Jones, 2001)

Graybeal (2010) tested six specimens in which precast decks were connected through continuous joints filled with ultra-high performance concrete (UHPC). UHPC is an advanced cementitious material developed in recent decades with superior properties such as higher strength, better durability, and improved ductility over conventional concrete. UHPC also provides an excellent bond to the reinforcement as well as the existing concrete. The research was focused on the performance of the longitudinal and transverse connections under both fatigue and static wheel loads. The connections were

fabricated utilizing straight lapped bars, headed bars, and intersecting hoop bars. Four specimens were built with transverse joints and two with longitudinal joints. Headed and straight bars were incorporated in the longitudinal connections (Fig. 2-2). Each specimen consisted of a female-female diamond shaped shear key that was 6.0-in. wide at the top and bottom. The lap-splices for the headed bar, the hooped bar, and the straight bar specimens were respectively 3.5 in., 3.9 in., and 5.9 in. The headed bars utilized Dayton Superior D-158-B plain end anchors with a 2-in. head. The longitudinal specimens were 94.5 in. by 84.7 in. by 5.9 in. with top and bottom mats of reinforcing. The top and bottom meshes were made with No. 5 bars spaced at 17.7 in. and No. 5 bars spaced at 7.1 in., respectively.

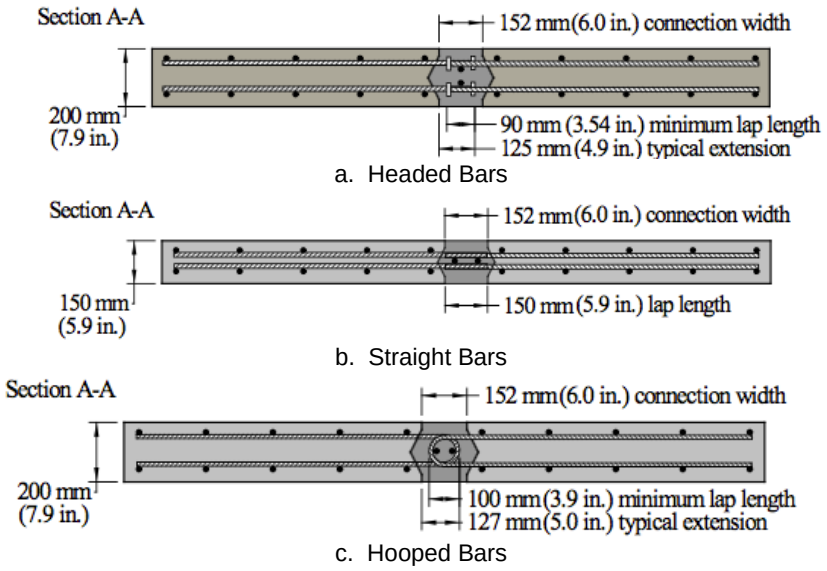

Figure 2-2. UHPC Longitudinal Reinforcing Details Used for Testing (Graybeal, 2010)

As was mentioned, the testing program for the longitudinal joints consisted of two specimens. The wheel load was simulated using a load patch of 10 in. by 20 in. located next to the joint. The distance between supports was 72 in. and the joint was located at the midspan. The cyclic loads were applied using a servo-hydraulic controlled actuator

with load frequency of 6 Hz. A sinusoidal loading protocol was used to apply 2 and 16-kip forces for two million cycles and 2 and 21.3-kip forces for remaining cycles to failure. The structural response included visual observation and instrumentation using five strain gauges mounted to the concrete, two displacement transducers, and a load cell attached to the actuator. Water ponds were placed on the top of the specimens and frequently checked throughout the cyclic testing. The specimens with the longitudinal connections withstood two million cycles under 2 and 16-kip loads and nearly seven million cycles of 2 and 21.3-kip loads. Throughout the cyclic testing no cracks or leaks were observed in the field-cast UHPC connections.

The results of the longitudinal joint with the straight bars was similar, however additional cyclic loading was applied to fail the specimen. The loading was 2 and 16 kips for the first 60 thousand cycles, 3 and 21.3 kips for 10 million cycles, 3 and 32 kips for 1.12 million cycles, and finally 340 thousand cycles of 3 and 40 kips. The testing was stopped when the bar fractured crossing the connection interface. No evidence of bonding failure of the UHPC to concrete or UHPC to rebar was observed. Figure 2-3 shows the failure of the rebar at the interface and the flexural cracking of the precast panels.

Figure 2-3. Failure of Longitudinal Joint Specimen with Straight Bars Under Fatigue Loading (Graybeal, 2010)

Design specifications, construction guidelines, and examples for superstructure connections suitable for precast bridge systems were presented in National Cooperative Highway Research Program (NCHRP) report No. 173 (French, et al., 2011). Two types of closure pour materials were evaluated with construction of a total of eight slab specimens. The closure materials consisted of magnesium ammonium phosphate (MAP) based grout, SET-45 HW (overnight cure material), and a high-performance concrete (HPC) mix (7-day cure material). The SET-45 HW was used with 60% extension (pea-gravel) in two specimens and without extension in the other two specimens. HPC mix was used in four specimens. All specimens were tested after a 7-day cure to simulate rapid construction. Specimens were 72-in. wide, 64-in. long and 6.5-in thick. The specimens were tested for static flexure, static shear, fatigue flexure, and fatigue shear loads. Figure 2-4 shows the longitudinal joint detail which was used for all specimens. The clear cover was 2 in. and 1 in. at the top and bottom, respectively. The spacing of No. 5 U-bars was 4.5 in. The length of the lap-splice for No. 5 U-bar was 6 in. with the inner bend diameter of $3d_b$., where d_b is the bar diameter. No. 4 lacer bars were used as

the longitudinal reinforcement. The shear key outer and inner widths were 11 in. and 8 in., respectively.

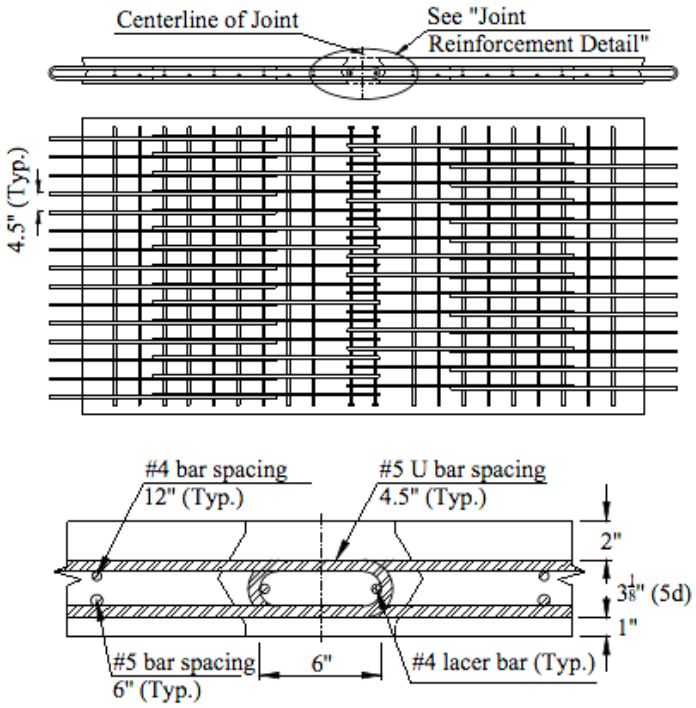

Figure 2-4. Longitudinal Reinforcement Detail Utilizing Hooped Bars (French, et al., 2011)

The NCHRP 173 test results suggested:

- Fatigue loading had negligible impact on the behavior of the longitudinal joints in terms of curvature, deflection, and relative deflection of the joint.
- After 2 million cycles the specimens with overnight cures had less capacity than the corresponding static load tests.
- Joints with 7-day cure material performed better that the overnight cure material in static shear and fatigue shear tests. The reason was that the 7-day cure materials achieved higher compressive strength than the overnight cure.
- Based on the results the detail was considered as a viable connection for longitudinal joints between precast deck panels and decked bulb-tees.

With the current focus on rapid construction methods, the durability of the longitudinal joints is becoming a concern. Excessive cracking allows moisture and chlorine penetration into the joint, which results in the corrosion of the reinforcing steel, thus rapid structural degradation. Baer (2013) proposed the incorporation of a new closure material, latex modified concrete (LMC), as a durable alternative. The proposed connection as shown in Fig. 2-5 had hooped bars with an 8-in. shear key with a panel depth of 8 in. The specimen was subjected to two million cycles of fatigue loading from 4.4 and 25 kips at a frequency of 1.5 Hz. Before fatigue loading, water ponds were constructed around the joint. Upon completion of the fatigue loading water tightness of the joint was investigated. Water ponds were placed on the joint for 4 days in which no water leakage was observed. The results of the fatigue test demonstrated no permanent failure. It was concluded the connection detail was capable of resisting fatigue loading without any damage over the bridge lifespan.

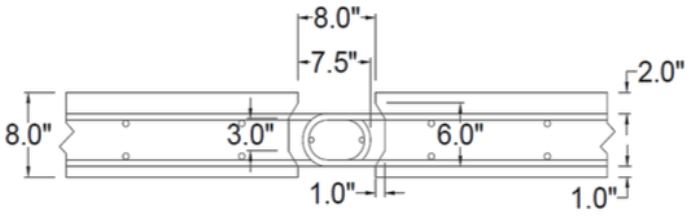

Figure 2-5. Longitudinal Reinforcement Detail Utilizing Hooped Bars and LMC (Baer, 2013)

Konrad (2014) studied the fatigue performance of the existing and a new longitudinal double-tee girder joint funded by SDDOT and MPC. The concern was reflective cracking of the longitudinal joints that might affect the structural performance of the bridge superstructure. The experimental results based on the AASHTO fatigue loading requirements concluded that the discrete welded steel connections were inadequate. Bridges are designed for a lifespan of 75 years. The test results showed a failure at

62,000 load cycles equivalent to 11.3 years in service. Figure 2-6 shows the measured girder load-deformation relationships for the conventional specimen. The failure mode was the headed stud pulling out from the girders at approximately 70 kips. The relative deflection between the girders shows the inability of the welded connections to transfer the shear between girders. In other words, the longitudinal joints acted as pin connections early in the tests. The proposed continuous joint detailing (Fig. 2.7) was tested for more than 800,000 cycles with insignificant stiffness degradation. The load carrying capacity of the proposed specimen was 1.5 times greater than the conventional connections with girder flexural failure (strength test was carried out after fatigue testing). Figure 2-8 shows the proposed detailing force-deformation relationships. The proposed specimen showed a 113–kip strength that was 40 kips higher than that of the conventional specimen. The test showed that the proposed connection can provide adequate load path between girders, and each girder will exhibit relatively the same displacements.

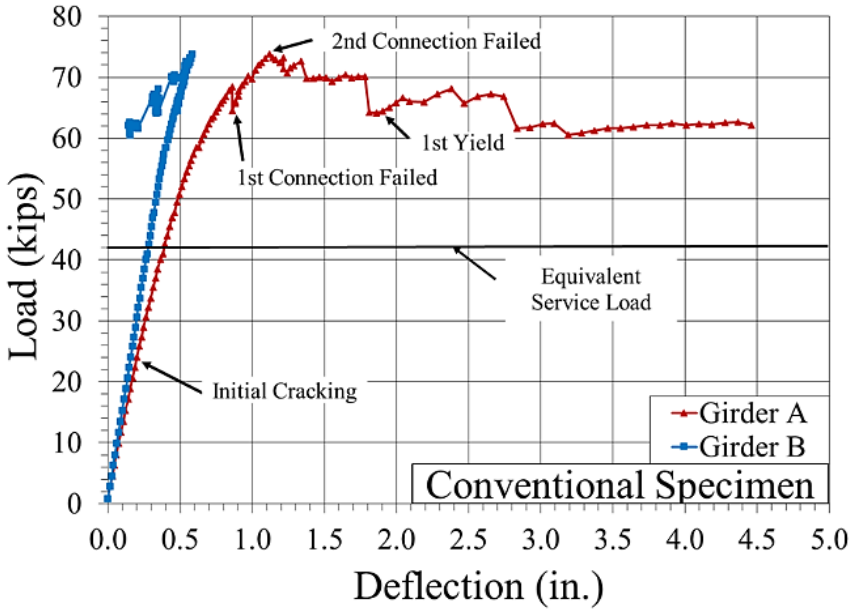

Figure 2-6. Measured Load-Deflection Relationship Under Static Loading for Conventional Specimen (Konrad, 2014)

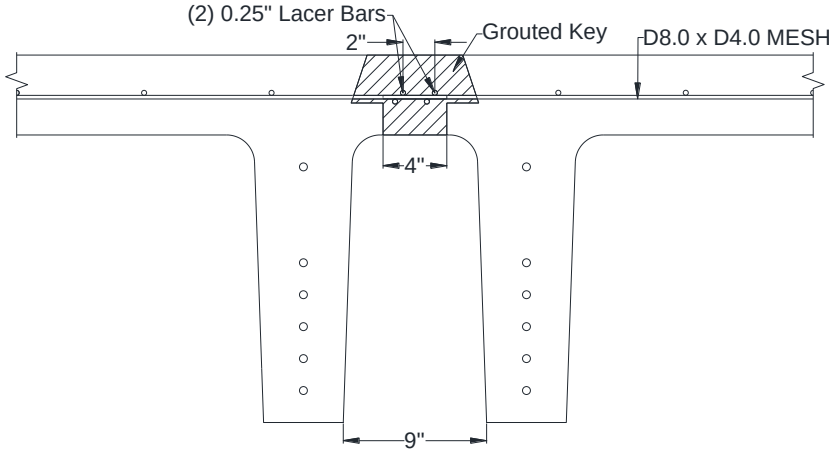

Figure 2-7 Proposed Continuous Joint Detailing (Konrad, 2014)

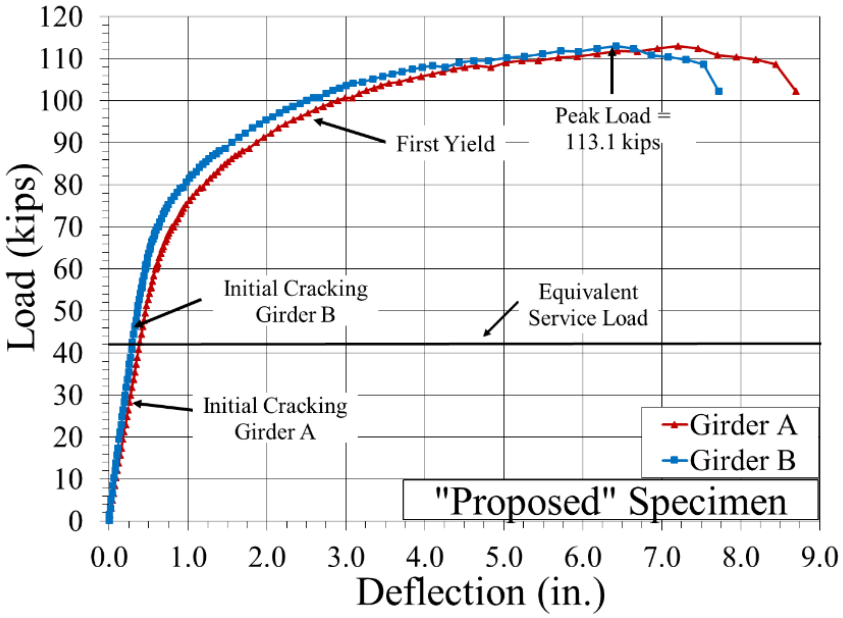

Figure 2-8. Measured Load-Deflection Relationship Under Static Loading for Proposed Specimen (Konrad, 2014)

Haber and Graybeal (2014) performed precast deck panel connection beam tests at the Federal Highway Administration (FHWA) Turner-Fairbank Highway Research Center to better understand the performance of the deck panel connections under extreme demands. The tests consisted of specimens (Fig. 2-9) with combinations of different grouts, lap-splices, rebar type, surface preparation, and keyway geometry. The loading protocol used for the beam specimens consisted of three loading protocols: cyclic crack loading, fatigue loading, and monotonic ultimate loading. The results concluded:

- Selection of grout material is critical for deck-level precast connections.
- Depending on the selected grout, surface treatment can have significant impact on tensile bond strength.
- Shear key geometry had no influence on deck panel connection performance.
- Exposed aggregate surface treatment was the best for bond strength performance.

- Non-shrink and magnesium phosphate grouts may lead to inadequate performance regardless of surface treatment in terms of bond strength and cyclic loading.
- Epoxy grout and ultra-high performance concrete provide best value when considering long-term performance and maintenance costs.

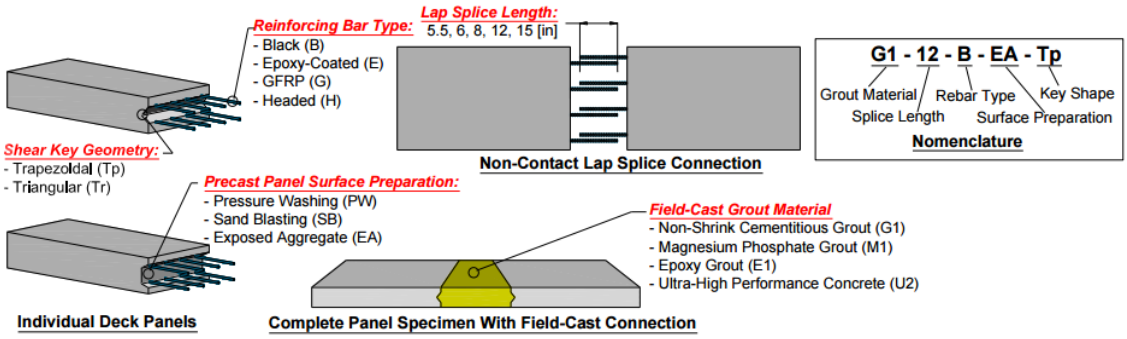

Figure 2-9. Testing Variables Used for Deck Panel Precast Connections (Haber and Graybeal, 2014)

Jones and Saiidi (2015) performed a survey of state DOTs regarding practical longitudinal and transverse joints suitable for precast bridge panels. Thirty-two DOTs participated in the survey. The survey concluded the most common type of longitudinal connections among DOTs are UHPC-filled joints with spliced reinforcement and post-tensioned joints filled with standard grout (Fig. 2-10). Deck panel performance was surveyed for common observed problems among DOTs for both full-depth and partial-depth deck systems. The most common issues pointed out by the participants were cracking within the filler material, joint leakage, and reflective cracking.

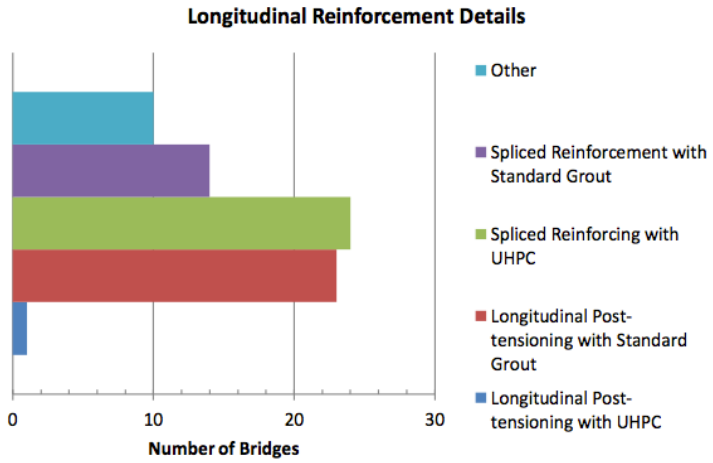

Figure 2-10. Survey Results for Various Longitudinal Joint Detailing (Jones et al., 2015).

2.3 Dowel bar Retrofit

One alternative to the continuous joint connection detail is the use of the dowel bar retrofit technique that has been frequently utilized by many state DOTs on paved highways. The technique involves saw-cutting a small slot on both sides of the joint. The material is typically removed by hammer-chipping and cleaned by air-blasting. A smooth dowel is placed and the slot is then filled with a cement-based material. Washington State DOT (WSDOT) has been using the dowel bar retrofit technique since 1992 to extend the lifespan of the pavement beyond the original intended 20 years. Since 1992, WSDOT has retrofitted over 225 miles of pavement using the dowel bar technique. The study by Pierce et al. (2002) was to investigate the performance, application, and lessons learned from the 10 years of service of the dowel bar retrofit. The report concluded that the overall performance of the dowel bar retrofit on Portland cement concrete (PCC) was acceptable. However, some issues were observed:

- Studded tire damage – accelerated wear from the use of studded or chained tires.

- Longitudinal cracking – cracks that intersect dowel bar pockets, typically occur where dowel bar is placed over existing longitudinal crack. Failure mode was debonding of the filler material from substrate.
- 45-degree cracking caused by
    - Saw cutting too deep where the dowel bar is located below mid-depth of the slab.
    - The use of heavy jackhammers that punch through the bottom of the slots during removal (deep damage in the slab or pavement).
- Spalling – caused by misalignment of the core board. The core boards intent is to re-establish the existing transverse joint and allow for expansion of the filler material.

The study concluded that construction inspection is the primary factor in successful execution of dowel bar retrofit. Furthermore, one of the most critical parts of the process is the saw-cutting of the slots to remove the material.

The dowel bar retrofit was suggested to be a viable option in the rehabilitating of concrete pavement. However, the use of the dowel bar retrofit technique on the rehabilitation of deck longitudinal joints may be impractical since the deck main reinforcement may be cut.

2.4 Joint Filler

2.4.1 Ultra-High Performance Concrete (UHPC)

UHPC refers to a class of advance cementitious composite materials, which has been developed in recent decades. Comparing UHPC to other conventional cement-based materials; UHPC exhibits superior properties in terms of strength, durability, and long-term stability. UHPC uses a very low water-to-cement ratio along with an optimized matrix. UHPC can provide an excellent bond with reinforcement as well as the existing substrate and significantly shorten the development length of the embedded rebar. Table 2-1 provides typical UHPC composition, and Table 2-2 shows average results of typical UHPC material properties (Graybeal, 2010).

Table 2-1. UHPC Material Composition (Graybeal, 2010)

Material	Percent by Weight
Portland Cement	28.5
Fine Sand	40.8
Silica Fume	9.3
Ground Quartz	8.4
Superplasticizer	1.2
Steel Fibers	6.2
Water	5.2

Table 2-2. UHPC Material Properties (Graybeal, 2010)

Properties	Average Result
Compressive Strength	18.3 ksi
Modulus of Elasticity	6,200 ksi
Split Cylinder Cracking Strength	1.3 ksi
Prism Flexure Cracking Strength	1.3 ksi
Direct Tension Cracking Strength	0.8-1.0 ksi
Long-Term Shrinkage	555 micro-strain
Chloride Ion Penetrability	360 coulombs
Freeze-Thaw Resistance	112%

FHWA report No. 041 investigated different field-cast materials that might be considered to complete the connection between precast bridge members (Swenty and Graybeal, 2013). The insufficient performance of connections between precast bridge members can be generally contributed to the closure material type and detailing. The research consisted of a series of tests that investigated constructability, material characterization, and bond strength for nine potential candidates. The results concluded that UHPC filled connections exhibited acceptable performance because of:

- Sufficient strength
- Good workability
- High tensile strength
- High modulus of elasticity
- Excellent durability
- Cost effective compared to epoxy grouts

Non-shrink, magnesium phosphate and epoxy grouts were also considered in the study that will be discussed further in the following sections.

FHWA report No. 084 on the "Design and Construction of Field-cast UHPC Connections" discussed 30 projects where UHPC was incorporated in precast bridge deck connections (Graybeal, 2014), which are the most common connection involving lap-splicing of mild steel reinforcing bars. Currently AASHTO requires a minimum development length of 24 times the bar diameter (d_b). However, UHPC substantially reduces the development length ($8d_b$ is sufficient to fracture the bar) compared to that of conventional concrete or grout resulting in smaller pockets for precast deck panels. This decreases the cost of reinforcing, fabrication, and field assembly. Examples of

proprietary products that meet the UHPC material properties: BCV, BSI, Cor-Tuf, CRC, Densit, and Ductal. The performance and workability of UHPC decreases when UHPC mix temperature is too high. UHPC can be mixed and placed using conventional methods. Finishing of UHPC is usually done in a closed form to avoid losing moisture.

2.4.2 Latex Modified Concrete (LMC)

Bridge deck deterioration has been a problem wherever salts are used to de-ice roads. The de-icing salts contribute to the corrosion of the bar in the bridge deck. The use of latex in concrete resists the penetration of water and salts and improves the bond to existing concrete. Latex is an additive to Portland cement concrete mixes to reduce the amount of water required to achieve adequate workability for placement. The lower water content increases the compressive strength of concrete. The latex forms an elastic membrane within the concrete matrix reducing the number of voids and micro-cracks. Also, the flexural strength and abrasion resistance are improved using latex (BASF, 2011).

Wenzlick (2006) examined the suitability of very high-early strength latex modified concrete (LMC-VE) for the repair of bridge decks in Missouri. A trial repair was conducted on I-70 near downtown St. Louis to verify how well the process of quick repair would work. Compressive tests performed on cylinders of LMC-VE showed that the compressive strength was 3,000 psi in three hours and 6,000 psi in three days. Chlorine penetration was 100 coulombs, which is negligible. The study reported that two other projects in St. Louis County and St. Charles County utilized LMC-VE. Based on the cost difference of 25% to 53% between regular LMC and LMC-VE, MoDOT

recommends using LMC-VE on bridge deck repairs in areas of extreme traffic congestion.

The durability of the longitudinal joint is a primary concern for connections between precast bridge girders. The longitudinal joints have experienced reflective cracking, which leads to moisture and chlorine corrosion of the reinforcing steel. Baer (2013) proposed LMC as a closure material with a better durability. LMC was selected because of the high bond to the existing concrete and the familiarity of contractors and designers. The objective of the study was to determine the performance of LMC as closure material for a new longitudinal joint connection that features a continuous joint with spliced reinforcement. The latex modifier used in this project was Styron Mod A/NA, which was a preapproved modifier for South Carolina Department of Transportation (SCDOT). Eclipse 4500 shrinkage reducing admixture was used to reduce the drying shrinkage. The test mixture was designed for 6,000 psi compressive strength and exhibited adequate workability (slump of 5 in.). Table 2-3 presents three different mix designs for LMC utilized in Baer (2013).

Table 2-3. LMC Material Composition (Baer, 2013)

Mix Designs	CPTM-1	CPTM-2	CPTM-3
W/C ratio	0.33	0.33	0.28
Coarse Aggregate (lb/yd^3)	1,720	1,260	1,260
Fine Aggregate (lb/yd^3)	1,048	1,505	1,596
Latex Modifier (lb/yd^3)	208	208	208
Air Entrainer (fl oz/yd^3)	1.5	1.5	1.5
Super Plasticizer (fl oz/yd^3)	24.4	0	0
Water Reducer (fl oz/yd^3)	15	15	15
Shrinkage Reducer (lb/yd^3)	11.55	11.55	11.55

Shrinkage tests were performed at 28 days and the length change was from 0.02 to 0.025%. The new connection with LMC was exposed to two million cycles of fatigue loading with no observed cracking in the joints. The study concluded that LMC is a viable filler material for longitudinal joint connections between precast bridge girders.

2.4.3 Grout Materials

Champa et al. (1995) analyzed different grout materials suitable for a keyway joint between adjacent box beams, voided slabs, and bulb tees. A standard non-shrink grout and magnesium ammonium phosphate (MAP) mortar were the two candidates selected for testing. Inspections of bridges have brought attention to the connection with problems of longitudinal cracking allowing water leaking along with salt and chlorides, which expedite the bar corrosion. Shrinkage and debonding of the joint material can be the cause of the deterioration of these keyways. Longitudinal cracking observed along the joint was the primary concern of the study. Polymer modified grouts exhibit advantageous properties compared to conventional grouts for use in bridge joint keyways because of:

- Better bond to substrate
- Less permeability

- Internal self-curing after moist curing
- Better freeze-thaw durability
- Lower creep

MAP has been used on several bridge projects in the northwest including Alaska. Tests on shear keys were performed with three different loading cases: vertical shear, tension, and longitudinal shear. The non-shrink grout failed at the interface and the Set-45 (MAP) failed at the concrete substrate. The study concluded that MAP grouted specimens performed significantly better compared to non-shrink grouted specimens in terms of strength, chloride absorption, and shrinkage.

The study reported that MAP grout has been successfully implemented in several field applications involving bridge keyways. The report concluded that the use of MAP grouts is encouraged to improve keyway performance, and non-shrink grouts were not recommended.

Barde et al. (2006) studied the repair of concrete pavements with rapid-setting materials. These materials can be placed and cured in a short period of time. In recent years, many high-early strength repair materials have been developed, both generic and proprietary. This study explored materials with early high-strength and excellent durability. A total of 11 different proprietary repair materials were selected for testing. Each material was extended with 3/8-in. pea-gravel and mixed per manufacture specifications. The specimens were tested for both strength and durability. The results provided information on initial set, final set, compressive strength, flexural strength, elastic modulus, shrinkage, and bond strength. The repair materials exhibited a wide range of properties. The study recommended the best repair materials as Fox Industries

FX-928, Chemrex SET45 Regular, and Sika Corporation SikaSet Roadway Patch 2000. However, further testing for freeze-thaw and potential corrosion was recommended.

NCHRP report No. 173 evaluated closure materials with improved properties that can enhance the performance of longitudinal joints in precast bridge decks (French, et al., 2011). Many different types of materials have been used since 1973. Materials include sand-epoxy mortars, latex modified concrete, cement-based grouts, non-shrink cement grout, epoxy mortar grout, calcium aluminate cement mortar, methylmethacrylate polymer concrete, and polymer mortar. Epoxy grouts exhibit excellent strength and durability with high strength (20 ksi in 6 hours), low shrinkage, and low chloride permeability. However, they are considered very expensive and less compatible with the surrounding concrete. Cement-based grouts main disadvantage is durability that leads to reflective cracking, which are unavoidable even with non-shrink based grouts. MAP grouts extended with pea-gravel can meet all the requirements with several other studies stating that MAP grout performs better than non-shrink grout.

The report tested eight closure materials to determine a candidate for long-term applications. Among the candidates four grout materials and four HPC materials were selected. Preliminary tests were performed based on strength tests to narrow the candidates down to two materials, an "overnight cure" and a "7-day cure" material. The final selection for long-term testing was based on the following properties: compressive strength, shrinkage, chloride penetration, freeze and thaw, and bond strength. The results concluded that the overnight cure material, MAP grout (Set 45HW), and the 7-day cure material, HPC mix1, were the best candidates. These two closure materials exhibited the best strength and durability properties of the eight materials tested (French, et al., 2011).

2.5 Joint Reinforcement

2.5.1 Introduction

Two reinforcing bar types that might be suitable for double-tee girder longitudinal joint rehabilitation are headed bars and wire meshes. The transverse reinforcement used in the rehabilitated longitudinal joint must be able to transfer required shear and bending moment. The transfer of shear and bending moment between girders depends on the splice lengths of the headed bar or wire mesh. AASHTO provides equations for development of wire mesh. However, AASHTO requires lab testing of any mechanical anchorage. International Code Council Report No. ES ESR-2935 (2016) provides development length equations for headed bars.

2.5.2 Headed bar

Headed bars are alternatives to hooked bars when anchorage length, congestion, and construction time become an issue. A major advantage of using headed bar is the shorter lap-splice that is required to fully develop a bar. Article 5.11.2.6.2 (Development by Mechanical Anchorages) of AASHTO LRFD Bridge Design (2013) states that any mechanical device capable of developing the strength of the reinforcement without damaging the concrete may be used as an anchorage. The performance of a mechanical anchor shall be verified by lab testing. Some of requirements regarding headed bar applications are presented herein.

Section 8.4.4 of ICC-ES ESR-2935 states when headed bars (HRC 555) are used as an alternative to standard deformed bars, the minimum lap length must be in accordance to Eq. 2-1 as

$$L_s = 1.3[L_a + S_b \tan(35)] \qquad \text{Eq. 2-1}$$

$$L_a = 8\,d_b \text{ or } 6 \text{ in.} \qquad \text{Eq. 2-2}$$

where:

L_s is the minimum lap length (in.).

S_b is the centerline spacing between lapped headed bars (in.).

L_a is the minimum anchorage length (in.).

Section 8.4.2 of ICC-ES ESR-2935 states that bars shall be placed so that c_b/d_b is equal to or greater than 2.5. Installation of the headed bars must be in accordance to Eq. 2-3 as

$$f_{c,bear}\,A_{brg} \geq f_y\,A_b \text{ (lbs)} \qquad \text{Eq. 2-3}$$

$$f_{c,bear} = \frac{0.6\,f_c^{'}\,\omega_t\,2c_b}{\sqrt{A_{brg}}} < 8\,f_c^{'} \text{ (psi)} \qquad \text{Eq. 2-4}$$

$$\omega_t = 0.6 + 0.4\frac{c_2}{c_b} < 2.0 \qquad \text{Eq. 2-5}$$

where:

f'_c is the specified compressive strength of concrete at 28 days limited to 6,000 (psi).

c_b is the minimum of half the center-to-center bar spacing or the least concrete cover dimension measured to center of bar (in.).

c_2 is the dimension perpendicular to c_b (in.).

c_2 shall always be equal or greater than c_b.

A_{brg} is the net headed bearing area (in^2).

A_b is the nominal cross-sectional area of the reinforcing bar (in^2).

f_y is the specified yield strength of reinforcing bars (ksi).

d_b = diameter of rebar (in.).

2.5.3 Wire mesh

Wire mesh is a mat of reinforcement with wires in both the longitudinal and transverse directions welded together. Two types of wires are commonly used: plain wire and deformed wire. In the present study, the focus is on the welded deformed wire mesh since they are used in the construction of double-tee girders in SD.

According to the AASHTO LRFD Bridge Design Specifications (2013):

1. Section *5.11.2.6.3 – Anchorage of Wire Fabric Reinforcement:* at each end of a single-leg stirrup of deformed wire fabric there should be two longitudinal wires at minimum spacing of 2.0 in.
2. Section *5.11.2.5.1 – Deformed Wire Fabric:* the development length of welded deformed wire for other than shear reinforcement is the lesser of the two equations:

$$l_{hd} \le 0.95\, d_b \frac{f_y - 20.0}{\sqrt{f'_c}} \text{ or} \qquad \text{Eq. 2-6}$$

$$l_{hd} \le 6.30\, d_b \frac{A_w f_y}{s_w \sqrt{f'_c}} \qquad \text{Eq. 2-7}$$

where:

l_{hd} is the development length for welded wire fabric (in.).

A_w is the area of an individual wire to be developed or spliced (in^2).

s_w is the spacing of wire to be developed or spliced (in^2).

f_y is the specified yield strength of reinforcing bars (ksi).

f'_c is the specified compressive strength of concrete at 28 days (ksi).

According to the AASHTO LRFD Bridge Design Specifications (2013), the length of lap-splice for welded wire mesh reinforcement in tension is

$$L_s = 1.3\, l_{hd} \text{ or } 8.0 \text{ in.} \qquad \text{Eq. 2-8}$$

where l_s is the splice length (in.). The overlap between the outermost cross wires of each fabric shall not be less than 2.0 in.

Graybeal (2014) suggested that the development length (l_d) (Eq. 2-9) of field-casted UHPC with 2% steel fiber and a compressive strength of at least 14 ksi as

$$l_d = 8\, d_b \qquad \text{Eq. 2-9}$$

where d_b is the diameter of the rebar (in.)

Other requirements for the development length of bars in UHPC are: l_d shall be at least $3d_b$ and yield stress (f_y) shall not exceed 75 ksi, and bars shall not be greater than No. 8 bar.

2.6 Demolition methods

2.6.1 Hydro-demolishing

Wenzlick (2002) concluded that hydro-demolition is a better alternative for concrete removal from bridge decks than the conventional methods using jackhammers. MoDOT reported debonding and cracking of the rehabilitated bridge decks using conventional demolishing methods. The MoDOT report highlighted the major advantages of hydro-demolition versus jack-hammering:

- Hydro-demolition does not damage the concrete that is to stay in place. Jack-hammering causes micro-fractures in the concrete surface that leads to poor bond.

- Bond strength of repaired concrete with hydro-demolition is on average two times higher than that repaired with jack-hammering.
- Hydro-demolition exposes the reinforcement with no additional damage, and no additional operation is needed before casting while jack-hammering requires sand-blasting of the reinforcement after material is chipped away.
- Cost for hydro-demolishing in Missouri in 2002 was $\$12/yd^2$ to $\$75/yd^2$ compared to $\$260/yd^2$ to $\$300/yd^2$ for conventional removal.

The only disadvantage noted in the report was the limited mobilization and availability of hydro-jets in 2002, but this problem may be resolved when demands.

3. Rating System

3.1 Introduction

The FHWA and many DOTs currently use accelerated bridge construction (ABC) to increase construction speed and to limit the impact on the public. Successful implementation of ABC relies heavily on the field-casted connections between adjacent precast elements. Performance and durability are essential factors for identifying an adequate ABC connection. As was presented, there are several filler materials, joint detailing, and reinforcements that might be suitable for double-tee longitudinal joint rehabilitation. A rating system is needed to rank the different alternatives. A rating system developed under NCHRP Report 698 (Marsh et al., 2011) was adopted in the present study to qualitatively rate each longitudinal joint rehabilitation alternative suitable for double-tee bridge girders. The rating system utilizes five levels for overall performance: construction risk, performance, durability, inspectability, and cost.

3.2 NCHRP Rating System

3.2.1 Construction Risk Rating

The evaluation of construction risk measures the difficulty to fabricate and install, the construction quality, and the scheduling risk for ABC construction:

- Complexity of detailing
- Construction tolerances

- Equipment required for installation
- Difficulty of work environment
- Vulnerability of construction mistakes
- Requirement for specialty trades
- Learning curve
- Sensitivity of installation schedule

3.2.2 Durability

The durability rating can be measured based on:

- Adequate protection of structural components
- Prevents paths for contaminants to structural components
- Durability affected by quality of construction

3.2.3 Performance

The evaluation of performance was measured based on:

- Strength of materials
- Data showing behavior during fatigue loading
- Proper development of bars
- Bond strength to existing substrate

3.2.4 Inspectability

The inspectability rating was based on the ability to assess structural damage by visual inspection after construction in which:

- Inspector can conclude no damage if none is visualized
- Inspector can visually inspect and recognize a failure
- Damage can be assessed with nondestructive methods

3.2.5 Cost

Cost-effectiveness is a main component in the overall problem statement of a project. It is necessary to include a cost rating component. Cost can be measured based on the unit price of the filler materials in this project. The cost of reinforcement is assumed to be the same in all variations thus it is not included in the rating.

3.3 Proposed Constituent Rating Criteria

The performance rating system developed under NCHRP Report 698 consisting of five levels of performance (construction risk, performance, durability, inspectability, and cost) was used to rate the three constituent parts of the longitudinal joint rehabilitation: connections, filler materials, and reinforcing bars. The rating criteria mentioned in the NCHRP Report was modified to fit the requirements necessary for a longitudinal joint rehabilitation detail to be used for double-tee girder bridges located on South Dakota local roads.

3.3.1 Connections

The construction risk criterion that was applicable to the double-tee rehabilitation was the potential damage to the members (e.g. bar damage during concrete removal), the requirement of skilled contractors, and equipment for demolishing. Durability is a major concern in this type of bridge system in which potential reflective cracks may expedite bar corrosion. The inspectability was assessed based on the ability to access cracking as a failure mode. The performance rating was based on the strength and fatigue capacity for each alternative found in previous research studies. Table 3-1 describes the evaluation criteria for the overall connection.

Table 3-1. Connection Rating Criteria

Criteria	Remarks
Construction Risk	Damage of existing elements, Requirement of skilled contractors and equipment
Durability	Potential for leakage, Potential for corrosion
Inspectability	Visualize cracking
Performance	Ultimate and fatigue strength
Cost	-

3.3.2 Filler material

The construction risk criterion that was applicable to the filler material was the working time, and curing time. Premix materials can be used to improve the material quality. The main concern was to allow sufficient time to place and finish the material with sufficient early strength to allow traffic flow within a reasonable time after the placement. Durability was measured by freeze-thaw cycles, chlorine penetration, and shrinkage properties. This measure was purely qualitative based on the results of previous studies. Inspectability was assessed based on the ability to access cracking as a failure mode. The performance rating was based on material data on compressive strength and bond strength to existing substrate. Cost was considered based on the price per cubic yard of the filler material. Table 3-2 provided the constituent rating criteria for the filler material.

Table 3-2. Filler Material Rating Criteria

Criteria	Remarks
Construction Risk	Working time, Curing time
Durability	Freeze-thaw, Chlorine penetration, Shrinkage
Inspectability	Visualize cracking
Performance	Compressive strength, Bond strength
Cost	Price per cubic yard

3.3.3 Reinforcing Bars

The construction risk criterion that was applicable to the reinforcing bars was the required cover and depth, and the potential of not meeting the required completion schedule. Durability was assessed based on the additional cover reinforcing bars would require. The performance rating was based on the ability to provide additional benefit in terms of developing the bar. Table 3-3 provides the constituent rating criteria for the reinforcing bars.

Table 3-3. Reinforcing Rating Criteria

Criteria	Remarks
Construction Risk	Risk of insufficient cover, Risk of not meeting schedule
Durability	Adequate cover
Inspectability	-
Performance	Development of bars
Cost	-

4. Evaluation and Selection of Joint Rehabilitation Methods

4.1 Joint Constituent Rating

4.1.1 Connection

The proposed continuous joint and dowel bar retrofit options were rated. Tables 4-1 and 4-2 present the quantitative criteria evaluation for each category. A score of +2 was assigned when the performance is highly desired. Undesired performance was scores as -2. If any criterion had neither a good nor bad effect, a zero score was assigned. Intermediate scores of ±1 were considered for intermediate performance. The construction cost of the connection was not considered. Table 4-3 shows the results of the connection type rating.

Table 4-1. Continuous Joint Evaluation

Criteria	Remarks	Score
Construction Risk	The potential of damaging the rebar is minimal when using hydro-demolition (Wenzlick, 2002) Potential for specialty contractors for demolition (Wenzlick, 2002)	Hydro-demolition: +1 Hammering: -1
Durability	The potential for water leakage and corrosion is minimized with continuous joint (Konrad, 2014)	+1
Inspectability	Failure of the joint would be easily identified through visual inspection of joint cracking (Konrad, 2014 and Graybeal, 2010)	0.
Performance	Research has shown adequate results of the continuous joint under static and fatigue tests (Konrad, 2014 and Graybeal, 2010)	+1
Cost	Hydro-demolition: $\$12/yd^2$ to $\$75/yd^2$ (Wenzlick, 2002) Hammer-chipping: $\$77/yd^2$ (SDDOT, 2015)	Not used in Rating

Table 4-2. Dowel Bar Retrofit Evaluation

Criteria	Remarks	Score
Construction Risk	The potential of damaging the rebar is significant when using the standard practice of saw-cutting the pockets (Pierce et al., 2002)	-1
Durability	The potential for water leakage and corrosion is significant with dowel bar retrofit because the method does not provide a continuous joint	-1
Inspectability	Failure of the joint would be easily identified through visual inspection of joint cracking (Pierce et al., 2002)	0.
Performance	No research has been found using dowel bar retrofit on bridge decks to transfer shear and moment. Dowel bar retrofit has been used on concrete pavements with a high degree of variability (Pierce et al., 2002)	-2
Cost	N/A	Not used in Rating

Table 4-3. Connection Type Rating

Performance Potential	Definition	Construction Risk Value	Durability Value	Inspectability Value	Performance Value	Cost
+2	Much Better					
+1	Better		CJ		CJ	
0	Equal	CJ		CJ, DB		
-1	Slightly Worse	DB	DB			
-2	Much Worse				DB	

CJ – Continuous joint, DB – Dowel bar retrofit

4.1.2 Filler material

A total of five premix filler materials were selected as possible candidates: ultra-high performance concrete (UHPC), latex modified concrete (LMC), magnesium ammonium phosphate grout (MAP), a fiber reinforced grout (FRG), and non-shrink grout. Tables 4-4 to 4-8 presents the results of the performance potential for each criterion. Table 4-9 presents the rating results for filler materials.

Table 4-4. UHPC Evaluation (Ductal JS1100 RS)

Criteria	Remarks	Score
Construction Risk	Working time: > 30 mins (Swenty and Graybeal, 2013) Curing time: 5 hrs.	0. for both
Durability	Chloride permeability: 200-800 coulombs (Swenty and Graybeal, 2013) Freeze-thaw: 100% Shrinkage: (28-days): 600 micro-strains	Permeability: 0. Freeze-thaw: +1 Shrinkage: 0
Inspectability	Not used in rating	Not used in rating
Performance	Compressive strength: (24-hr.): 10 ksi, (28-day): 18 ksi Slant cylinder bond strength: (7-day): 2.2 ksi (Swenty and Graybeal, 2013)	Strength: +2 Bond: +1
Cost	$2,200/yd^3 (Swenty and Graybeal, 2013)	-2

Table 4-5. LMC Evaluation (Dayton Superior HD-5)

Criteria	Remarks	Score
Construction Risk	Working time: 15 - 20 mins (Dayton, 2015) Curing time: 25 – 30 mins	Working: -1 Curing: +1
Durability	Chloride permeability: < 1,000 coulombs (BASF, 2011) Freeze-thaw: 300 cycles showed no loss (Dayton, 2015) Shrinkage: air cure: -1,100 micro-strains, water cure: 400 micro-strains	Permeability: +1 Freeze-thaw: +1 Shrinkage: -1
Inspectability	Not used in rating	Not used in rating
Performance	Compressive strength: (1-day): 5.2 ksi, (28-day): 8.1 ksi (Dayton, 2015) Slant cylinder bond strength: (1-day): 2.00 ksi, (28-day): 2.75 ksi	Strength: +1 Bond: +1
Cost	HD-50: \$35/bag (\$2,250/yd^3) (Keegan, 2015)	-2

Table 4-6. MAP Evaluation (BASF SET 45)

Criteria	Remarks	Score
Construction Risk	Working time: < 10 mins (Swenty and Graybeal, 2013) Curing time: 8 mins	Working: -1 Curing: +1
Durability	Chloride permeability: 1,000-1,800 coulombs (Swenty and Graybeal, 2013) Freeze-thaw: rapid degradation Shrinkage: (28-days): 300 micro-strains	Permeability: +1 Freeze-thaw: -2 Shrinkage: 0
Inspectability	Not used in rating	Not used in rating
Performance	Compressive strength: (24 hrs.): 8.4 ksi, (28-days): 9.91 ksi (Swenty and Graybeal, 2013) Slant cylinder bond strength: (7-day): n/a	Strength: +1 Bond: 0
Cost	$2,080/yd^3 (Swenty and Graybeal, 2013)	-2

Table 4-7. FRG Evaluation (Five Star Highway Patch FR)

Criteria	Remarks	Score
Construction Risk	Working time: 15 mins (Fivestar, 2015) Curing time: N/A	Working: -1 Curing: 0
Durability	Chloride permeability: low (Fivestar, 2015) Freeze-thaw: 90% Shrinkage: (28-days): 500 micro-strains	Permeability: +1 Freeze-thaw: 0 Shrinkage: 0
Inspectability	Not used in rating	Not used in rating
Performance	Compressive strength: (24 hrs.): 5.0 ksi, (7-day): 6.50 ksi (Fivestar, 2015) Slant cylinder bond strength: (7-day): 2.0 ksi	Strength: 0 Bond: +1
Cost	$1760/yd^3 (Fivestar, 2015)	-1

Table 4-8. Non-shrink Grout Evaluation (Five Star Grout)

Criteria	Remarks	Score
Construction Risk	Working time: > 30 mins (Swenty and Graybeal, 2013) Curing time: 7 hrs.	Working: 0 Curing: 0
Durability	Chloride permeability: 3,000-9,000 coulombs (Swenty and Graybeal, 2013) Freeze-thaw: 99% Shrinkage: (28-days): 1,200 micro-strains	Permeability: -1 Freeze-thaw: 0 Shrinkage: 0
Inspectability	Not used in rating	Not used in rating
Performance	Compressive strength: (24-hr.): 3.45 ksi, (28-day): 6.7 ksi (Swenty and Graybeal, 2013) Slant cylinder bond strength: (7-day): 0.2 ksi	Strength: 0 Bond: 0
Cost	Five Star Grout: $1,570/yd^3 (Swenty and Graybeal, 2013) Dayton Superior 1107 Advantage: $580/yd^3 (Keegan, 2015)	0

Table 4-9. Filler Material Rating

Performance Potential	Definition	Construction Risk Value	Durability Value	Inspectability Value	Performance Value	Cost
+2	Much Better		UHPC, LMC		UHPC, LMC	
+1	Better		FRG		MAP, FRG	
0	Equal	UHPC, LMC, MAP, NS		UHPC, MAP, LMC, NS, FRG	NS	NS
-1	Slightly Worse	FRG	MAP, NS			FRG
-2	Much Worse					MAP, UHPC, LMC

UHPC – Ultra-high performance concrete, LMC – Latex-modified concrete, MAP – Magnesium ammonium phosphate grout, FRG – Fiber reinforced grout, NS – Non-shrink grout

4.1.3 Reinforcing Bars

The headed bar and wire mesh reinforcement were proposed for the joint rehabilitation. Tables 4-10 to 4-11 presents the results of the performance criteria for each item. Table 4-12 summarizes the result of the reinforcing type rating.

Table 4-10. Headed Bar Evaluation

Criteria	Remarks	Score
Construction Risk	Increases the risk of not meeting cover requirements from the added head dimension	-1
Durability	The head of the bar increases the required cover	+1
Inspectability	Not used in rating	Not used in rating
Performance	Decreases the required development length of the bar (Headed, 2014)	+1
Cost	Not used in rating	Not used in rating

Table 4-11. Wire mesh Evaluation

Criteria	Remarks	Score
Construction Risk	Insignificant risk for not meeting cover requirement	0.
Durability	Insignificant changes in durability using wire mesh	0.
Inspectability	N/A	Not used in rating
Performance	Significantly higher development lengths than headed bar (AASHTO, 2013)	-1
Cost	Not used in rating	Not used in rating

Table 4-12. Reinforcing Type Rating Results

Performance Potential	Definition	Construction Risk Value	Durability Value	Inspectability Value	Performance Value	Cost
+2	Much Better					
+1	Better		HB		HB	
0	Equal	WM	WM	HB, WM		
-1	Slightly Worse	HB			WM	
-2	Much Worse					

WM – Wire mesh, HB – Headed bar

4.2 Joint Rating Results

With two connection types, five filler materials, and two reinforcing types, a total of 20 connection options were feasible for the double-tee joint rehabilitation. The results of each constituent rating including connection, filler material, and reinforcing were compiled into Table 4-13. The rating from construction risk value, durability value, inspectability value, and cost was summed together and an overall rating was assigned to each connection. The results concluded that alternatives with the dowel bar retrofit method are not adequate for the rehabilitation of the longitudinal joint. Overall, the alternatives with continuous joints and UHPC and LMC as filler were identified as the best alternatives. The rating favored the headed bar but the wire mesh was still a potential option. The top four candidates for the rehabilitation of double-tee longitudinal joints were: continuous joint with UHPC and headed bar (CUH), continuous joint with LMC and headed bar (CLH), continuous joint with UHPC and wire mesh (CUW), and continuous joint with LMC and wire mesh (CLW).

Table 4-13. Connection – Material – Reinforcing Rating System

Conn. #	Conn. Alt.	Filler Material	Reinforcing	Const. Risk Rating	Durability Rating	Perform. Rating	Inspect. Rating	Cost Rating	Overall Rating
1	CUH	UHPC	Headed-Bar	0, -1, 0	2, 1, 1	2, 1, 1	0, 0, 0	-2	5
2	CUW	UHPC	Wire-Mesh	0, 0, 0	2, 0, 1	2, -1, 1	0, 0, 0	-2	3
3	CNH	NSG	Headed-Bar	0, -1, 0	-1, 1, 1	0, 1, 1	0, 0, 0	0	2
4	CNW	NSG	Wire-Mesh	0, 0, 0	-1, 0, 1	0, -1, 1	0, 0, 0	0	0
5	CMH	MAP	Headed-Bar	0, -1, 0	-1, 1, 1	1, 1, 1	0, 0, 0	-2	1
6	CMW	MAP	Wire-Mesh	0, 0, 0	-1, 0, 1	1, -1, 1	0, 0, 0	-2	-1
7	CLH	LMC	Headed-Bar	0, -1, 0	2, 1, 1	2, 1, 1	0, 0, 0	-2	5
8	CLW	LMC	Wire-Mesh	0, 0, 0	2, 0, 1	2, -1, 1	0, 0, 0	-2	3
9	CFH	FRG	Headed-Bar	-1, -1, 0	1, 1, 1	1, 1, 1	0, 0, 0	-1	3
10	CFW	FRG	Wire-mesh	-1, 0, 0	1, 0, 1	1, -1, 1	0, 0, 0	-1	1
11	DUH	UHPC	Headed-Bar	0, -1, -1	2, 1, -1	2, 1, -2	0, 0, 0	-2	-1
12	DUR	UHPC	Rebar	0, 0, -1	2, 0, -1	2, -1, -2	0, 0, 0	-2	-3
13	DNH	NSG	Headed-Bar	0, -1, -1	-1, 1, -1	0, 1, -2	0, 0, 0	0	-4
14	DNR	NSG	Rebar	0, 0, -1	-1, 0, -1	0, -1, -2	0, 0, 0	0	-6
15	DMH	MAP	Headed-Bar	0, -1, -1	-1, 1, -1	1, 1, -2	0, 0, 0	-2	-5
16	DMR	MAP	Rebar	0, 0, -1	-1, 0, -1	1, -1, -2	0, 0, 0	-2	-7
17	DLH	LMC	Headed-Bar	0, -1, -1	2, 1, -1	2, 1, -2	0, 0, 0	-2	-1
18	DLR	LMC	Rebar	0, 0, -1	2, 0, -1	2, -1, -2	0, 0, 0	-2	-3
19	DFH	FRG	Headed-Bar	-1, -1, -1	1, 1, -1	1, 1, -2	0, 0, 0	-1	-3
20	DFW	FRG	Rebar	1, 0, -1	1, 0, -1	1, -1, -2	0, 0, 0	-1	-5

Notes: C – Continuous Joint Rehabilitation, D – Dowel Bar Retrofit, U – UHPC, L – LMC, F – FRG, N – NS, M – MAP, H – Headed Bar, W – Wire Mesh, R-Rebar

4.3 Proposed Joints

The top four alternatives suitable for double-tee girder longitudinal joint rehabilitation based on the proposed rating system are:

i. CUH - Continuous joint connection with UHPC and headed bar

ii. CLH - Continuous joint connection with LMC and headed bar

iii. CUW - Continuous joint connection with UHPC and wire mesh

iv. CLW - Continuous joint connection with LMC and wire mesh

Figure 4-1 shows the preliminary detailing for the rehabilitation of the longitudinal joint utilizing headed bars. Figure 4-2 shows the preliminary detailing for the

rehabilitation of the longitudinal joint utilizing wire mesh. The details are for both filler materials, UHPC and LMC. Further investigation of the proposed details evaluating the different filler materials and reinforcing type are discussed in Chapter 5.

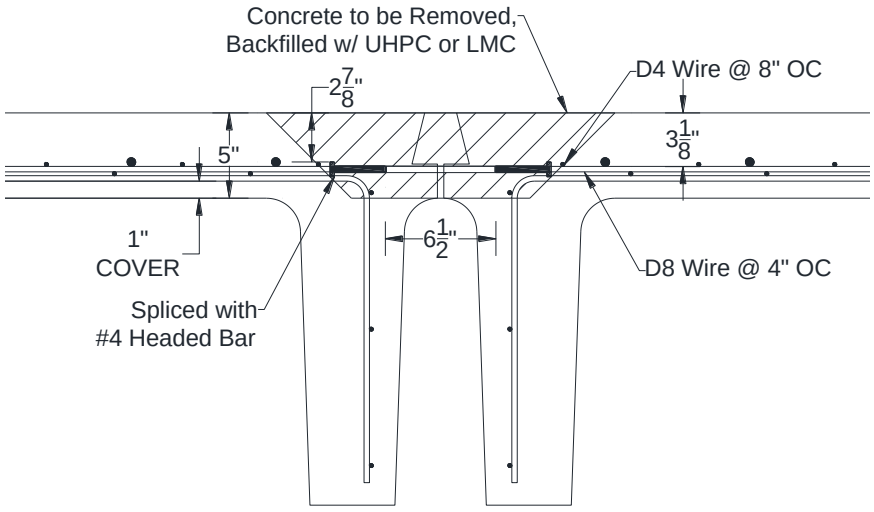

Figure 4-1. The preliminary proposed longitudinal reinforcing rehabilitation detail utilizing headed bar

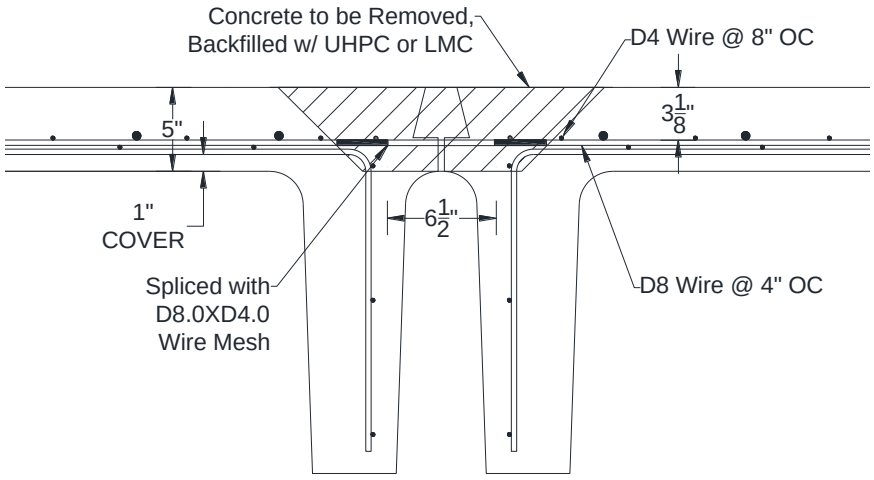

Figure 4-2. The preliminary proposed longitudinal reinforcing rehabilitation detail utilizing wire mesh

5. Development of Connection Detailing

5.1 Introduction

Twenty joint detailing alternatives for the rehabilitation of the longitudinal joint of double-tee girder bridges consisted of a combination of different connection types, joint filler materials, joint reinforcing, and demolition methods were proposed in the previous chapter. Of the 20 alternatives, continuous joint detailing has proven to improve the performance and durability of precast element connections, which are suitable for accelerated bridge construction (ABC). The proposed continuous joint rehabilitation detailing consists of exposing the transverse reinforcement of the deck, lap-slicing the reinforcement, and using a filler material to replace the removed concrete. Filler materials that are considered favorable must improve strength, durability, and bond properties over conventional cementitious materials. Previous studies have shown that ultra-high performance concrete (UHPC) and latex modified concrete (LMC) have been effectively used on new bridge construction. Because of their improved properties, they were selected for further testing.

The rating results showed that the top four alternatives are continuous joint with UHPC and headed bar (CUH), continuous joint with LMC and headed bar (CLH), continuous joint with UHPC and wire mesh (CUW), and continuous joint with LMC and wire mesh (CLW). Since it was not feasible to determine the best alternative using the

available test data from previous research studies, 13 large-scale beam tests were carried out to finalize the joint rehabilitation detailing.

An analytical study was conducted to optimize the joint detailing required for adequate load distribution that meets demands under fatigue, service, and strength limit states. The rehabilitation of the longitudinal joint requires concrete demolishing and using new cementitious materials. To optimize the performance and to minimize the cost, two joint concepts, "pocket" and "continuous", were developed and analytically investigated using linear finite element analyses considering several parameters under the AASHTO loads and limit states.

The results of the experimental and analytical studies were used to finalize the rehabilitation detailing for the longitudinal joints in double-tee girder bridges. The proposed detailing will be used in a full-scale bridge test to assess the structural performance. A summary of experimental and analytical studies as well as the findings of the studies are presented herein.

5.2 Experimental Study of Large-Scale Beams

This section includes the experimental study of large-scale beams built according to the proposed rehabilitation detailing discussed in the previous chapter. The beam test specimens were not rehabilitated but were constructed to simulate the rehabilitation methods and to evaluate the joint strength. The test matrix, test setup, test procedure, instrumentation, and results are discussed in this section.

5.2.1 Test Matrix

As discussed in the previous section, the joint rehabilitation detailing could not be finalized due to the lack of test data. Therefore, a testing program was planned to select

the best detailing for the next phase of the study, which was testing of a full-scale bridge model. This phase of testing included 12 spliced specimens incorporating different joint detailing as well as a reference reinforced concrete beam specimen (RCS) for comparison. Three variables were investigated (Table 5-1): filler material, reinforcement type, and splice length.

Table 5-1. Beam Test Specimens

Test Specimen	Filler Material	Splice Reinforcement	Splice Length
RCS	6000 psi NW Concrete	4 in. X 8 in., D8.0 X D4.0 Wire Mesh	None
U-H-3	UHPC	No. 3 Headed Bar	3 in.
U-H-5	UHPC	No. 3 Headed Bar	5 in.
U-W-3	UHPC	D8.0 X D4.0 Wire Mesh	3 in.
U-W-5	UHPC	D8.0 X D4.0 Wire Mesh	5 in.
L-H-3	LMC	No. 3 Headed Bar	3 in.
L-H-5	LMC	No. 3 Headed Bar	5 in.
L-W-3	LMC	4 in. X 8 in., D8.0 X D4.0 Wire Mesh	3 in.
L-W-5	LMC	4 in. X 8 in., D8.0 X D4.0, Wire Mesh	5 in.
LE-H-3	LMC– Extended w/ 3/8-in. Pea-gravel	No. 3 Headed Bar	3 in.
LE-W-5	LMC– Extended w/ 3/8-in. Pea-gravel	4 in. X 8 in., D8.0 X D4.0 Wire Mesh	5 in.
N-W-3	NSG	4 in. X 8 in., D8.0 X D4.0 Wire Mesh	3 in.
N-W-5	NSG	4 in. X 8 in., D8.0 X D4.0 Wire Mesh	5 in.

Filler Materials: UHPC (ultra-high performance concrete), LMC (latex modified concrete), and NSG (non-shrink grout)
Test specimens: RCS (reference concrete slab),
Specimen ID: Filler Material (U=UHPC, L=LMC, N=NSG) – Reinforcing (H=Headed steel bar, W=steel Wire) – Splice Length (e.g. U-H-3= UHPC – No. 3 Headed bar – 3 in. splice)

Figure 5-1 shows the geometry selection criteria for the beam test models based on the two-adjacent prototype double-tee girders. The thickness of the beam was the same as the girder flange thickness. The length of the beam was approximately 7.5 ft based on the centerline to centerline of the two exterior stems of the two girders. A 12-in. slice of the prototype bridge was selected as the width of the test specimens. The test beams were placed on two roller supports simulating the two left stems of the two girders. A point load was applied approximately at the right edge of the left girder to maximize the shear transfer. The effect of the right exterior stem as a support was ignored to maximize shear force demands on the joint. Figure 5-2 through 5-5 show the proposed joint detailing for all spliced test specimens. RCS had the same geometry as the spliced beams, but it was reinforced with a continuous wire mesh with the same size, type, and spacing as those that are currently utilized in the actual double-tee girders. The beam test model reinforcement followed the prototype double-tee girder mild steel reinforcement in terms of the total area but either wire mesh or headed bar was utilized in the beams. The concrete mix design was the same as that of actual double-tee girders used in the field to minimize test variations.

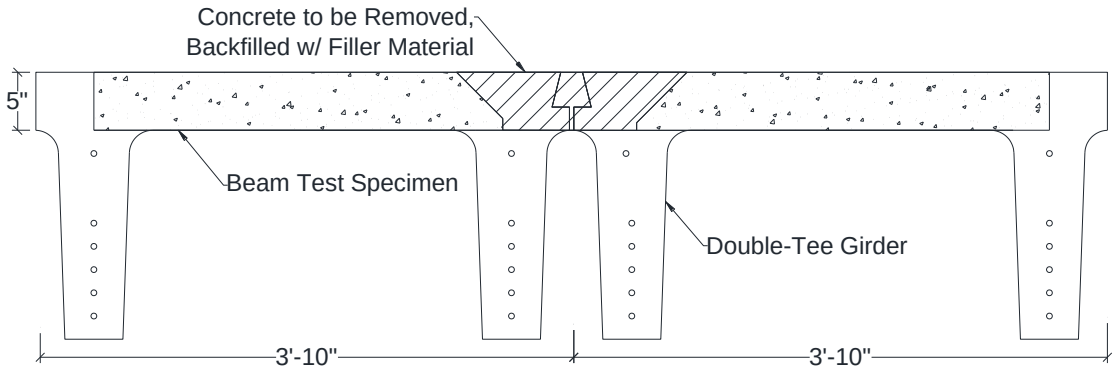

a. Profile View of Beam Test Superimposed onto Double-tee Girders

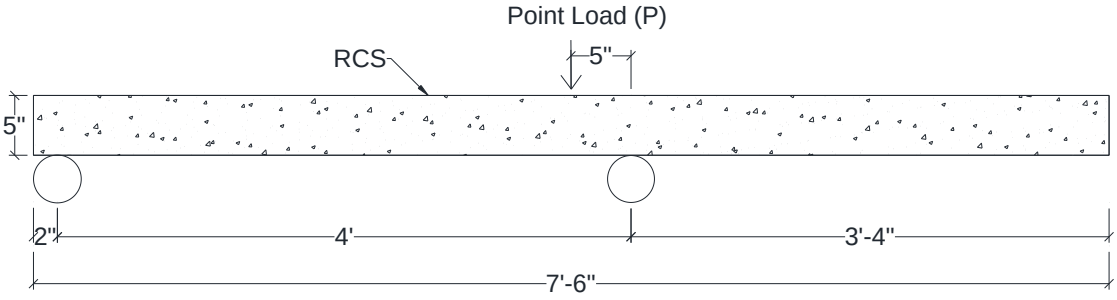

b. Reference Concrete Slab (RCS) Test Specimen

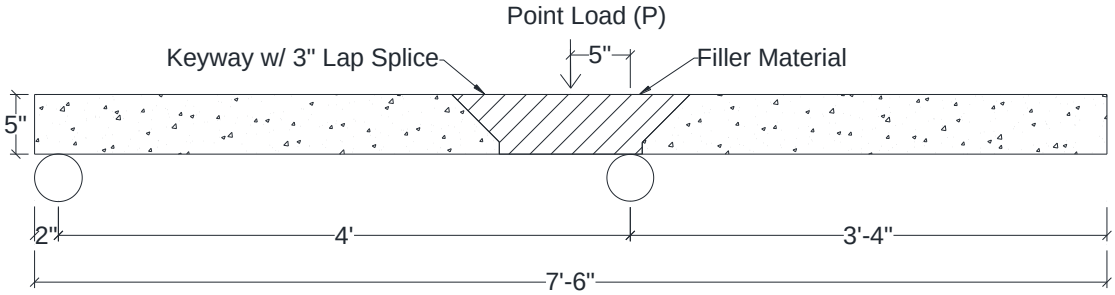

c. Test Specimen with 3-in. Lap-Splice

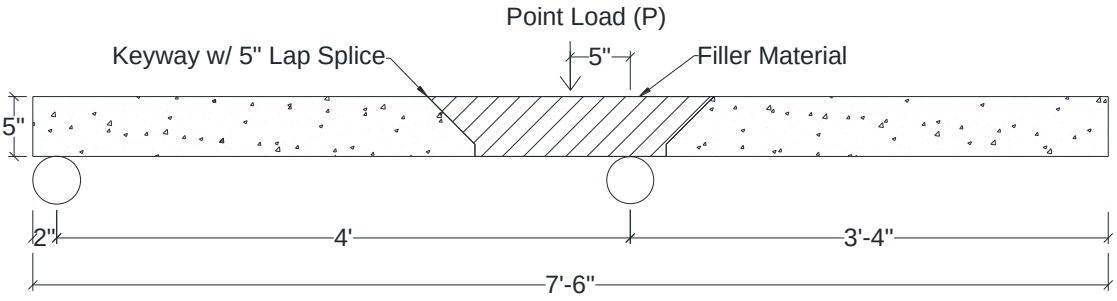

d. Test Specimen with 5-in. Lap-Splice

Figure 5-1. Geometry of Beam Test Specimens

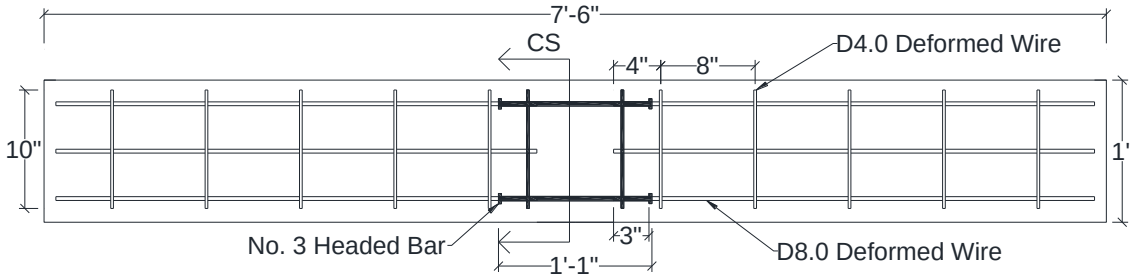

a. Plan View

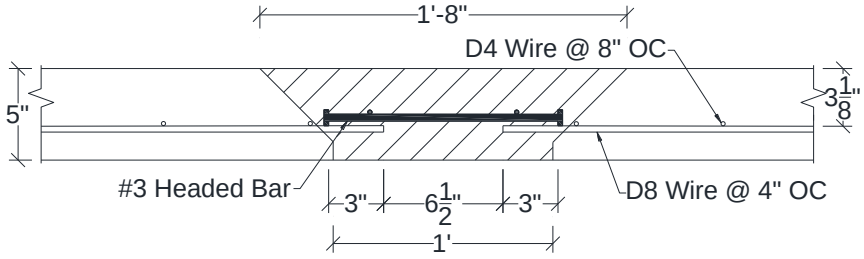

b. Profile View

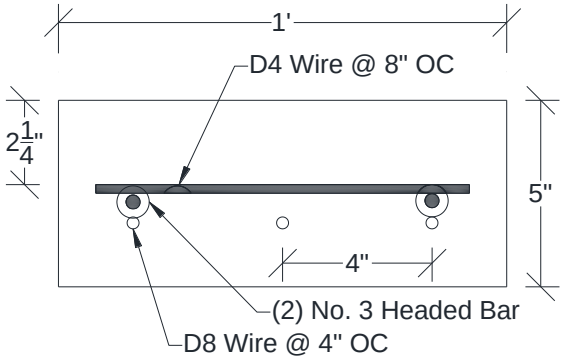

c. Cross-sectional View

Figure 5-2. Detailing for Beam Test Specimen with 3-in. Splice Lengths Utilizing No. 3 Headed Bars

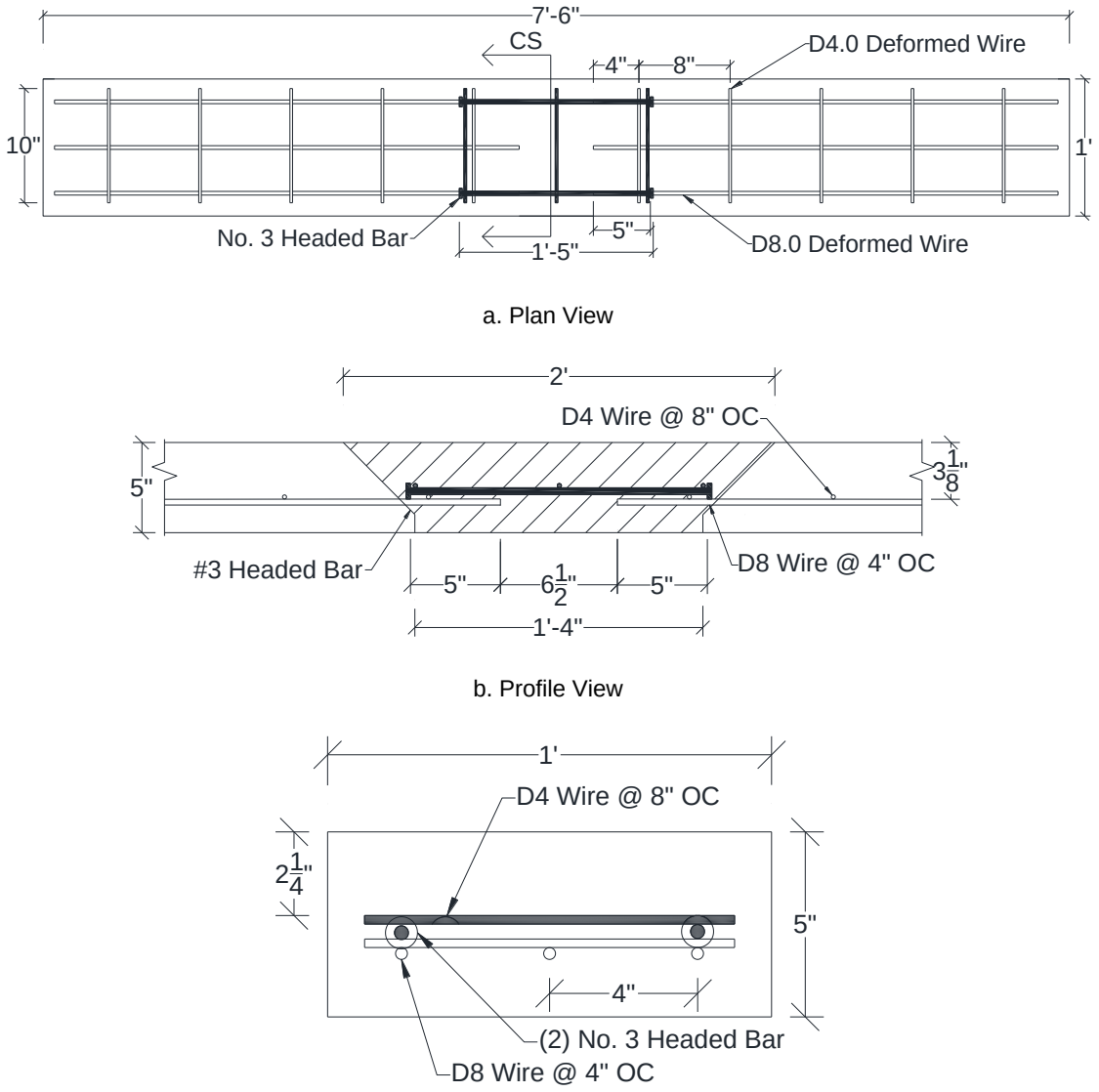

Figure 5-3. Detailing for Beam Test Specimen with 5-in. Splice Lengths Utilizing No. 3 Headed Bars

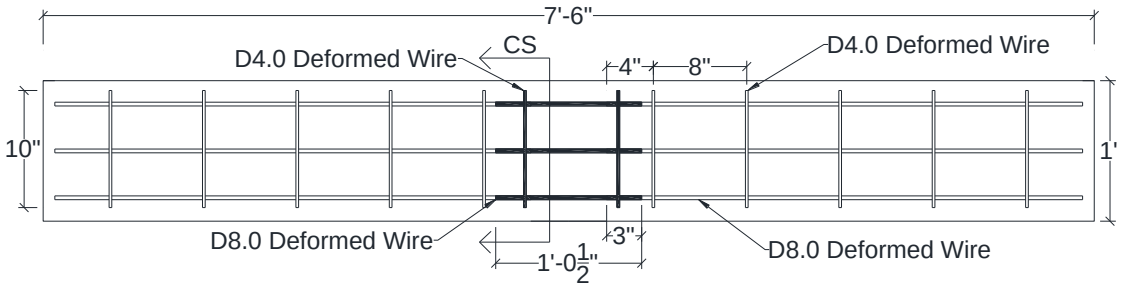

a. Plan View

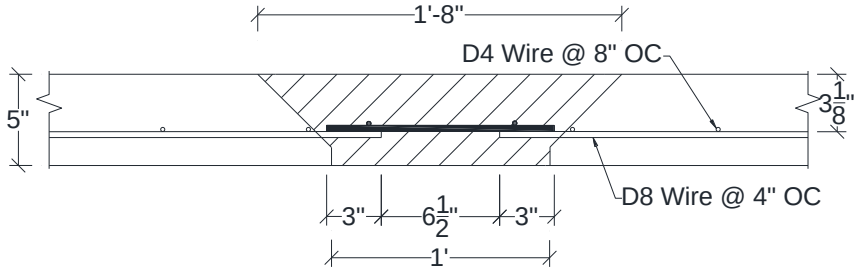

b. Profile View

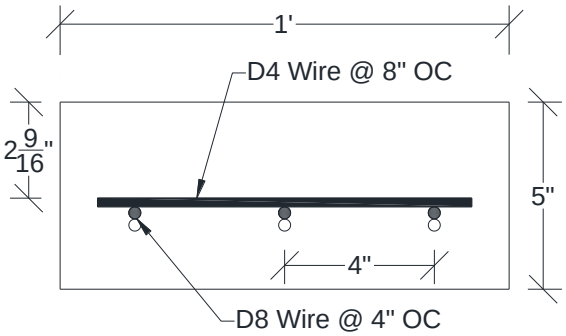

c. Cross-sectional View

Figure 5-4. Detailing for Beam Test Specimen with 3-in. Splice Lengths Utilizing D8/D4 Wire Mesh

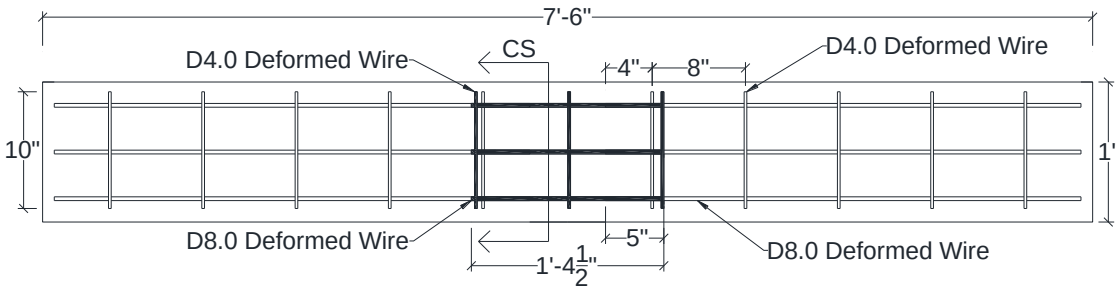

a. Plan View

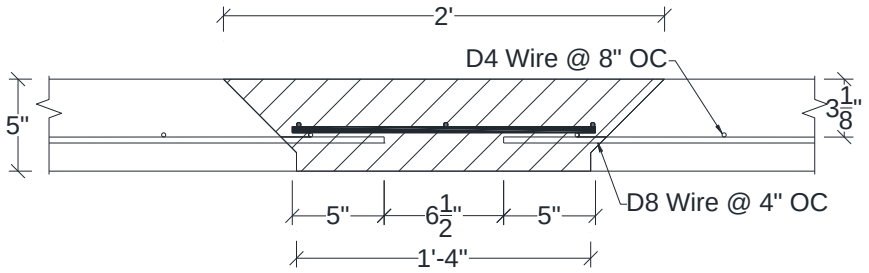

b. Profile View

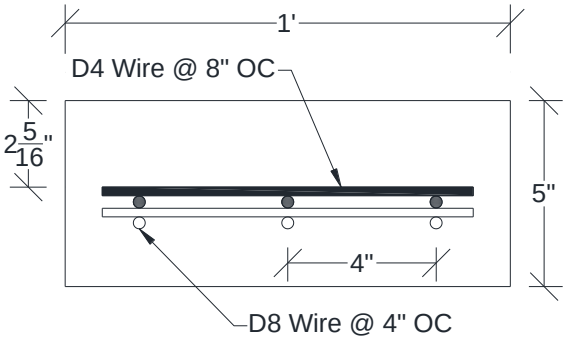

c. Cross-sectional View

Figure 5-5. Detailing for Beam Test Specimen with 5-in. Splice Lengths Utilizing D8/D4 Wire Mesh

5.2.2 Test Setup

The beam test setup is shown in Fig. 5-6. A point load was cyclically applied using a 146-kip actuator at 5 in. from the center of the middle support to maximize the shear demand.

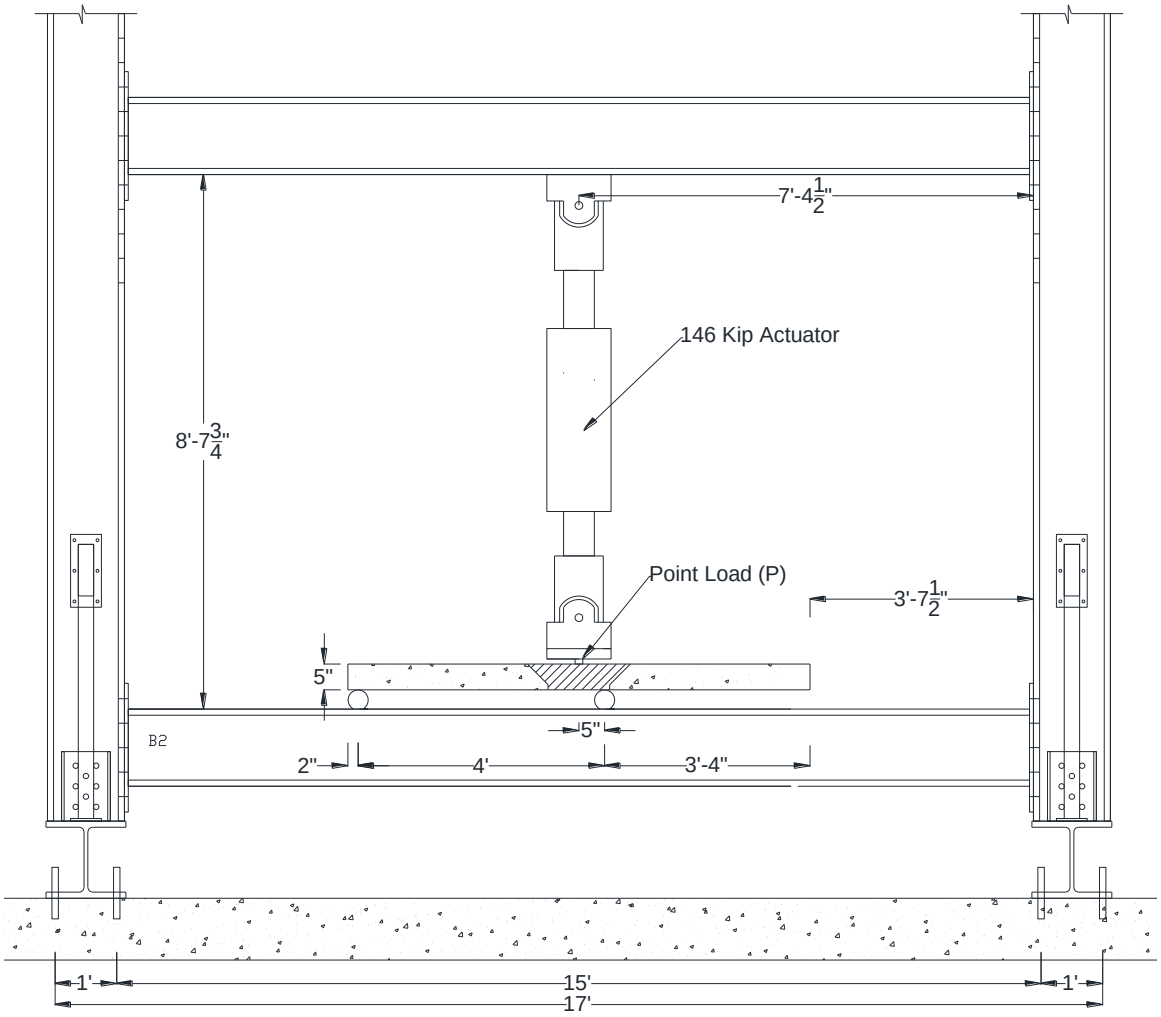

Figure 5-6. Elevation View of Test Setup

Plaster was used between the steel plate and the specimen to provide a level surface for the load plate and to avoid localized loading. For some of the specimens (e.g. those with UHPC), the surface was ground smooth with a hand grinder, and plaster was not

utilized to avoid failure of the plaster. The joint surface was painted white to visualize and document cracking between load cycles.

5.2.3 Construction

The formwork for the 13 test specimens was made with plywood. For specimens with splices, the two segments of the beam were separated using a divider (Fig. 5-7a) to be spliced and filled later. The reinforcement for the precast elements (the precast segments of the beams) was 4 in. by 8 in., D8/D4 welded wire mesh. The main reinforcement, ASTM A-497 (f_y=70 ksi) D8 welded wire with 4 in. center-to-center spacing, has a diameter of 0.32 in. with A_s of 0.24 in^2 per ft. The D4 wire with 8 in. center-to-center spacing has a diameter of 0.23 in. with A_s of 0.06 in^2 per ft.

The beams were fabricated in the Lohr Structures Laboratory at South Dakota State University. Ready mix concrete was utilized for construction. The fresh concrete temperature was 64°F with a slump of 6.0 in. The mix design was based on the current double-tee mix design provided by the manufacturer (Appendix A) targeting 6,000 psi compressive strength at 28-day and a 6-in. slump. A total of 15 standard test cylinders were casted to measure the compressive strengths at varies days. The cylinders were sealed and stored next to the test specimens. Vibration during the pour (Fig. 5-7b) was used to insure proper consolidation. Figure 5-7c shows the test specimens after the pour with plastic sheeting placed to facilitate a moist cured condition at ambient room temperature.

a. Formwork

b. Pouring Concrete

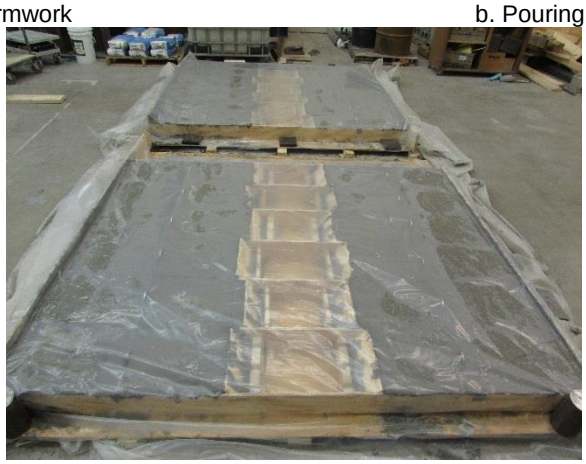

c. After Concrete Pour

Figure 5-7. Casting of Concrete Beam Elements

After 7 days of curing, the inner formwork was stripped to place the joint reinforcement. A previous study showed that roughening and pre-wetting the surface for 24 hours increases the bond between two cementitious materials (Graybeal, 2014). Since the concrete is usually demolished by hammer chipping in South Dakota, a hammer drill was used to roughen the splice surface (Fig 5-8a and 5-8b) to best resemble demolishing conditions. Figure 5-8c (left photograph shows a specimen with 3-in. lap-splice, right photograph shows a specimen with 5-in. lap-splice) shows the spliced 4 in. by 8 in. D8/D4 welded wire mesh and Figure 5-8d (left specimen with 3-in. lap-splice, right

specimen with 5-in. lap-splice) shows the spliced No. 3 headed bars. The head of the reinforcement was 0.5-in. thick with a diameter of 1 in.

a. Original Joint Surface

b. Roughened Joint Surface

c. Wire Mesh Joint Detail
Left=3-in. Splice; Right=5-in. Splice

d. Headed Bar Detail
Left=3-in. Splice; Right=5-in. Splice

e. Pouring UHPC

f. UHPC Static Flow Test

Figure 5-8. Casting Joint Filler UHPC and LMC

The joints were poured with a premix latex modified concrete, LMC (Appendix A), a premix UHPC (with 2% volumetric steel fibers), LMC extended with 3/8-in. diameter pea-gravel, or conventional non-shrink grout. The average batching time for two 50-lb bags of UHPC was 30 minutes using a six-cubic-ft mortar mixer. Each bag of LMC was mixed in a five-gallon bucket for two minutes using a rotary hand mixer. UHPC (Fig. 5-8e) was moderately flowable with an average static flow of 7.5 in. (Fig. 5-8f). LMC was very fluid with low viscosity. Two-inch standard cubes were utilized for LMC sampling, and 3-in. dia. cylinders were casted for both UHPC and LMC extended with pea-gravel. The cylinders were sealed and cured at ambient room temperature. The 2-in. LMC cubes were unmolded after 24 hours then placed in a steam room for curing.

5.2.4 Test Procedure and Instrumentation

A displacement-based half-cyclic loading protocol (Fig. 5-9) with a slow rate of 0.003 in./sec was used for the testing of the beam specimens. Cyclic as oppose to monotonic loading was chosen to maximize damages and to investigate the joint performance under large cyclic displacement demands.

Five linear voltage differential transformers (LVDTs) were mounted on all specimens at various locations (Fig. 5-10) to measure beam deflections and joint slippage.

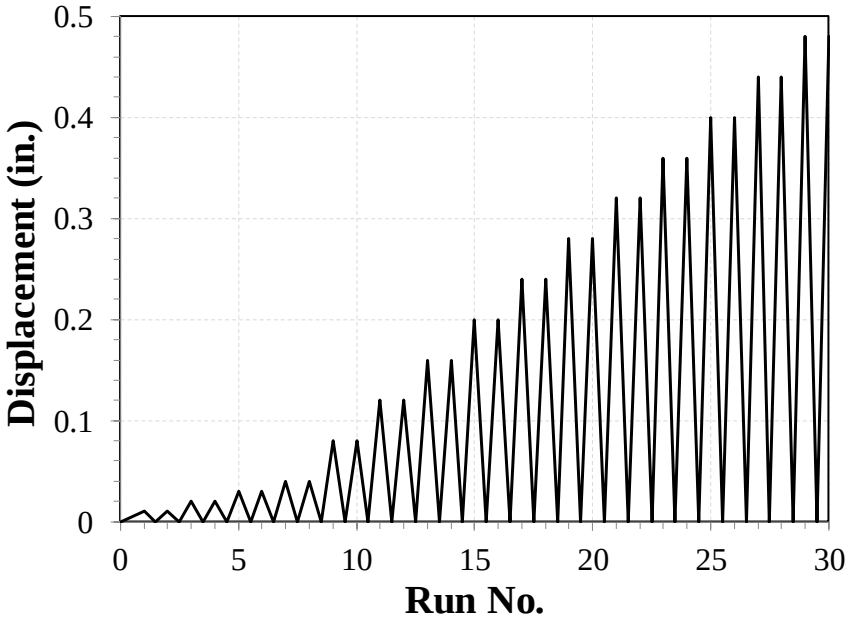

Figure 5-9. Loading Protocol

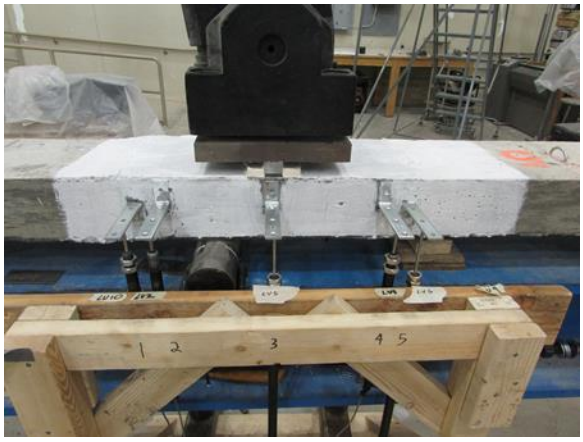

Figure 5-10. LVDT Instrumentation Plan

5.2.5 Test Results of Large-Scale Beams

5.2.5.1 Concrete Properties

The 7-day, 28-day, and test day compressive strengths of each cementitious material were measured per ASTM C39 (2016) and presented in Table 5-2. The target 28-day strength of the conventional concrete was 6,000 psi. The conventional concrete strength was 89% of the target capacity at 28 days. The 28-day non-shrink grout compressive

strength was not reported due to the steam room malfunctioning which caused shrinkage cracks on the test samples. The 28-day LMC-E strength was less than the 7-day value and therefore was not reported.

Table 5-2. Compressive Strength of Cementitious Materials

Material	Element	Specimen	Measured at	f'_c (psi)
Conventional Concrete	Beam	RCS	7-day	4,526
			28-day	5,336
			Test Day	5,324
			Mid Testing	6,224
			End Testing	6,084
UHPC	Joint		7-day	13,678
			28-day	20,671
		UW3	Test Day	19,001
		UW5	Test Day	17,380
		UH3	Test Day	20,652
		UH5	Test Day	20,945
LMC	Joint		7-day	7,608
			28-day	8,859
		LW3	Test Day	8,488
		LW5	Test Day	8,623
		LH3	Test Day	7,815
		LH5	Test Day	7,128
Non-Shrink Grout	Joint		7-day	5,394
			28-day	-
		NW3	Test Day	6,127
		NW5	Test Day	-
LMC Extended with Pea-Gravel	Joint		7-day	4,574
			28-day	5,192
		LEW5	Test Day	4,534
		LEH3	Test Day	4,534

5.2.5.2 Reinforcement Properties

The primary reinforcement used in the construction of the beam test specimens was D8 deformed wire (ASTM A497). The joints were constructed with either D8 deformed wire or No. 3 headed reinforcing steel bar (ASTM A706). According to the ASTM standards, the minimum yield strength (f_y) of the deformed wires and No.3 headed

bars should be 70 and 60 ksi, respectively. The measured mechanical properties of wires and bars are presented in Table 5-3 and their stress-strain relationships are shown in Fig. 5-11. The tensile tests were performed based on ASTM E8 testing procedures. The strain was measured using a 20-mm extensometer. The measured yield strength was determined based on the 0.2% offset method since the bars did not show a yield plateau.

Table 5-3. Tensile Properties of Steel Reinforcement Used in Beam Test Specimens

Properties	D8 Wire (ASTM A497)	No. 3 Headed Bar (ASTM A706)
Yield Strength, fy (ksi)	108	80
Ultimate Strength, fu (ksi)	112	105
Strain at Peak Stress, ε_u	1.8%	8.5%
Strain at Break, ε_r	7-11%	15%

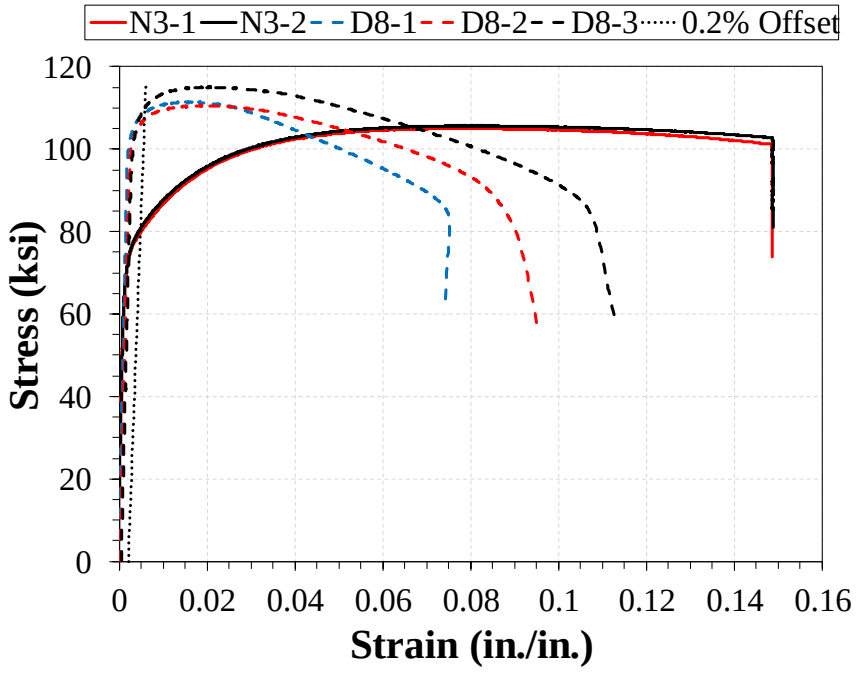

Figure 5-11. Stress-strain Relationships of Beam Test Specimen Reinforcement

5.2.5.3 Cyclic Strength Testing

This section presents the experimental results of the cyclic strength tests performed on the 13 beam specimens. A cast-in-place beam (RCS) with continuous reinforcement was tested as the benchmark model. Table 5-4 presents RCS geometry and the capacities.

Table 5-4. RCS Beam Geometry and Capacity

Parameter	Value
Beam Length (in.)	90
Span (in.)	48
Area of Steel Wire (in^2)	0.24
Effective Depth (in.)	3.7
Measured Peak Shear Force (kips)	20.0
Measured Moment Capacity (k-in.)	99.75
Measured P_{max} (kips) for 7.5-in. Load Eccentricity	15.6
Equivalent P_{max} (kips) for 5-in. Load Eccentricity	22.3

The calculated load caring capacity ($P_{max\text{-}cal.}$) for RCS based on the shear and moment capacities according to Eq. 5-1 to 5-3 was 6.7 kips and 12.0 kips, respectively. Due to the proximity of the applied load to the support combined with conservatism of the shear equation, the test specimens exhibited much higher shear capacity than expected. Initially, a 22-kip actuator was used for the testing of RCS with 5-in. eccentricity (Fig. 5-6). Since the test beam capacity was higher than that calculated, the support was shifted 2.5 in. outward resulting in a larger span (50.5 in.) and a larger load eccentricity to fail the specimen without the need of utilizing a larger-capacity actuator. The failure mode of RCS was bar rupture under the applied load of 15.6 kips. Since the load eccentricity was 5 in. for all other test specimens, the RCS failure load with 5-in. eccentricity was calculated as 22.3 kips using statics. Note, a 146-kip actuator was used for all other beam test specimens.

The measured moment capacity of RCS (99.8 kip-in.) was close to the calculated moment capacity (93.5 kip-in. from Eq. 5-1) using the measured mechanical properties for steel wires and concrete (Tables 5-2 and 5-3).

$$M_p = f_y A_s (d - \frac{a}{2}) \text{ (kip-in.)} \quad \text{Eq. 5-1}$$

$$a = \frac{f_y A_s}{0.85 f'_c b} \text{ (in.)} \quad \text{Eq. 5-2}$$

where:

f_y is the yield stress of reinforcing bar (ksi),

A_s is the area of reinforcing bar (in^2),

d is the effective depth of the reinforcement (in.),

f'_c is the compressive strength of concrete (ksi).

The measured shear capacity of RCS was much higher than the calculated value from AASHTO. The maximum shear demand based on a 22.3-kip applied load is 20 kips for RCS, while the beam shear capacity according to AASHTO equation 5.8.3.3-3 (repeated in Eq. 5-3) is 6.7 kips. In an attempt to better estimate the shear capacity for RCS, AASHTO equation 5.8.4.1-3 for shear friction (Eq. 5-4) with μ=1.4 (monolithic) and c = 0.40 ksi (monolithic) was used, which resulted in a shear capacity of 44.2 kips. This suggests the shear friction equation is a better tool to estimate the shear capacity of the beam specimens.

$$V_c = (0.0316)(2)^2 \sqrt{f'_c} b_v d_v \quad \text{Eq. 5-3}$$

$$V_{ni} = c A_{cv} + \mu (f_y A_s + P_c) \quad \text{Eq. 5-4}$$

where:

b_v is the effective web width (in.),

d_v is the effective shear depth (in.),

A_{cv} is the area of concrete engaged in interface shear transfer (in^2),

μ is the friction factor (AASHTO 5.8.4.3),

c is the cohesion factor (AASHTO 5.4.4.3) (ksi),

P_c is the permanent net compressive force normal to shear plane (kips).

The failure mode of the remaining test specimens was either bar pullout or bar fracture. All test specimens with 5-in. lap-splice (Fig. 5-12) exhibited bar fracture except NW5 (a joint reinforced with wire mesh and filled with conventional non-shrink grout) and LH5 (a joint with headed bars and latex modified concrete). UW3 (a joint with wire mesh and UHPC) and UH3 (a joint with headed bars and UHPC) were the only test specimens with a 3-in. lap-splice (Fig. 5-13) exhibiting bar fracture. Table 5-5 presents a summary of the beam test results including the initial cracking load, the strength load, and the failure mode. The load corresponding to the initial cracking was based on visual inspection of the test beams.

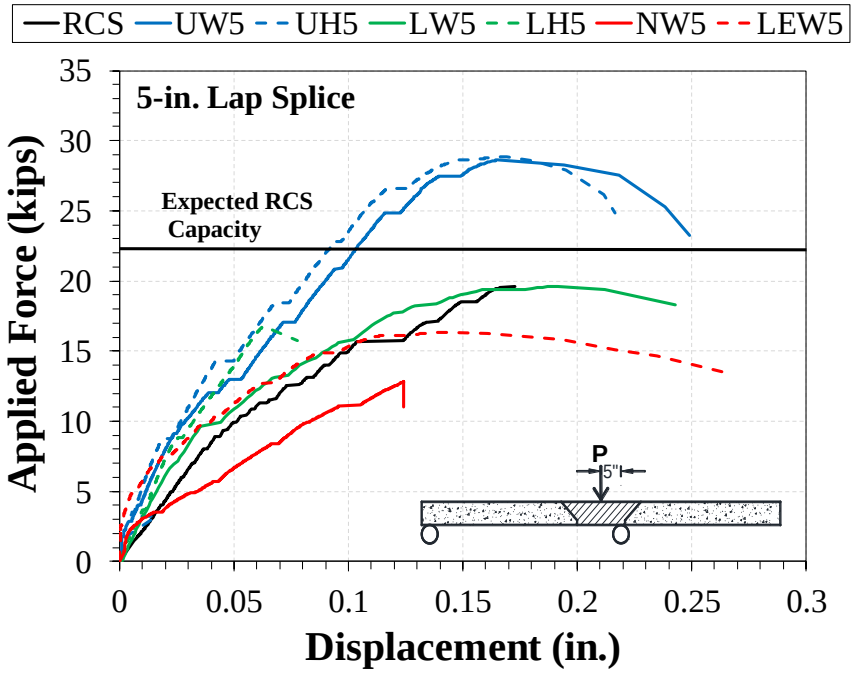

Figure 5-12. Load-Displacement Relationships for beams with 5-in. Lap-Splice

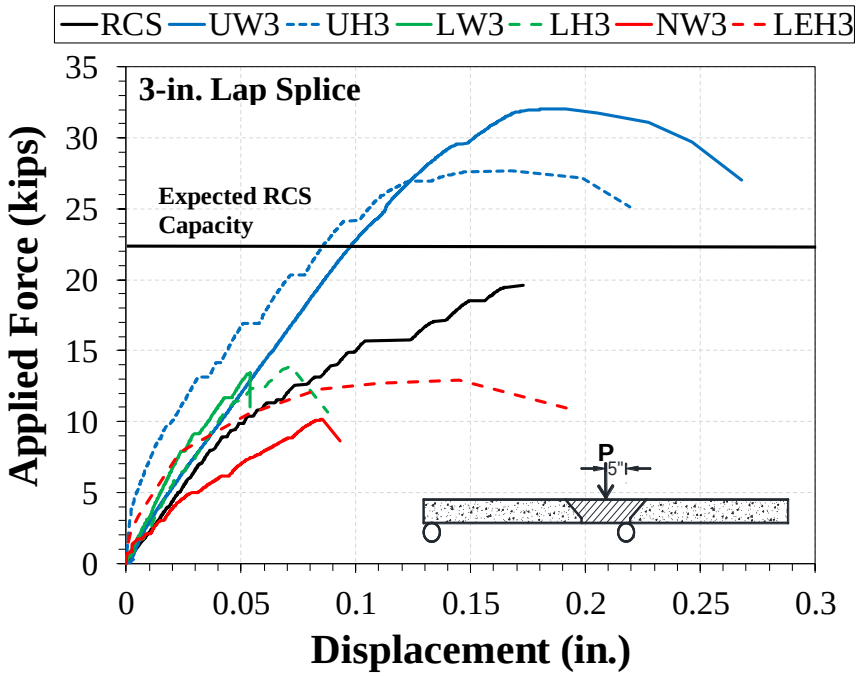

Figure 5-13. Load-Displacement Relationships for Beams with 3-in. Lap-Splice

Table 5-5. Mode of Failure and Load Capacities for Beam Specimens

Specimen	Measured P_{crack} (kips)	Measured P_u (kips)	Mode of Failure
RCS	8.8	22.3	Bar rupture in joint
LW5	9.9	20.1	Bar rupture in joint
UW5	13.3	29.4	Bar rupture in precast concrete segment
LEW5	7.2	16.8	Bar rupture in joint
NW5	3	13.6	Bar pullout
LH5	14.3	16.4	LMC compressive failure
UH5	14.7	29.6	Bar rupture at interface
LW3	12	13.8	Bar pullout
UW3	16.4	32.9	Bar rupture at interface
NW3	9.1	10.4	Bar pullout
LH3	11.7	14.9	Bar pullout
UH3	13.5	28.5	Bar rupture at interface
LEH3	10.5	12.9	Bar pullout

The UHPC test specimens had a 30% higher capacity than the reference specimen. This may be attributed to the 400% higher compressive strength and additional tensile strength provided from the 2% volumetric ratio steel fibers. The first crack (Fig. 5-14) then failure (Fig. 5-15) of all specimens except those incorporating UHPC occurred inside the joint directly under the applied load where the bending moment was maximum. In the UHPC specimens, all the flexural cracking was shifted outside of the joint.

LH5 had a different failure mode compared to the rest of the specimens in which LMC crushed directly under the applied load. This was attributed to the lower effective depth for LH5 (3.2 in.) compared to that for LW5 (3.7 in.) as well as the 50% higher strain capacity for No. 3 headed bar reinforcement compared to that of D8 reinforcement. The combination of the two parameters resulted in a condition in which the beam concrete (LMC) failed in compression in a brittle manner. On the other hand, LW5 exhibited bar fracture. Also, LEW5 had an effective depth of 3.2 in. that resulted in 16% lower capacity compared to LW5.

a. RCS

b. LW3

f. UW5

j. LEW5

c. LW5

g. UH5

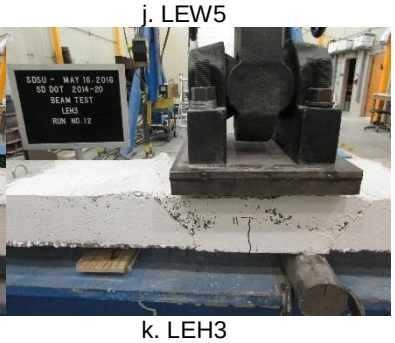

k. LEH3

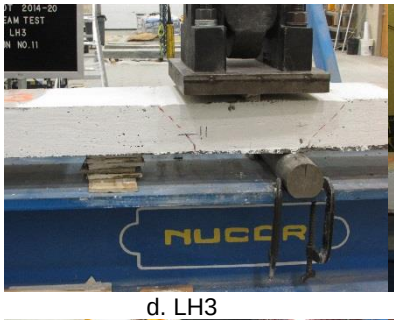

d. LH3

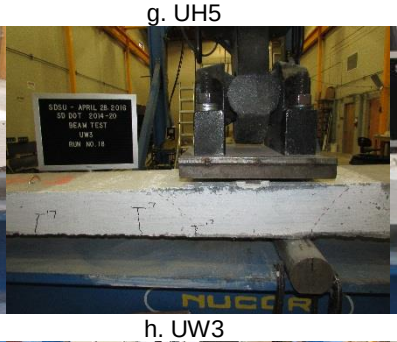

h. UW3

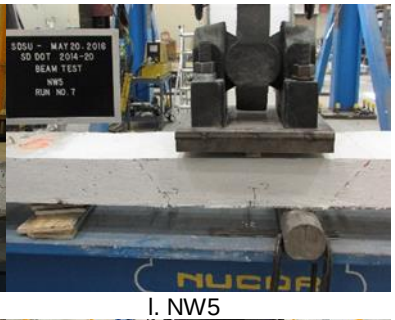

l. NW5

e. LH5

i. UH3

m. NW3

Figure 5-14. Photographs of Test Specimens at First Cracking

a. RCS

b. LW3

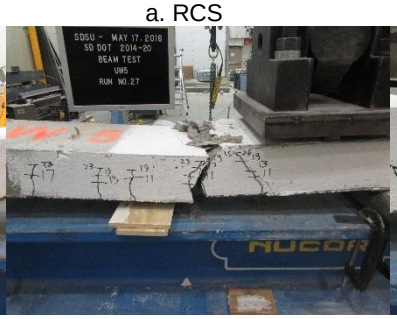

f. UW5

j. LEW5

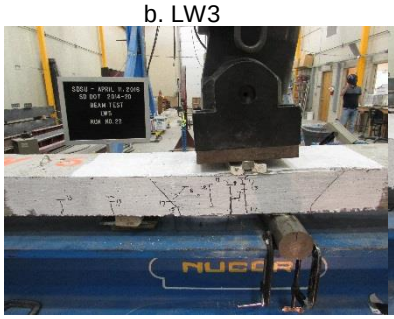

c. LW5

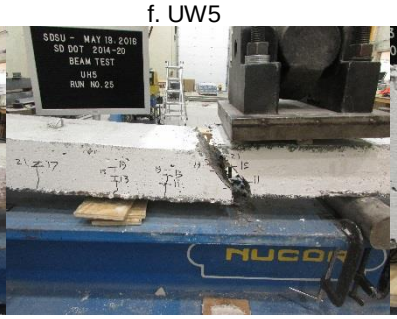

g. UH5

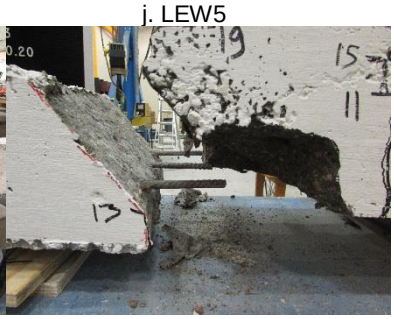

k. LEH3

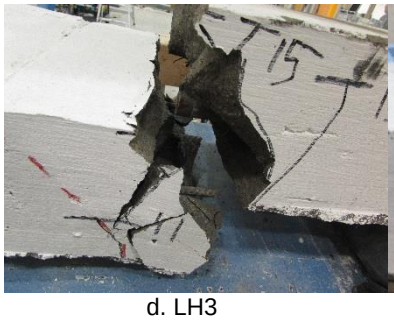

d. LH3

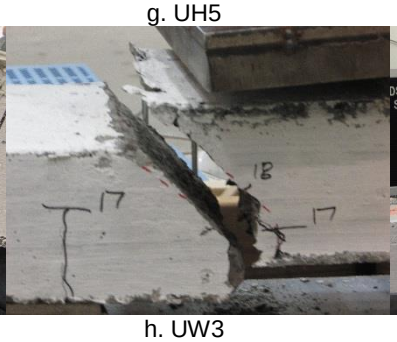

h. UW3

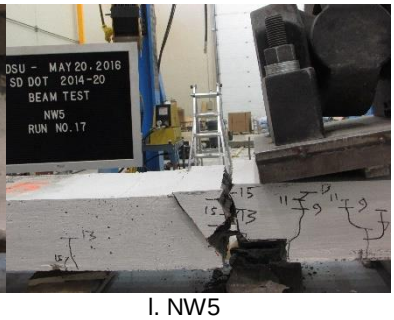

l. NW5

e. LH5

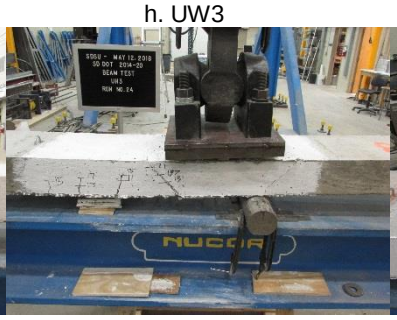

i. UH3

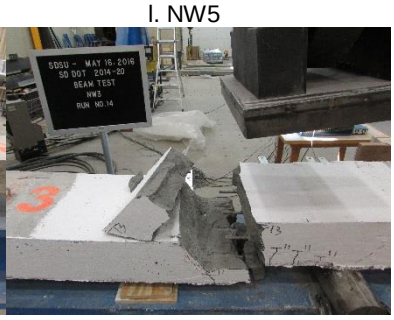

m. NW3

Figure 5-15. Photographs of Test Specimens at Failure

The bond between the UHPC and concrete was high resulting in monolithic behavior. Slippage between the two materials measured with LVDTs was insignificant. In UW5, the steel wire fractured outside the UHPC joint in the precast concrete. The steel wires fractured at the UHPC-concrete interface in other UHPC specimens (UW3). However, concrete aggregate was attached to the UHPC at the interface indicating sufficient bond.

5.3 Analytical Study

Performance of a full-scale precast double-tee bridge incorporating the proposed rehabilitation detailing was analytically investigated. The modeling method, model verification, analysis of parameters, loading, and a summary of the results are discussed herein.

5.3.1 Introduction

An analytical study was necessary to optimize the joint detailing with a capacity that exceeds demands under fatigue, service, and strength limit states. Rehabilitation of the double-tee girder longitudinal joints requires demolishing of existing concrete and filling the voids with new materials. It is obvious that joints with minimal concrete removal and minimal filler material will be more cost-effective. In an attempt to minimize the cost, the performance of two joint rehabilitation concepts were analytically investigated using linear finite element analyses:

Option I – "continuous" concept (Fig. 5-16a) in which the girder flange reinforcement will be exposed along the length of the girder using a demolishing technique to be spliced with a new welded wire mesh. The joint can be filled with either LMC or UHPC.

Option II – "pocket" concept (Fig. 5-16b) consisted of discrete pockets exposed by demolishing the girder flange concrete and reinforced with steel bars. In between the pockets the damaged material in the longitudinal joint is removed and replaced with a filler material such as UHPC.

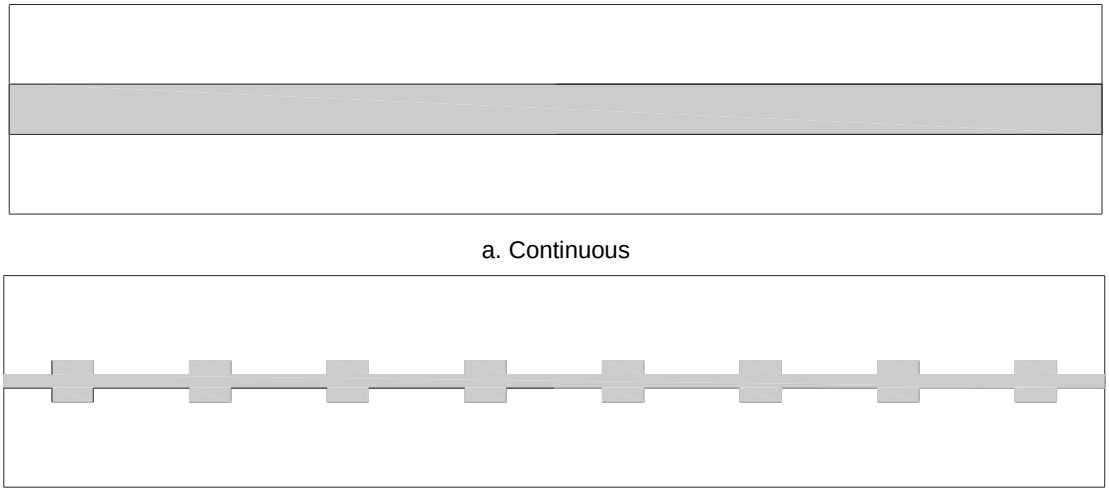

a. Continuous

b. Pocket

Figure 5-16. Rehabilitation Concepts - Bridge Plan View

5.3.2 Modeling Method

Linear finite element analyses (FEA) were performed on two adjacent 23-in. deep double-tee girders (Fig. 5-17a). The double-tee stems are 18-in. tall, 5-in. wide at the bottom tapered to 6.125 in. at the top. The double-tee deck is 5-in. thick and 46-in. wide.

SAP2000 ver. 18 (2016) was selected for the analytical study. The stems were modeled with frame elements. Pin supports were assigned to the end of each stem. The deck (the flange of the girders) was modeled using solid shell elements. The connection between the frame and shell elements was provided utilizing body constraints fixing all degrees of freedom (DOFs) between the two end nodes. The connection allows the deck and stems to act compositely. The section properties for each girder was according to the

actual double-tee section with an area of 426 in^2 and a moment of inertia of 18,640 in^4 about the strong axis. The compressive strength (f'_c) for the deck and stems were 6,000 psi based on the target 28-day compressive strength of the actual double-tee girder mix design. The concrete modulus of elasticity (E_c) was 4,415 ksi.

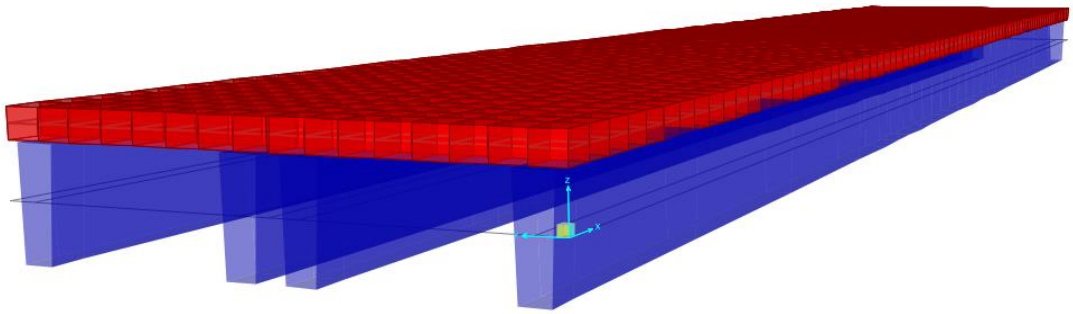

a. Extruded View of FEA Model – Continuous Joint

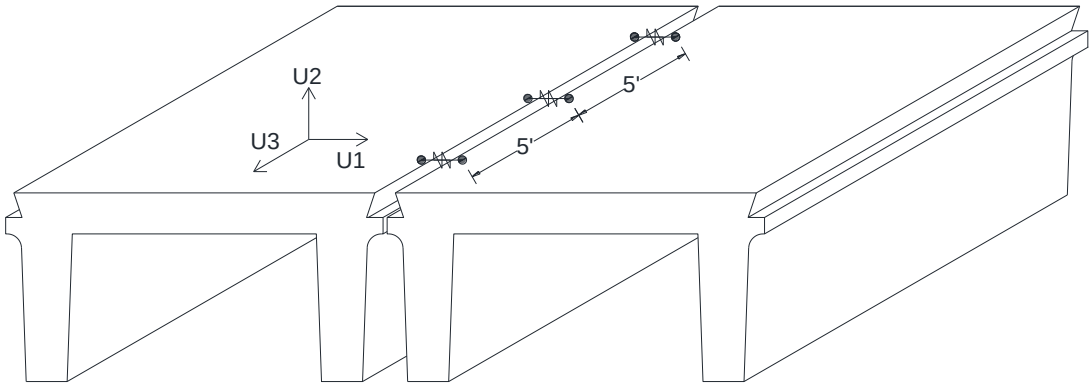

b. Illustration of Link locations and Local Axis

Figure 5-17. Finite Element Analysis (FEA) Model

Point loads were applied at the midspan of the bridge to produce the peak moment from moment envelopes calculated for an interior double-tee girder under the AASHTO Service I, Fatigue II, and Strength I limit states. The loads were applied on an area of 10 in. by 20 in. at the midspan adjacent to the longitudinal joint to maximize the shear load demand on the joint. The area load was to simulate a truck tire load.

In an attempt to evaluate the performance of the proposed rehabilitation detailing, two analytical models were created:

i. "Continuous" model (Fig 5-17a) in which the longitudinal joint of the girders was monolithically constructed with shell elements.

ii. "Pocket" model (Fig 5-17b) in which the girders were connected by a series of links spaced along the length of the longitudinal joint.

The "pocket" model was constructed using "link" elements consisting of linear springs in all six DOFs to connect the girders as shown in Fig. 5-17b. The spring properties (Table 5-6) were based on the properties of UHPC and reinforcement. UHPC was assumed to have a compressive strength (f'_{UHPC}) of 18 ksi, a modulus of elasticity (E_c) of 6,200 ksi, and Poisson's ratio of (v) of 0.2 (Graybeal, 2010). The axial stiffness (U_1) (Eq. 5-5), shear stiffness (U_2) (Eq. 5-6), and rotational stiffness (R_3) (Eq. 5-7) were calculated based on assumed properties of E_s = 29,000 ksi and A_s = 0.8 in^2 for steel bars; A_c = 90 in^2 and I = 187.5 in^3 for filler material; and a spring length of L = 4.25 in. Shear stiffness (U_3), rotational stiffness (R_1), and (R_2) were considered rigid.

$$U_1 = \frac{AE}{L} \qquad \text{Eq. 5-5}$$

$$U_2 = \frac{GA}{L} \qquad \text{Eq. 5-6}$$

$$R_3 = \frac{EI}{L} \qquad \text{Eq. 5-7}$$

Table 5-6. Input for Pocket Springs

Link Properties	Values
Axial Stiffness (U_1)	92,800 kip/in
Shear Stiffness (U_2)	54,700 kip/in
Shear Stiffness (U_3)	Fixed
Rotational Stiffness (R_1)	Fixed
Rotational Stiffness (R_2)	Fixed
Rotational Stiffness (R_3)	273,500 kip-in/rad

5.3.3 Model Verification

The accuracy of the proposed continuous model was verified by comparing the response against that calculated from structural theory (Eq. 5-8 and 5-9). The calculated deflection of two 40-ft long girders using Eq. 5-8 with a 25-kip point load at the midspan was 0.7 in. The calculated bending stress in the deck using Eq. 5-9 was 1.22 ksi.

$$\Delta = \frac{PL}{48EI} \qquad \text{Eq. 5-8}$$

$$\sigma = \frac{My}{I} \qquad \text{Eq. 5-9}$$

Two mesh sizes of 3 in. by 3 in. and 6 in. by 6 in. were used in shell elements to construct the deck. It was found that the fine mesh did not significantly improve the accuracy of the results, thus the course mesh was used in further analysis. Body constraints were spaced every 1 or 2 ft along the length of the girder to compositely connect the girder stems and deck. The effect of this parameter was found to be insignificant. The midspan deflection of the final "continuous" model was 0.67 in. and the deck bending stress (S_{11}) was 1.21 ksi. The differences between the FEA model and the hand calculation were less than 5 and 1% for the girder deflection and the deck bending stress (S_{11}), respectively. Therefore, the proposed modeling method for continuous model was valid.

5.3.4 Parametric Study

5.3.4.1 Parameters

A parametric study was conducted to determine the minimum pocket spacing for the rehabilitation of longitudinal joints in double-tee girder bridges. The goal was to determine a pocket spacing by which the rehabilitated bridge response was the same as that of a cast-in-place monolithic bridge.

The models were constructed with different link spacing of 5, 8, and 13 ft to compare relative deck deflections and support reactions with those of cast-in-place double-tee bridges. Furthermore, the bridge length was varied from 30 to 50 ft to investigate the force transfer mechanism and to optimize the pocket spacing for a wide range of spans.

5.3.4.2 Applied Girder Loads

The loads applied to the bridge in the parametric study was based on AASHTO Article 3.4.1 “Load Factors and Load Combinations.”

- 3.6.1.2.2 Design Truck (HL-93) – (Fig. 5-18).
- 3.6.1.2.3 Design Tandem – pair of 25-kip axles spaced 4.0 ft apart.
- 3.6.1.2.4 Lane load – 0.64 klf uniformly distributed load.

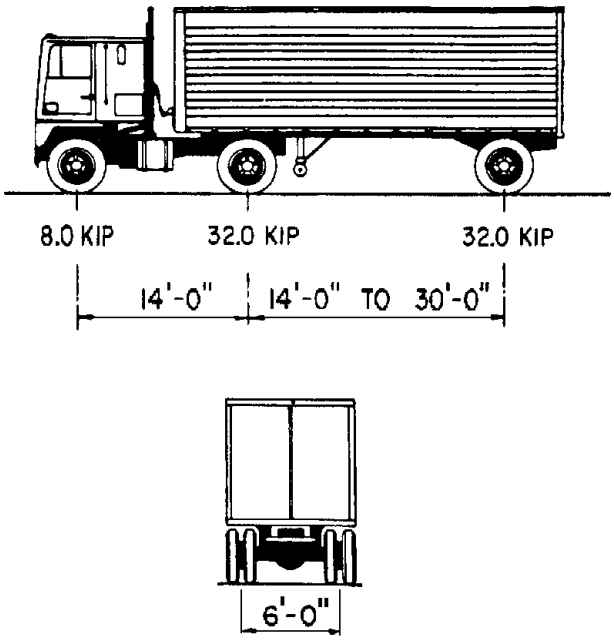

Figure 5-18. HL-93 Design Truck

The dynamic load allowance (*IM*) for the bridge system was 33% for the Service I limit state, 15% for the Fatigue II limit state, and 75% for the Strength I limit state based on AASHTO Article 3.6.2.1. The dynamic load factor was determined by Eq. 5-10.

$$Load\ Factor = 1 + \frac{IM}{100} \qquad \text{Eq. 5-10}$$

The girder distribution factor was 0.35 using AASHTO Table 4.6.2.2.2b-1. Appendix A presents the detail of calculations. Three limit states were selected as:

- Service I: (1.0) DC + (1.33) Truck Load + (1.0) Lane Load
- Fatigue II: (0.863) Truck Load
- Strength I: (1.25) DC + (3.063) Truck Load + (1.75) Lane Load

The moment demand based on the moment envelope for HL-93 as well as tandem under the Service I, Fatigue II, and Strength I limit states was 728, 298, and 1,606 kip-ft,

respectively. The Fatigue II limit state for HL-93 was calculated with 30-ft axle spacing. The Strength I limit state moment envelope was used for connection design.

Equivalent point loads (*P*) were applied at the midspan of the bridge to produce a bending moment equivalent to the peak moment demands at different limit states. The equivalent point loads were determined using Eq. 5-11.

$$P = \frac{4(M)(GDF)(N_g)}{L} \qquad \text{Eq. 5-11}$$

where:

P is the point load (kips),

M is the peak moment demand from the moment envelope (kip-ft),

GDF is the girder distribution factor,

N_g is number of girders.

In summary, the calculated point load for different AASHTO limit states were:

- Service I – 51 kips
- Fatigue II – 21 kips
- Strength I – 112 kips

All three equivalent point loads were applied at the mid-span of the bridge to determine adequate pocket spacing to meet AASHTO limit state requirements. Note the aforementioned Strength I load is for the design of the connections (e.g. pocket connection) not the girder design.

5.3.4.3 Results of Parametric Study

This section includes a summary of the findings of the parametric study on the effect of the pocket spacing and the bridge span length on joint load transfer mechanism and overall behavior of the rehabilitated bridge.

The performance of two adjacent double-tee girders connected with pocket detailing (Fig. 5-16b) was evaluated by comparing the amount of load being transferred to stems of each girder as shown in Figure 5-19. Three different pocket (link) spacing of 5, 8, and 13 ft were included in the analysis, and the response was compared to that of a monolithic (continuous) bridge model. It can be seen that the difference between the stem forces for the monolithic and pocket models increases when the pocket spacing increases. For example, the end reactions of stem A and D of the pocket model with 13-ft link spacing were respectively 7 and 6% higher than those in the model with 5-ft pocket spacing. For stem B, there difference was 11%.

The stem force differences in the monolithic model and the model with 5-ft pocket spacing were within 10% for all stems. Therefore, it can be concluded that the pocket spacing of 5 ft results in a monolithic behavior for a double-tee bridge rehabilitated with the pocket option. This pocket spacing was selected for further analysis.

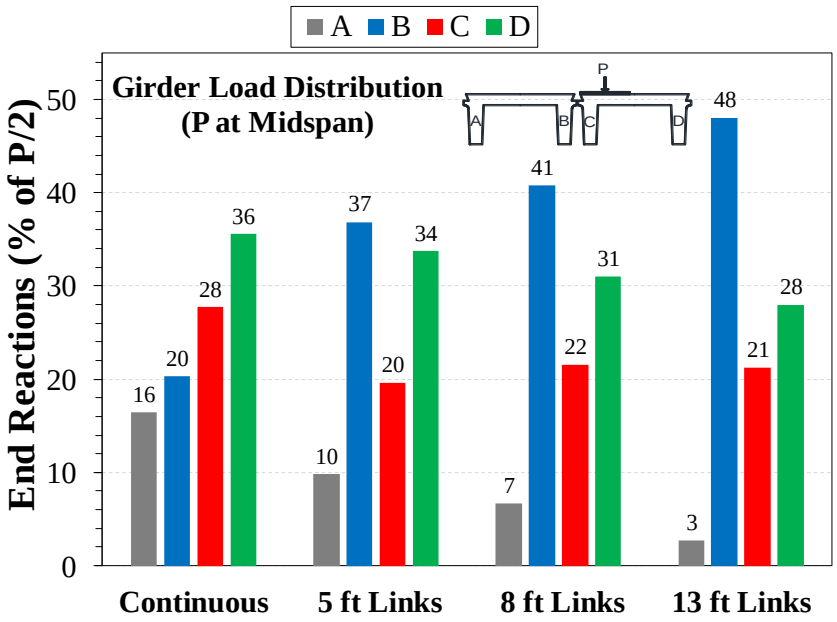

Figure 5-19. Effect of Pocket Spacing on Double-Tee Girder Load Distribution

In an attempt to better comment on the suitability of a rehabilitated bridge with 5-ft pocket spacing, the calculated stem forces of the rehabilitated bridge were compared with those measured in previous experimental studies (Fig. 5-20). Two full-scale double-tee bridge models were tested by Konrad (2014), one specimen with continuous joint detailing (which behaved as a monolithic bridge) and one specimen with welded plate detailing (conventional double-tee bridge detailing that is currently used in practice). It can be seen that the girder stem end reactions for the analytical continuous model were close to those measured in the test with only 5% difference in all stems except in stem A in which the difference was 11%. Furthermore, the pocket model performed better compared to the original double-tee specimen with welded plates in terms of the load transfer mechanism.

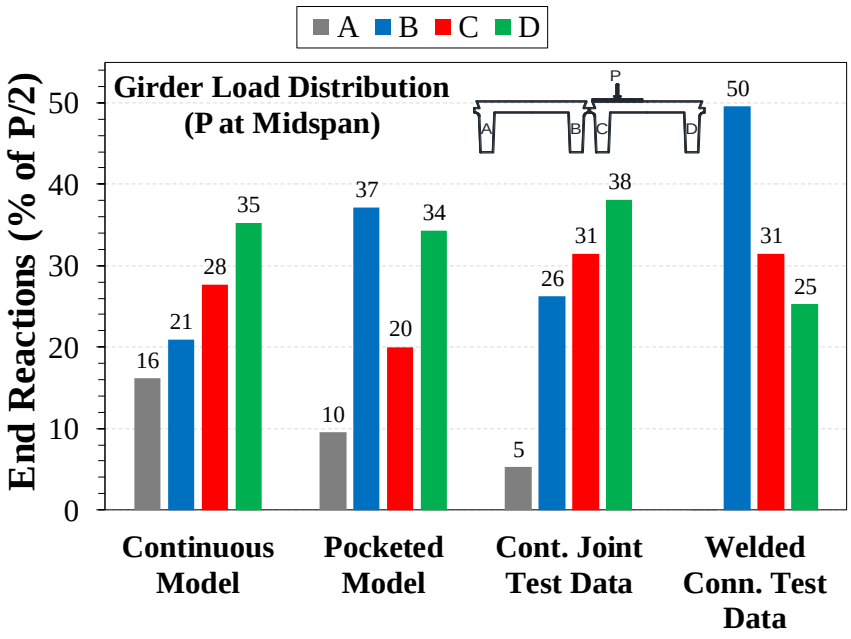

Figure 5-20. Calculated and Measured Double-Tee Girder Load Distribution

In South Dakota, double-tee bridges with span lengths other than 40 ft may be in-service. In an attempt to investigate the feasibility of the "pocket" detailing on bridges with different span lengths, "pocket" models with span lengths of 30 to 50 ft were studied using the stem load distribution (Fig. 5-21). It can be seen that the stem loads slightly increase (e.g. 2% in stem A) from 40 ft span to 50 ft span and slightly decrease (e.g. 5% in stem A) from 40 ft span to 30 ft span. Overall, the effect of the span length on the stem loads was 5% or less for all stems.

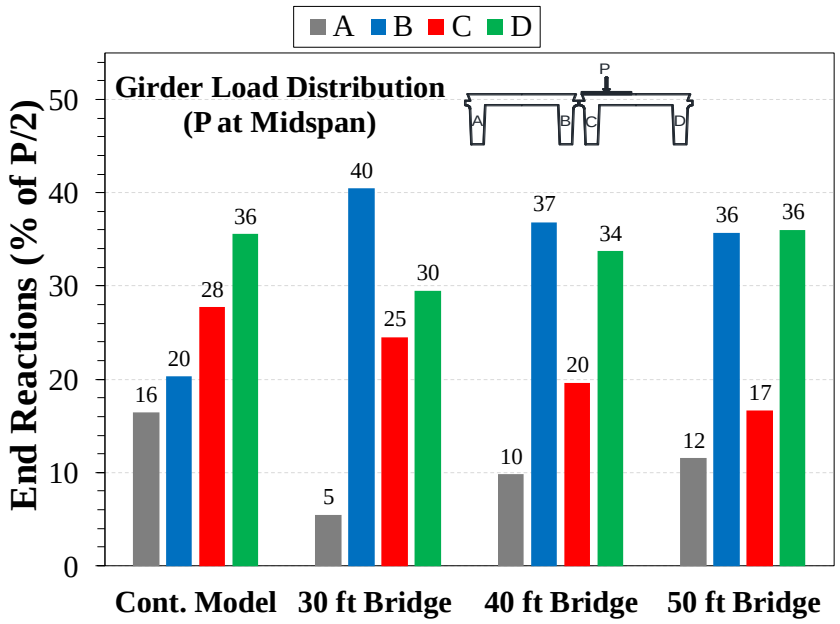

Figure 5-21. Rehabilitated Double-Tee Girder Load Distribution vs. Span Length

The effect of pocket spacing on the deflection of the rehabilitated double-tee bridges was also investigated. The parametric study showed that the differential deck deflection between the two-adjacent double-tee girders is maximum at the midspan of the bridge. The calculated girder differential deflections for the rehabilitated double-tee bridges with 5, 8, and 13-ft pocket spacing were respectively 0.02, 0.03, and 0.05 in. under service limit state loading. Therefore, the rehabilitated bridge model with 5-ft pocket spacing exhibits the minimal differential deck deflection.

Overall, the finite element analysis showed that "pocket" rehabilitation detailing is a viable solution specifically when the pocket spacing is 5 ft. Furthermore, the continuous detailing is another viable solution for the rehabilitation of double-tee longitudinal joints.

5.4 Design of Joint Rehabilitation Alternatives

The design forces of the pocket and the continuous joint rehabilitation alternatives can be found using the aforementioned finite element modeling methods.

5.4.1 Design of Pocket Joint Alternative

The design of the pocket connection can be based on the Strength I limit state demands. The pocket maximum shear and moment demands for a 40-ft bridge with 5-ft pocket spacing are 24.4 kips and 160 kip-in, respectively. The moment capacity of a 5-in thick pocket is 178 kip-in at the section with new reinforcement assuming four No. 4 bars with a yield strength of 60 ksi are used in the pocket. The shear capacity of the pocket can be determined based on the AASHTO shear friction equation. The friction and cohesion factors for roughened surface condition are 1.0 and 0.24 ksi, respectively. The pocket shear capacity is 36.7 kips for a 5-in. thick and 18-in. wide pocket at a section with exposed double-tee deck reinforcement (D8 steel wire with A_s = 0.24 in^2 per ft). The shear capacity of the pocket section with new reinforcement will be higher since the total bar area will be higher. The required minimum splice length for a Grade 60 No. 4 bar and exposed D8 reinforcement shall be 3 in. based on the findings of the beam tests (section 5.2) if UHPC is used as the pocket filler material.

Note, the intermediate continuous joint between the pockets (Fig. 5-16b) was neglected in the analytical models. If UHPC is used in the pocket joint rehabilitation alternative, it can be assumed that the joint remains monolithic under the Service I limit state based on the superior bond strength between UHPC and precast concrete. The slant shear bond strength between UHPC and roughened precast concrete is 2,200 psi (Swenty and Graybeal, 2013). The direct tensile bond strength between UHPC and concrete is approximately 300 psi (Li and Rangaraja, 2016).

The shear stress contour of a 40-ft long double-tee bridge rehabilitated with “pocket” model at the Service I limit state is shown in Figure 5-22. It can be seen that the

maximum shear stress is 210 psi for an 18-in. wide pocket (or 630 psi for a 6-in. wide pocket). Since this shear stress is less than the bond strength between UHPC and concrete, no cracking is expected under the service limit state loads. Furthermore, the maximum shear stress at the Strength I limit state is 533 psi for an 18-in. wide pocket (or 1,400 psi for a 6-in. wide pocket).

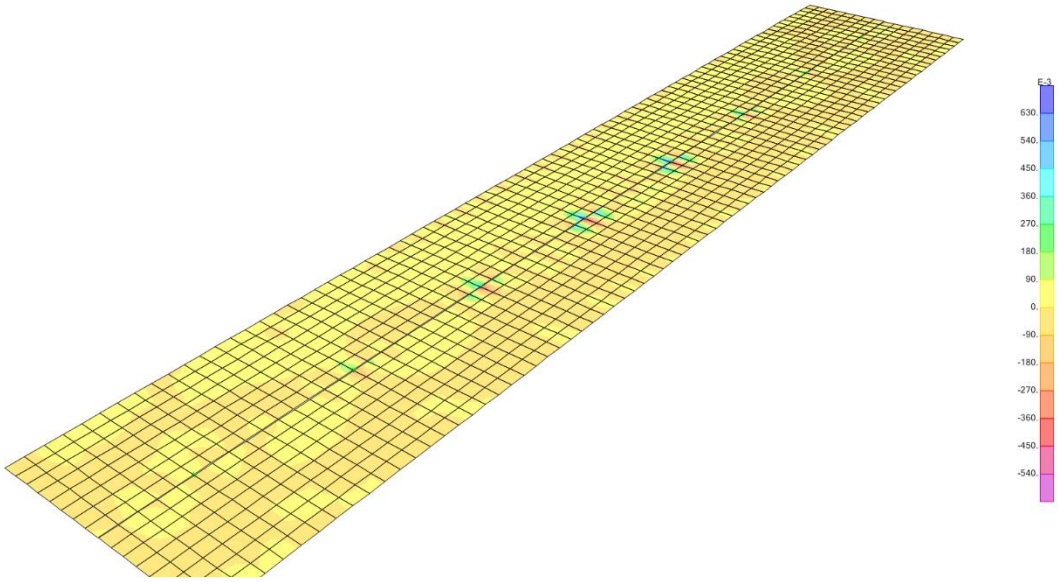

Figure 5-22 "Pocket" Model S_{23} Stress contour at Service I Limit State

5.4.2 Design of Continuous Joint Alternative

Either LMC or UHPC can be incorporated in the continuous joint rehabilitation alternative. Based on the findings of the beam tests, wire mesh is the best reinforcement type for this joint detailing. It is recommended to use 4 in. by 4 in. D8/D8 welded wire mesh (A_s = 0.24 in^2/ft) as the joint reinforcement to provide higher amount of steel compared to the deck existing reinforcement (which was 4 in. by 8 in. D8/D4 welded wire mesh). The minimum required lap-splice for the wire mesh shall be 5 in. according to the beam test data assuming LMC is used as filler material.

The maximum calculated shear stress in the connection of the "continuous" analytical model was 160 psi at the Service I limit state (Fig. 5-23) and 360 psi at the Strength I limit state. The continuous joint shear capacity is 408 psi (13% greater than the demand) based on the AASHTO shear friction equation for a 5-in. thick LMC continuously reinforced with D8 steel wire mesh (A_s = 0.24 in^2 per ft).

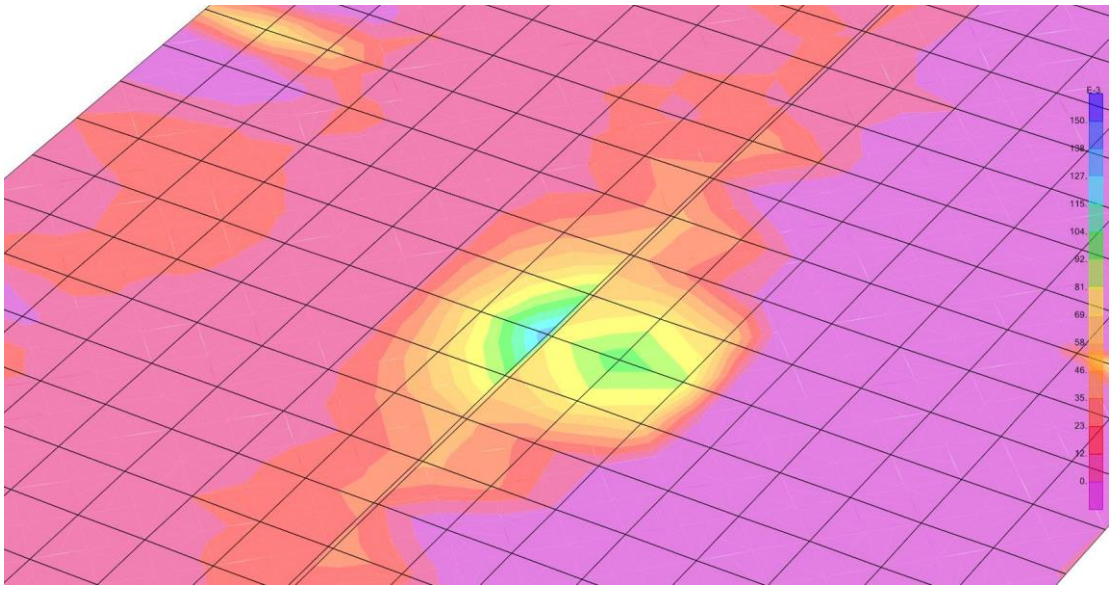

Figure 5-23. "Continuous" Model S_{23} Stress Contour at Service I Limit State

5.5 Proposed Rehabilitation Methods for Full-Scale Bridge Testing

This section includes the proposed rehabilitation methods for a full-scale prefabricated prestressed double-tee bridge test model. The proposed joint rehabilitation details, special requirements for demolition and construction, and cost estimates are discussed herein.

Based on the results of the parametric study, both the "pocket" and "continuous" concept are feasible for the rehabilitation of the double-tee bridges. The "pocket"

concept offers several advantages such as 50% reduction in material, significantly lower cost, and better bridge stability during construction.

To investigate the performance of bridges rehabilitated with the proposed detailing, testing of a full-scale bridge test specimen consisting of two simple span interior prefabricated prestressed double-tee girders was proposed. Each girder was 23-in. deep, 3.83-ft wide, and 40-ft long.

In an attempt to evaluate the performance of the both joint rehabilitation alternatives using only one test specimen, half of the test bridge was proposed to be rehabilitated with the "pocket" detailing utilizing UHPC and the other half of the bridge to be rehabilitated with the "continuous" detailing incorporating LMC (Fig. 5.24). Hammer-chipping demolition technique was selected for concrete removal. The proposed rehabilitation detailing for the bridge test model is summarized as follows:

Option I – "pocket" detailing

- Prepare 18 in. by 18 in. pockets to be filled with UHPC. The pocket spacing should not exceed 5 ft (Fig. 5-24) center-to-center.
- Pockets should be reinforced with four ASTM A706/A615 Grade 60 No. 4 bars in both longitudinal and transverse directions (Fig. 5-25).
- A minimum of 3-in. lap-splice between the pocket reinforcement and the deck existing wires is required to ensure full development (Fig. 5-25).
- A 5.875-in. continuous shear key filled with UHPC and longitudinally reinforced with two No. 4 bars should be provided (Fig. 5-26).

Option II – "continuous" detailing

- Prepare a 22-in. wide continuous opening to be filled with LMC (Fig. 5-24).

- Continuous joint should be reinforced with ASTM A497 Grade 70, 4 in. by 4 in. D8/D8 welded wire mesh (Fig. 5-27).
- A minimum of 5-in. lap-splice between the new and existing reinforcement should be provided to fully development the wires (Fig. 5-27).
- If wire mesh is not continuous over the length of the bridge, the mesh should be spliced as shown in Fig. 5-28.

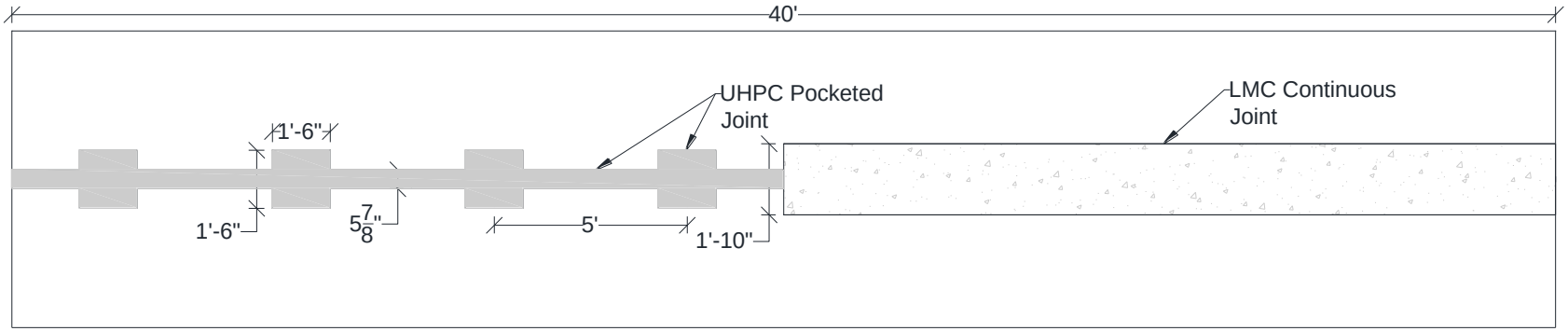

Figure 5-24. Proposed Rehabilation Plan Drawing

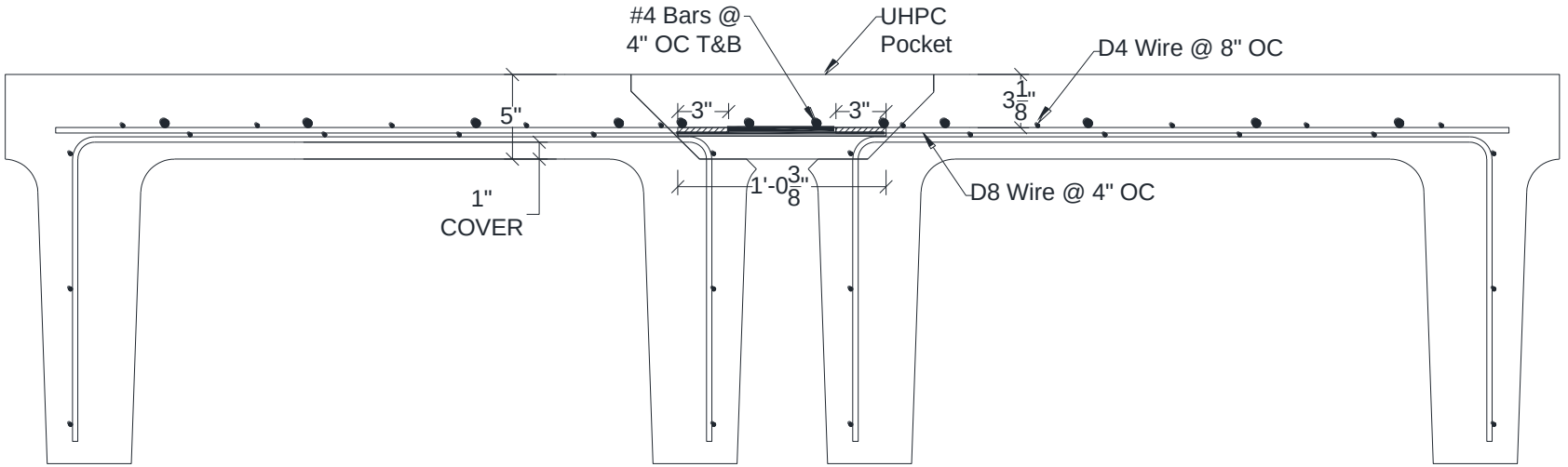

Figure 5-25. Proposed UHPC Pocket Detail

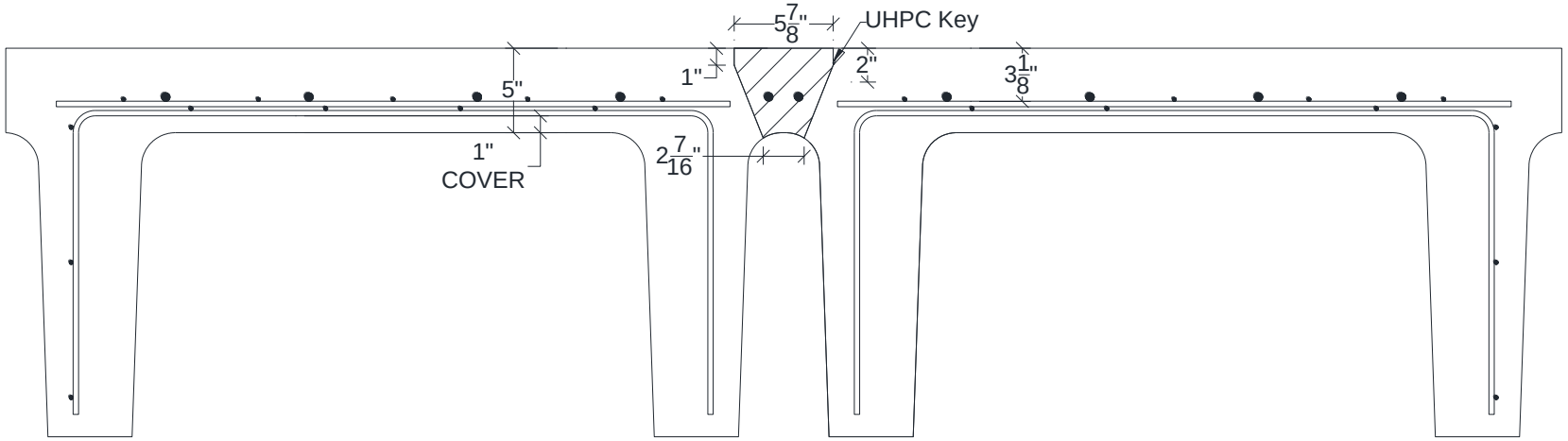

Figure 5-26. Proposed UHPC Intermediate Pocket Detail

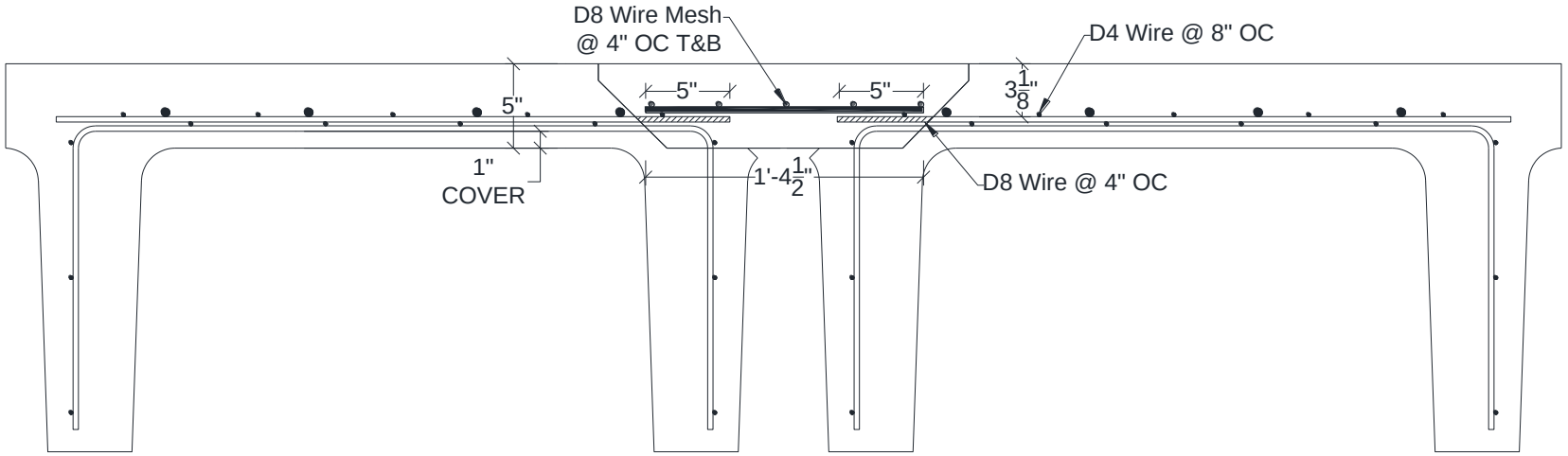

Figure 5-27. Proposed LMC Continuous Joint Detail

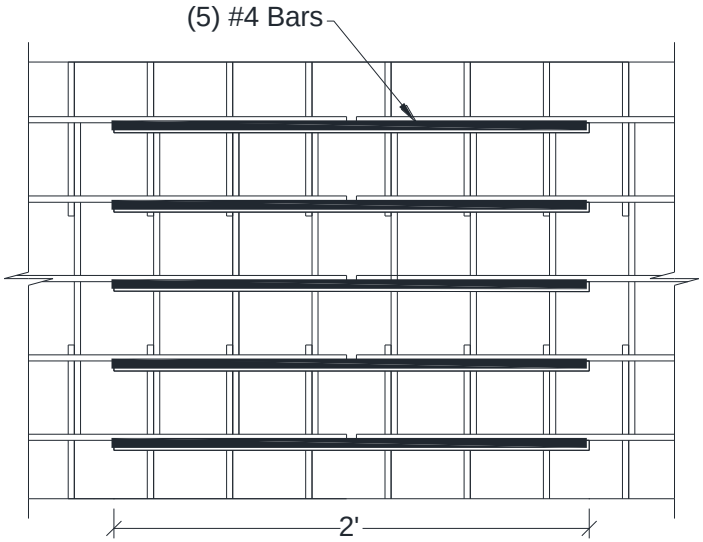

Figure 5-28. Proposed Continuous Joint Splice Detail

5.5.1 Special Requirements for Demolition and Construction

Special requirements for demolition and construction methods are necessary to successfully rehabilitate the longitudinal joints of double-tee bridge girders. These requirements can improve the overall durability and stability of the rehabilitated bridge. The special requirements for demolition and construction for the bridge test model are summarized as follows:

- A maximum one-in. saw-cut shall be used around the perimeter of the joint.
- Hammer-chipping can be used as the demolishing method if:
    - The pockets are chipped with a minimum of 45° inclination.
    - The intermediate pocket joint is chipped with a minimum of 20° inclination.
    - The continuous joint is chipped with a minimum of 45° inclination.
- 30-lb and 15-lb pneumatic hammer chippers are permitted.
    - 30-lb hammer chippers shall only be used to break up the top layer of existing concrete.
    - Only 15-lb hammer chippers shall be used when finishing and chipping around the reinforcement.
- Hydro-demolition may be used in lieu of hammer chipping.
- Demolition and construction for each longitudinal joint of the bridge using the "continuous" detailing shall be facilitated using segmental construction with quarter-span increments. In other words, the joint shall not be rehabilitated along the length of the bridge all at once.

- The joint surface shall be sand blasted and pre-wetted with burlap for at least 24 hours prior to pouring filler material.
- Formwork shall be used to prevent falling debris.

6. Full-Scale Double-Tee Bridge Test Specimens

A full-scale double-tee bridge was constructed using conventional detailing then tested under fatigue loading to crack the longitudinal girder-to-girder joint. Subsequently, the bridge was rehabilitated according to the two proposed detailing presented in Chapter 5. The rehabilitated specimen was then tested under fatigue and strength loading to evaluate the performance of the bridge and to comment on the suitability of the proposed joint rehabilitation alternatives. This chapter presents design, fabrication, test setup, instrumentation, and test procedure for both the conventional and the rehabilitated test specimens.

6.1 Design of Bridge Test Specimen

Many of the double-tee bridges located on local roads in South Dakota consist of eight girders providing two lanes of traffic with a total width of 30 ft-8 in. (Fig. 6-1). A 40-ft long full-scale bridge with only two interior girders (shaded area in Fig. 6-1) was selected for testing in the present study. The 40-ft span length is common for this particular section. Furthermore, two double-tee bridges with the same lengths were tested by Wehbe et al. (2016).

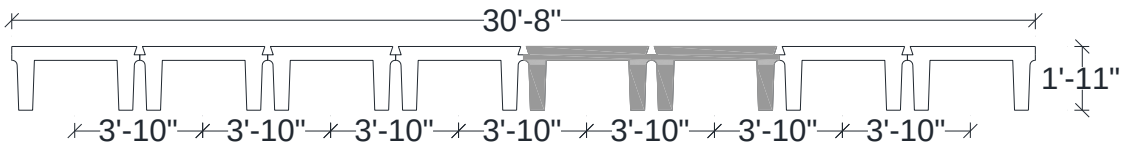

Figure 6-1. Cross-Section of Typical Double-Tee Girder Bridges

The bridge was designed according to the AASHTO LRFD Bridge Design Specifications (2013) with live loading consisting of a truck or tandem and a lane load. The design live load was based on an HL-93 truck (two 32-kip axles and one 8-kip front axle spaced 14 to 30 ft apart) or two 25-kip tandem axles 4-ft apart as well as a 10-ft wide 0.64 klf distributed lane load.

The design led to a double-tee girder (Fig. 6-2) with a depth of 23 in., a width of 46 in., and a length of 40 ft. The deck was 5-in. thick reinforced with a 4 in. by 8 in. ASTM A-497 D8/D4 welded wire mesh. D8 wires provided 0.24 in^2 per foot steel reinforcement in the transverse direction of the bridge. Each stem was 5-in. thick at the bottom tapered to 6.25 in. at the top, and was reinforced with six 0.5-in. diameter ASTM-416 Grade 270 low relaxation 7-wire strands. The tendons were straight over the length of the girder (Fig. 6-2b). Each tendon was blanketed (debonded) 5 ft from each girder end and was initially pulled 10.75 in. equivalent to 202.6-ksi stress (or 31-kip force) per tendon. The girder shop drawings are provided in Appendix B.

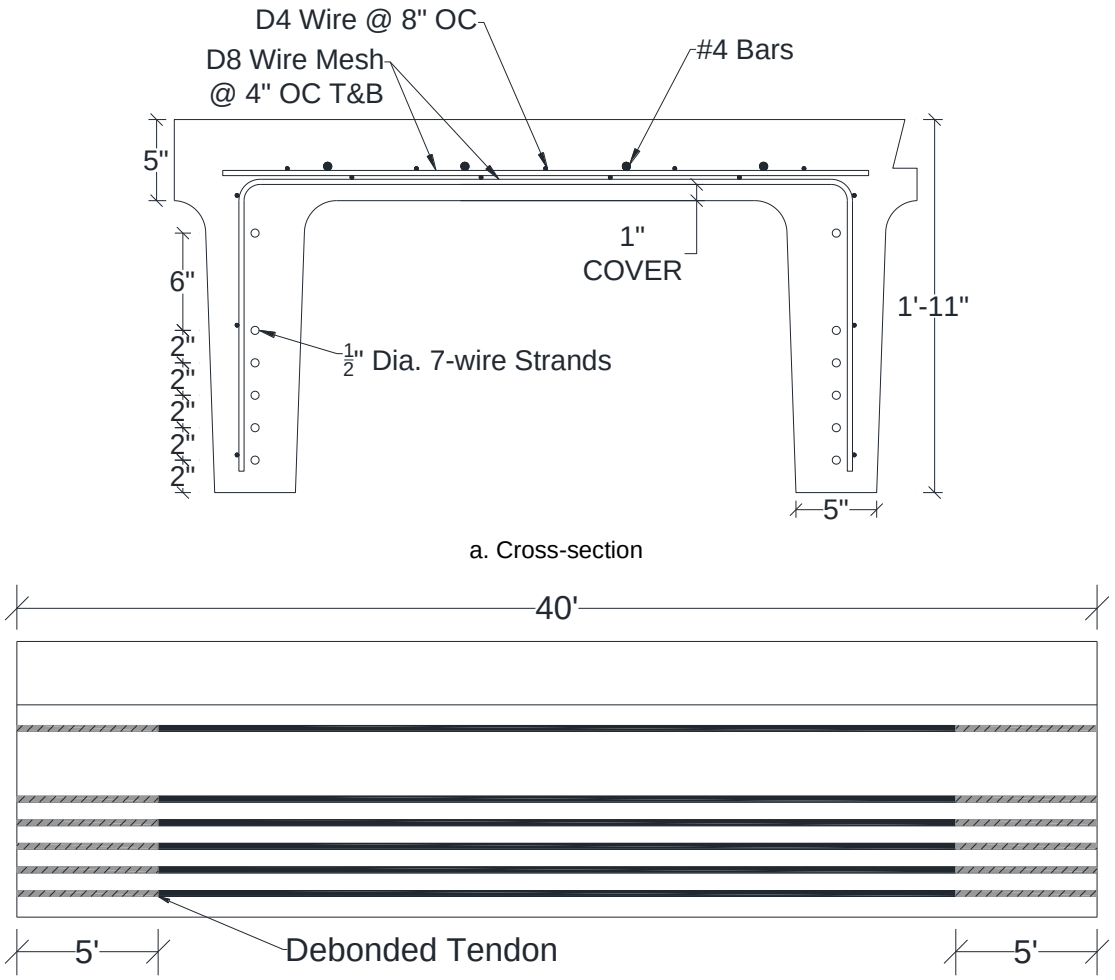

a. Cross-section

b. Tendon Profile in Girder Elevation View

Figure 6-2. Detailing of a 23-in. Double-Tee Section

6.1.1 Conventional Test Specimen

The longitudinal joint of the conventional specimen (Fig. 6-3) consisted of discrete welded plates spaced at 5 ft with a continuous grouted keyway. The welded plate detailing (Fig. 6-4) consisted of two 1.25 in. by 1.25 in. by 3/16 in. (L 1 ¼ - 1 ¼ - 3/16 in.) angles each 6-in. long embedded in the concrete with two 3/8-in. diameter 4-in. long headed studs. The angles of the two adjacent girders were connected using 1/4 in. by 1 in. by 5 in. steel plates with 3/8-in. field weld. A non-metallic non-shrink grout preapproved by South Dakota Department of Transportation with a minimum compressive strength of 4,500 psi (SDDOT Standard Specification for Roads and Bridges, 2004) was used to fill the keyway.

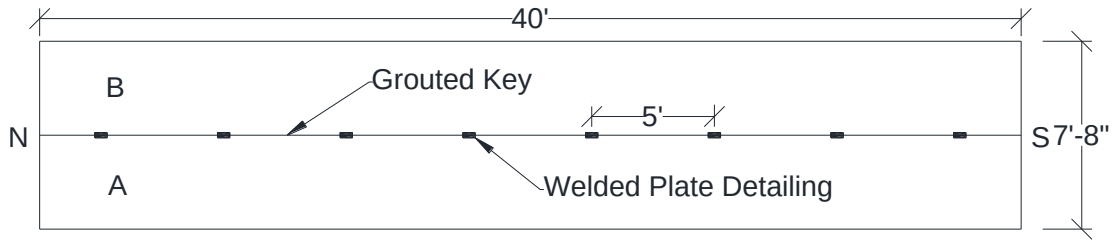

Figure 6-3. Plan View of Conventional Test Specimen

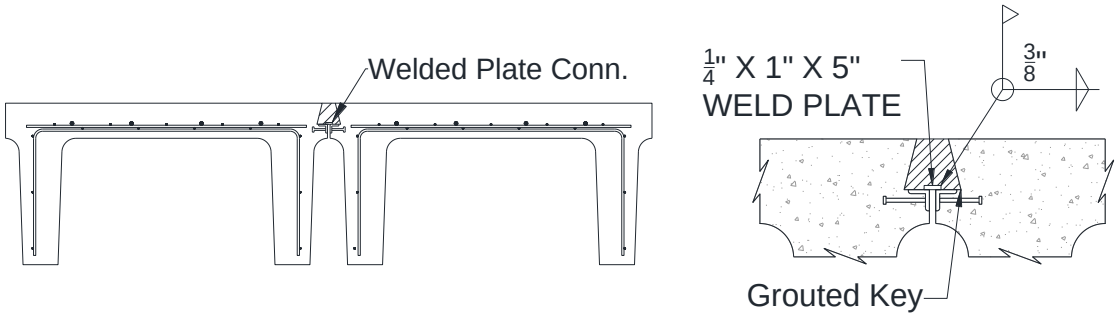

a. Cross-Section with Welded Plate Connection b. Welded Plate Detailing

Figure 6-4. Conventional Test Specimen Details

6.1.2 Rehabilitated Test Specimen

After testing the conventional bridge specimen, the longitudinal girder-to-girder joint was rehabilitated with two different methods (Fig. 6-5): Ultra-high performance concrete (UHPC) pocket detailing (Fig. 6-6 and 6-7), and latex modified concrete (LMC) continuous detailing (Fig. 6-8).

The UHPC pockets were 5-in. deep (the same as the deck thickness), 18-in. wide, and 18-in. long reinforced with a mesh of four No. 4 bars in each direction of the bridge. The pocket spacing was 5 ft, and the pocket side slope was 45 degree. The new steel bars were lapped three inches with the exposed deck D8 wires. This splice length is sufficient to fracture the new reinforcement based on the beam test data presented in Chapter 5. The intermediate UHPC keyway (between the pockets) was 5-in. deep and 5.87-in. wide with a side slope of 20 degree. The UHPC keyway was longitudinally reinforced with two No. 4 continuous bars to improve the integrity of the joint.

The LMC continuous joint was 5-in. deep and 22-in. wide reinforced with 4 in. by 4-in., D8/D8 welded wire mesh. The new wire mesh was spliced to the deck existing wire mesh with at least 5-in. splice length in the transverse direction of the bridge. Furthermore, two 10-ft long meshes were lap-spliced with No. 4 bars in the longitudinal direction of the bridge to complete the joint and to provide continuity.

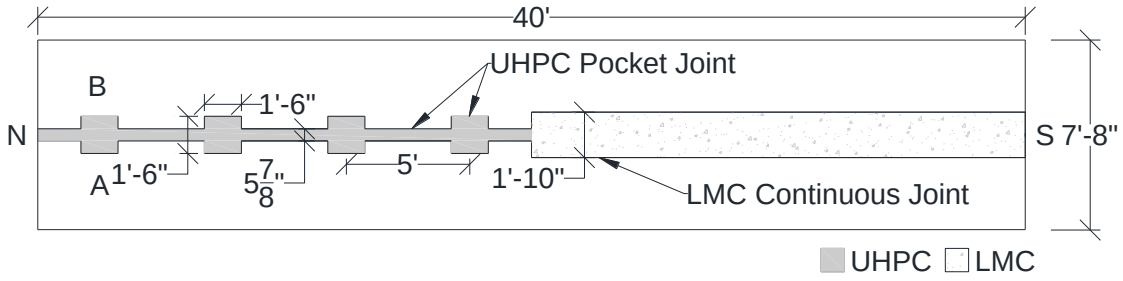

Figure 6-5. Plan View of Rehabilitated Test Specimen

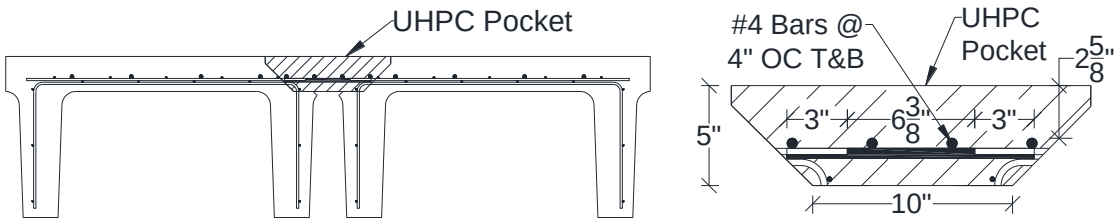

a. Cross-Section with UHPC Pocket b. UHPC Pocket Detailing

Figure 6-6. UHPC Pocket Rehabilitation Detailing

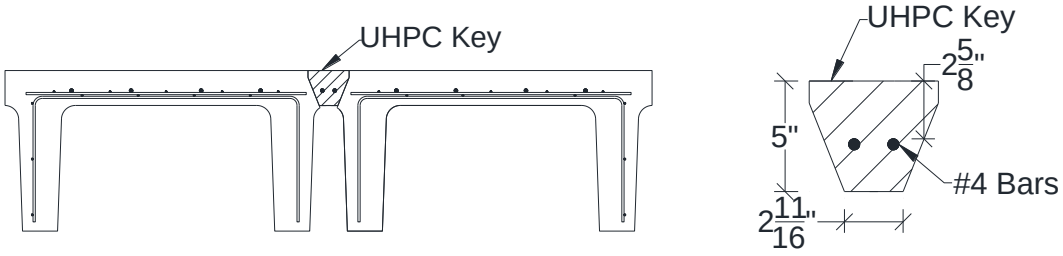

a. Cross-Section with UHPC Key b. UHPC Key Detailing

Figure 6-7. UHPC Intermediate Pocket Rehabilitation Detailing

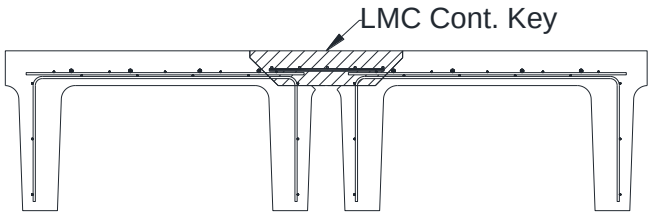

a. Cross-Section with LMC Continuous Key

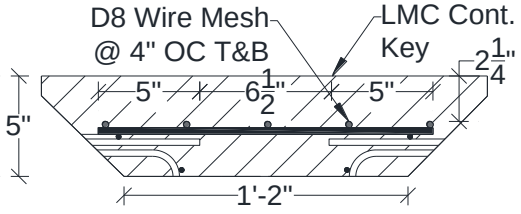

b. LMC Continuous Detailing

Figure 6-8. LMC Continuous Rehabilitation Detailing

6.2 Fabrication and Assembly of Test Specimen

The girders were fabricated in Mitchell, South Dakota. The girders were prepared and cast in four days on a 140-ft long prestressing bed (Fig. 6-9a). On day one, the prestressing strands were initially tensioned to 3,000 lbs to remove slack in the tendons,

and strain gauges were installed on the tendons. On day two, the strands were jacked to 31 kips then wire mesh and longitudinal joint anchors were placed in the prestressing bed. On day three, the embedded concrete strain gauges were installed in the deck between wires in the mesh. Subsequently, the girders were casted (Fig. 6-9b). Fresh concrete properties (e.g. slump, air, density, and temperature) were measured and 18 standard cylinders were collected. The girders were covered and steam cured overnight. On day four, the concrete strength was 5,680 psi, which was higher than the minimum release strength of 5,000 psi. Subsequently, the strands were cut with a torch (Fig. 6-9c) and the girders removed from the prestressing bed (Fig. 6-9d). Strain data was measured during various stages of the construction to measure elastic shortening losses.

a. Prestressing Bed

b. Concrete Casting

c. Cross-section with Torched Stands

d. Removal from Formwork

Figure 6-9. Fabrication of Double-Tee Girders

The test girders were stored in the manufacturer yard for six months then delivered to the Lohr Structures Laboratory at South Dakota State University (SDSU) with a semi-truck trailer. The girders were unloaded using a 15-ton overhead crane (Fig. 6-10a) then were placed on reaction blocks (Fig. 6-10b)

a. Unloading b. Placement on Abutment

Figure 6-10. Unloading and Placement of Girders

The girders were surveyed to measure cambers. The camber of girder A and B was 0.85 and 0.6 in., respectively with a 0.25-in. differential camber.

6.2.1 Conventional Bridge Joint Completion

The girder steel angles and steel plates were welded in the lab (Fig. 6-11a) by a certified welder to connect the adjacent girders. Subsequently, the keyway was filled with non-shrink grout (Fig. 6-11b) to complete the joint. The grout was cured three days in which the compressive strength reached 5,853 psi.

a. Welded Plate b. Grouting

Figure 6-11. Fabrication and Grouting of Conventional Joint Detailing

6.2.2 Rehabilitated Bridge Joint Completion

Since double-tee bridges are common in rural areas, simple and locally available techniques were sought for the rehabilitation. Saw-cutting and hammer-chipping were then selected in the present study to rehabilitate the joint.

The continuous joint was demolished and cast in two segments to avoid instability of the bridge. Each segment was 25% of the bridge length. An actual double-tee girder with continuous exposed bars at the both sides of the girder may become unstable in the field. The rehabilitation began with saw-cutting (Fig. 6-12a) the perimeters of the joint with a depth of 1 in. Then, 15- and 30-lb pneumatic hammer chippers (Fig. 6-12b) were utilized to remove the deck concrete with a 45-degree side slope for both the continuous (Fig. 6-12c and 6-12d) and pocket joints (Fig. 6-12e).

a. Saw-cutting

b. Pneumatic Hammer Chipper

c. Continuous Joint Demolishing – Segment I

d. Continuous Joint Demolishing – Segment II

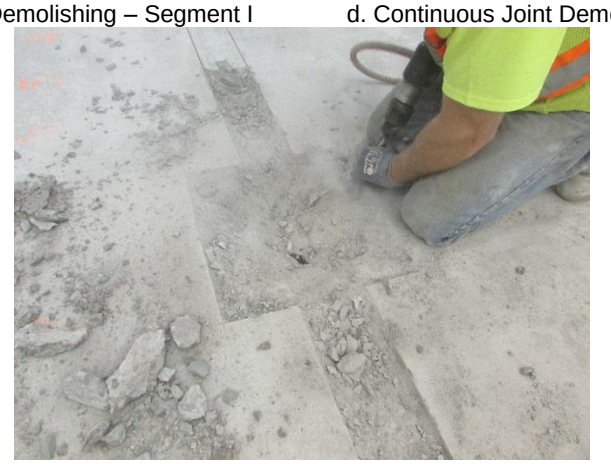

e. Pocket Demolishing

Figure 6-12. Demolition of Longitudinal Connection

After chipping the concrete and exposing the deck reinforcement, the surface was cleaned with compressed air then wetted for 24 hours (Fig. 6-13). Sand-blasting should be used to improve the bond. However, it wasn't feasible in this experimental study due to laboratory restrictions.

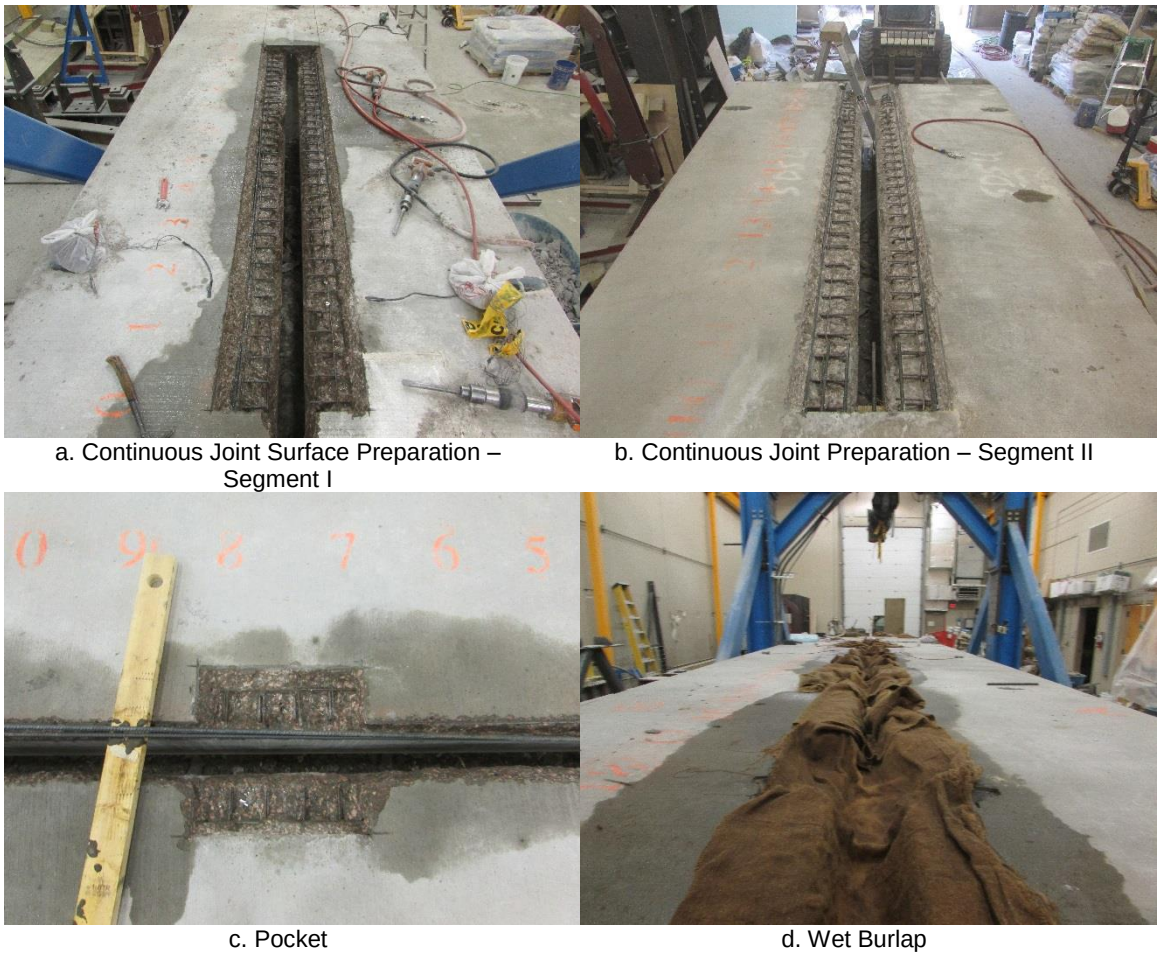

a. Continuous Joint Surface Preparation – Segment I

b. Continuous Joint Preparation – Segment II

c. Pocket

d. Wet Burlap

Figure 6-13. Surface Preparation for Joint Rehabilitation

The formwork for Segment I of the continuous joint was made with plywood with intermediate blocking (Fig. 6-14a-b). A Styrofoam (Fig. 6-14c) was used to separate the segments. A significant LMC leak was noticed using this method. For Segment II of the continuous joint, the formwork was modified using Styrofoam (Fig. 6-14d) and no leak was observed.

The as-built continuous joint reinforcement (Fig. 6-14e) was 4 in. by 4-in., D8/D8 welded wire mesh with a total width of 16 in. installed 2.25 in. below the deck surface. A minimum splice length of 5 in. was provided on the both sides of the joint. The pocket reinforcement (Fig. 6-14f) was 12.5-in. long in both directions and was installed with a clear cover of 2.75 in. from the top of the deck. A minimum splice length of 3 in. was provided in the transverse direction of the bridge in each pocket.

a. Top View
Continuous Joint Segment I Formwork

b. Underneath View
Continuous Joint Segment I Formwork

c. Block-out Formwork

d. Continuous Joint Segment II Formwork

Figure 6-14. Formwork and Reinforcement of Rehabilitated Joints

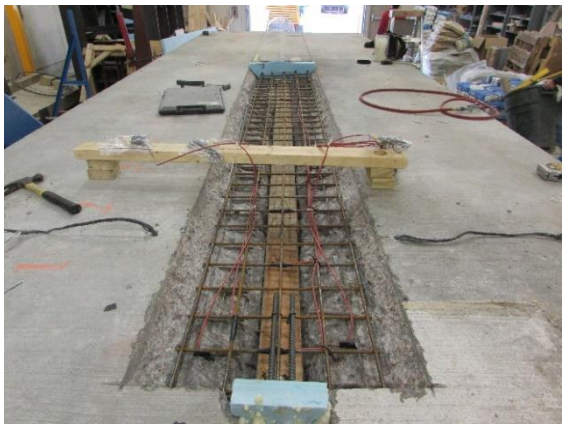

e. Continuous Joint Reinforcement

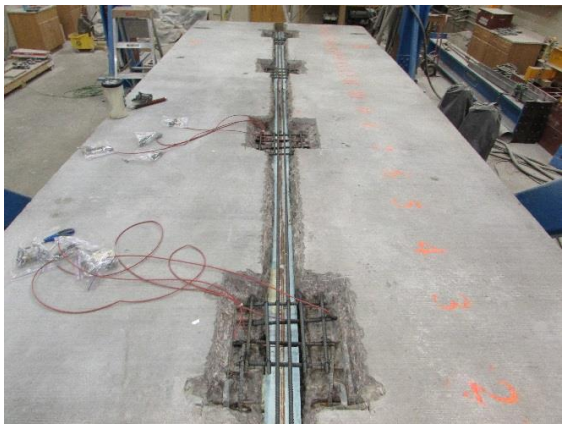

f. Pocket Reinforcement

Figure 6-14. Continued

The continuous joint was poured with a premix latex modified concrete, LMC (Appendix C), using a 12-cubic ft drum mixer (Fig. 6-15a) batching six 50-lb bags for three minutes. As previously mentioned, the continuous joint was poured in two segments. Wheel-barrels (Fig. 6-15b) were lifted onto the bridge using a forklift to pour the joints. Figure 6-15c shows the finished continuous joint poured with LMC.

The pocket joint was poured with a premix UHPC (with 2% steel fibers). The average batching time for four bags of UHPC was 20 minutes using a seven cubic ft mortar mixer (Fig. 6-15d). The average static flow of the UHPC was 8 inches. Figures 6-15e to 6-15f shows the pouring and the finishing of the pocket joint.

Two-in. standard cubes were casted for LMC, and 3-in. diameter cylinders were casted for UHPC. The cylinders were sealed and cured at ambient room temperature. The 2-in. LMC cubes were unmolded after 24 hours then placed in a steam room for curing.

After pouring, the joints were covered with wet burlaps and plastic sheets. The test specimen was cured for 14 days to allow UHPC to gain a compressive strength of 18 ksi.

a. Mixing LMC b. Pouring LMC

c. Finished LMC d. Mixing UHPC

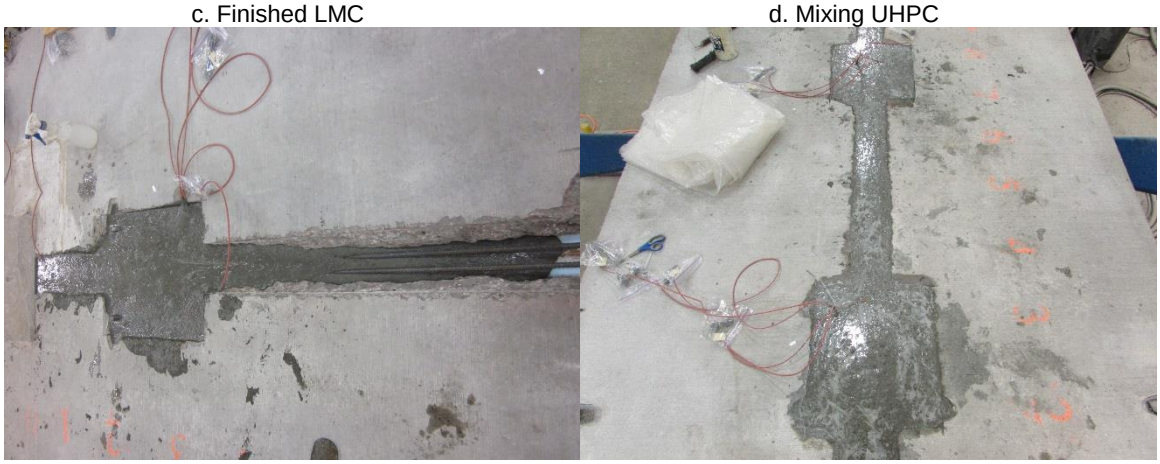

e. Pouring UHPC f. Finished UHPC

Figure 6-15. Casting UHPC and LMC in Rehabilitated Joints

6.3 Instrumentation

The instrumentation used in the experimental programs consisted of strain gauges, linear voltage differential transformers (LVDTs), load cells, and string potentiometers (string pots). This section presents the instrumentation plan of the bridge test specimen.

6.3.1 Strain Gauges

Strain gauges were used for measuring the strains of the girder and joint reinforcement as well as the girder concrete strains. Table 6-1 presents the type and number of gauges used in the project. Sixteen strain gauges were installed on the reinforcement of the rehabilitated joint (Fig. 6-16). The labeling system for the strain gauges consisted of four sublabels including type, location, direction, and unique number of the gauge as shown in the figure. Twelve gauges were installed on the girder tendons (Fig. 6-17) and six concrete strain gauges were embedded in the deck.

Table 6-1. Strain Gauge Types

Material	Resistance (Ω)	Length (mm)	Gauge Type	Direction of Loading	No. of Gauges
Concrete	120	60	PMFL-60-2LT	Long.	6
P/S Strand	121	2	YEFLA-2-5L	Long.	12
Mild Steel	121	2	YEFLA-2-5L	Trans.	14
Mild Steel	121	2	YEFLA-2-5L	Long.	2

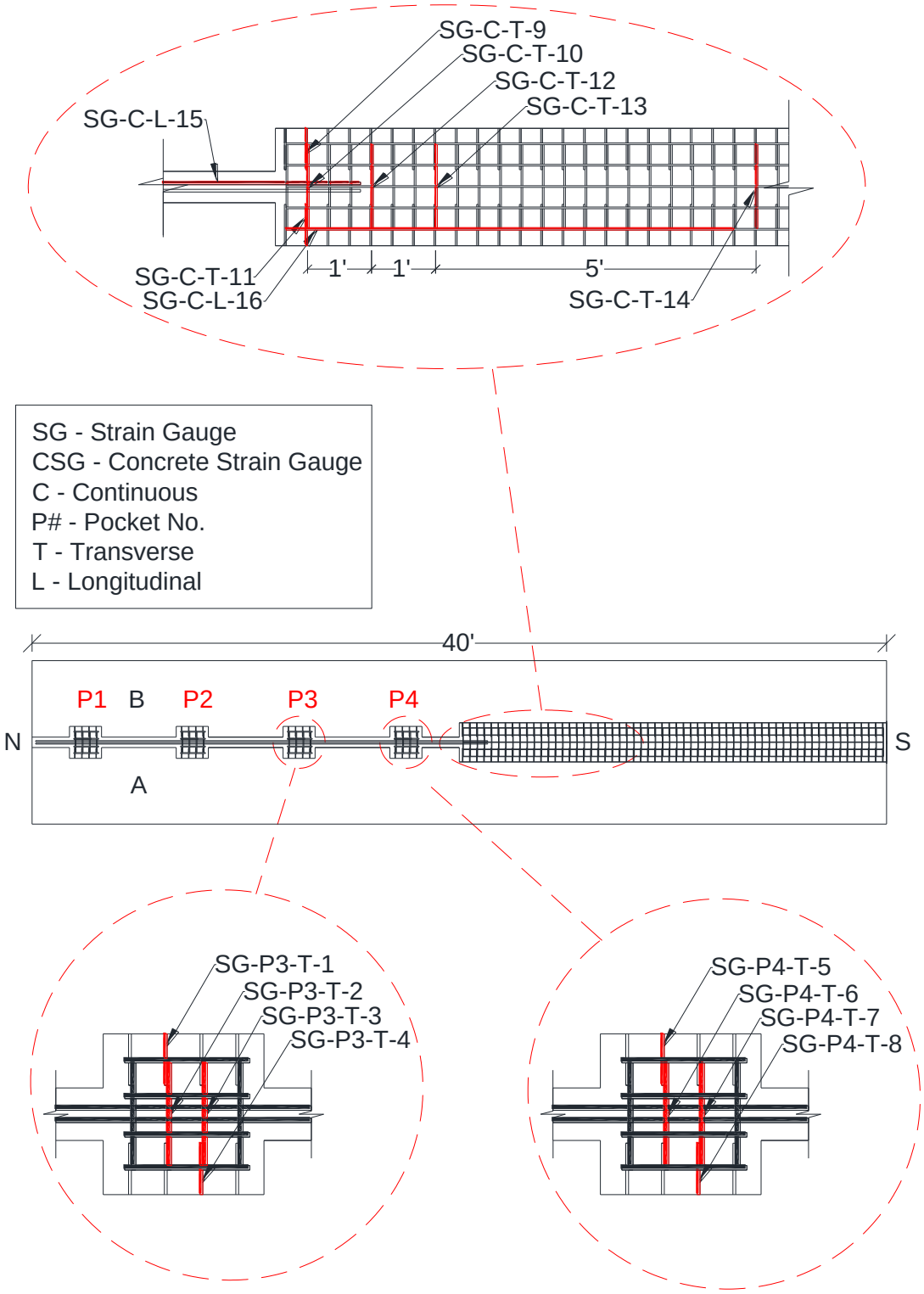

Figure 6-16. Rehabilitated Joint Strain Gauge Plan

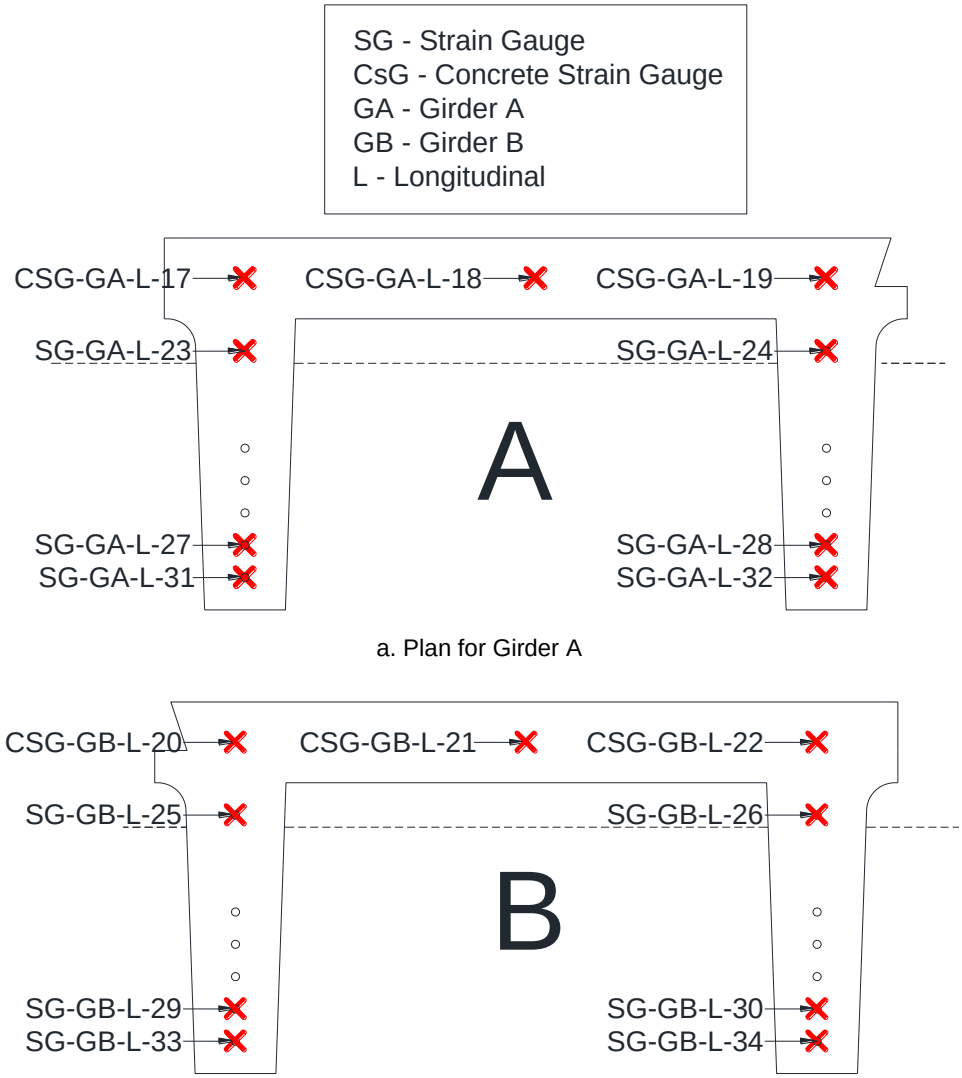

a. Plan for Girder A

b. Plan for Girder B

Figure 6-17. Girder Strain Gauge Plan

The prestressed strands were first cleaned by removing all debris and grease. Next, the strands were sanded with fine grit sand paper. After sanding, the surface was cleaned with an acid then neutralized with a base solution. The tendon strain gauges (SG) were placed at the midspan by offsetting them from the center of the girders based on the elongation of the tendons at full tension (31 kips), which was done after strain gauge installation. The gauges were attached to the tendons with an adhesive supplied by the

manufacturer (Fig. 6-18a). Finally, the gauge was waterproofed with a nitrile compound and wrapped with several layers of tape and rubber. The concrete strain gauges (CSG) were placed at the midspan between the welded wire mesh (Fig. 6-18b). The gauges were tied to the wire mesh with wires. Samples of steel reinforcement strain gauges are shown in Fig. 6-18c before casting.

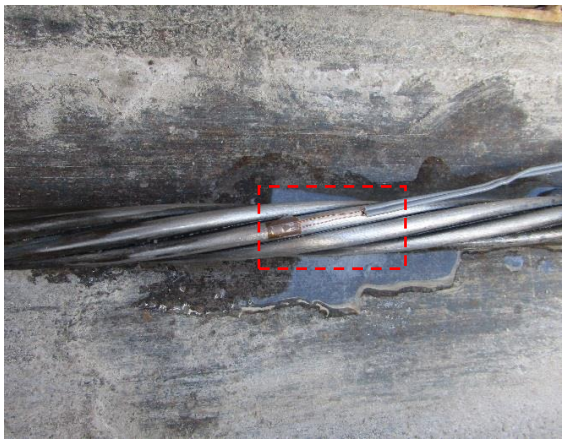

a. Strain Gauge on Prestressing Strand

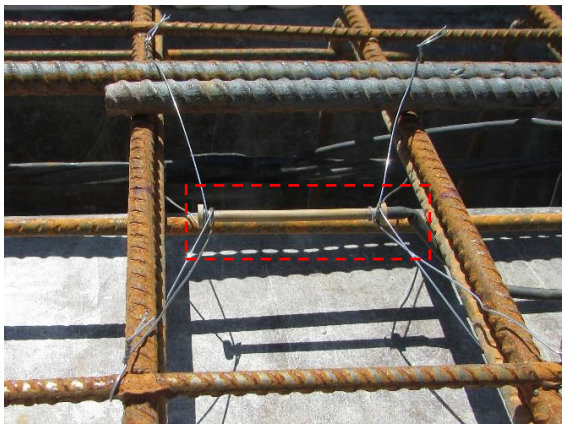

b. Embedded Concrete Strain Gauge

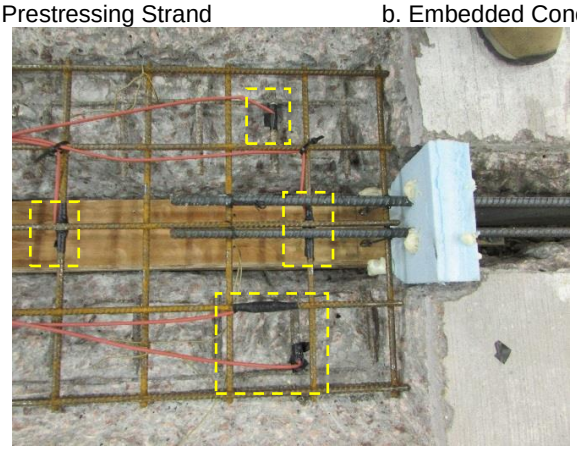

c. Strain Gauge on Mild Steel Bars

Figure 6-18. Strain Gauge Installation

6.3.2 Linear Variable Differential Transformers (LVDTs)

Thirteen LVDTs were used to measure displacements, slippage, and rotations of critical locations in the experiment (Fig. 6-19 and Fig. 6-20). The four midspan LVDTs (Fig. 6-21a) measuring vertical deflection of the stems from the bottom were removed

during strength testing and were replaced with four string pots to prevent damage of LVDTs. Two LVDTs (Fig. 56-21b) were used to measure vertical compression of the elastomeric bearing pads at the support to calculate the net midspan deflections. Six LVDTs were used to measure either vertical (Fig. 6-21c) or horizontal (Fig. 6-21d) relative displacements between the deck and the longitudinal joint. Two LVDTs (one on the top of the deck as shown in Fig. 6-21e and one at the bottom of the girders as shown in Fig. 6-21f) were used to measure the rotation of the girders in the transverse direction of the bridge.

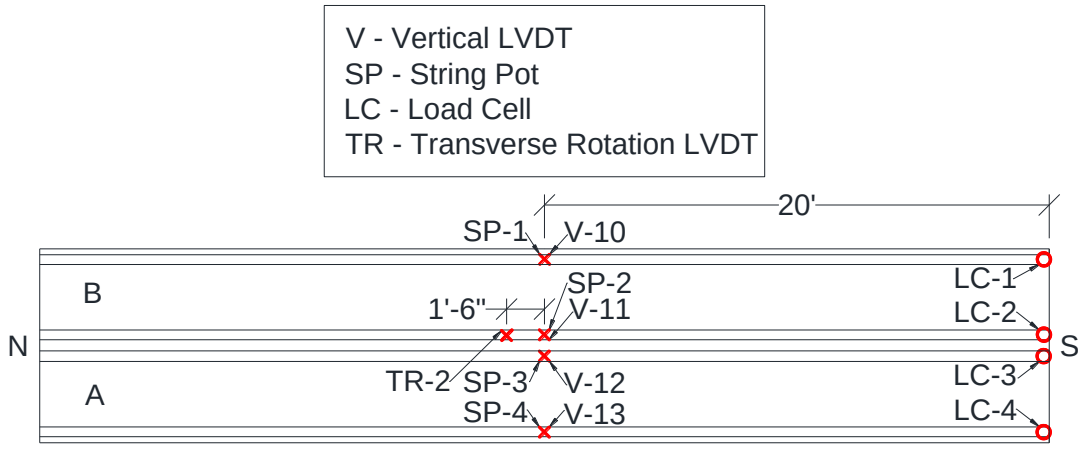

Figure 6-19. LVDT Instrumentation Plan Below Deck

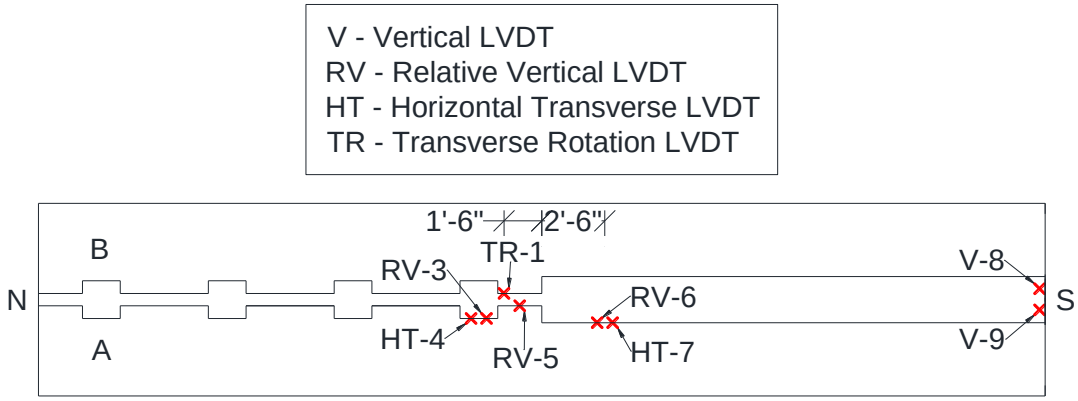

Figure 6-20. LVDT Instrumentation Plan above Deck

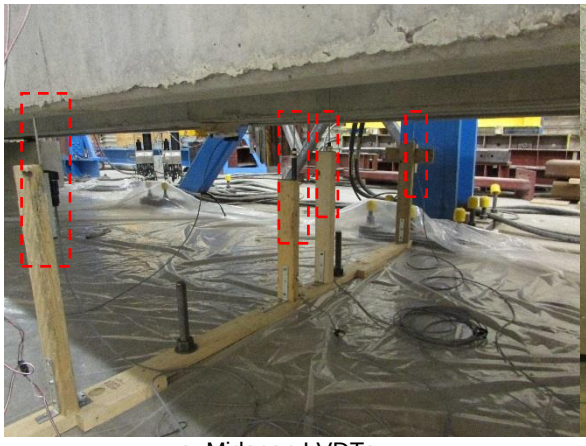

a. Midspan LVDTs

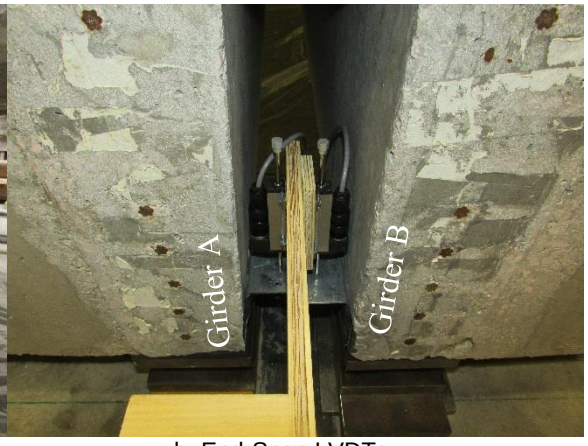

b. End-Span LVDTs

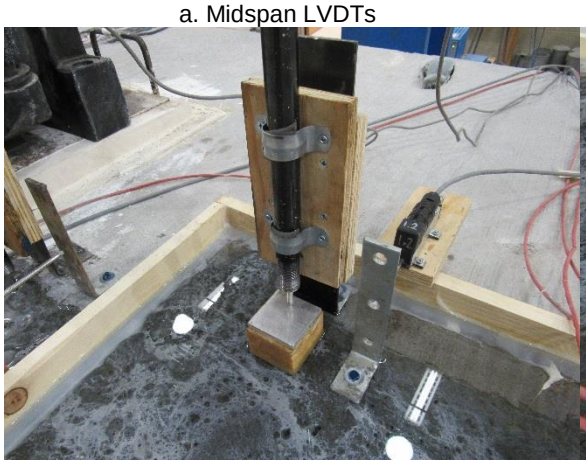

c. Vertical LVDT to Measure Joint Slippage

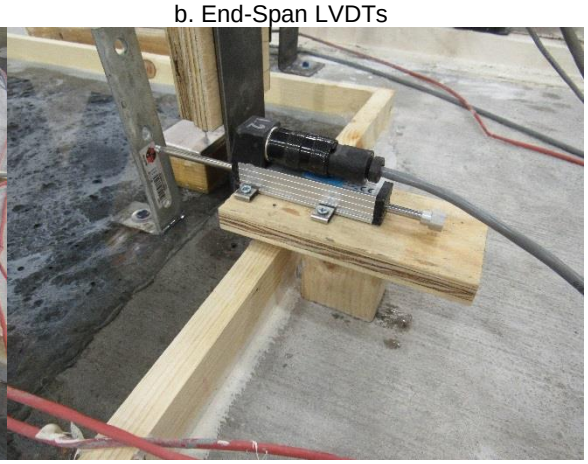

d. Horizontal LVDT to Measure Joint Slippage

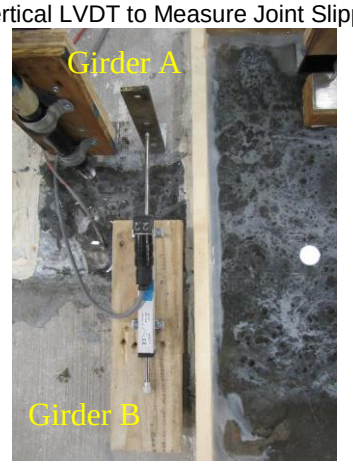

e. Top LVDT to Measure Girder Rotation in Transverse Direction

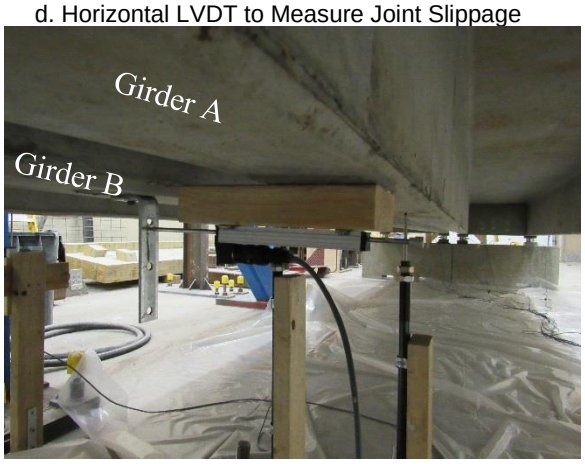

f. Bottom LVDT to Measure Girder Rotation in Transverse Direction

Figure 6-21. LVDT Installation

6.3.3 Load cells

The end reactions of each girder were determined by placing four 100-kip load cells under each stem at the south end (Fig. 6-19). The load cells were placed between two 1 by 6 in. by 6 in. steel plates for adequate bearing. An elastomeric bearing pad was placed between plate and girder to allow free rotation (Fig. 6-22).

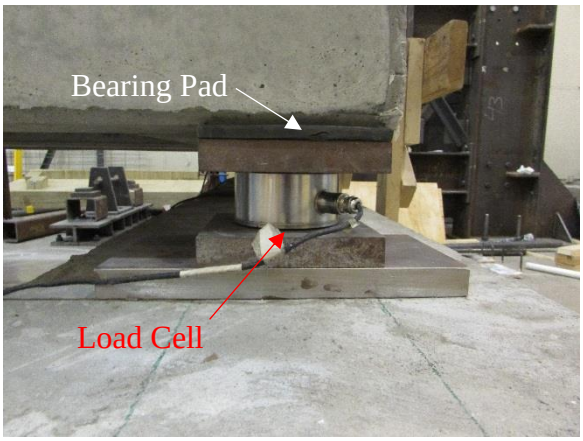

Figure 6-22. Load Cell Installation at Girder South End

6.3.4 Data Acquisition System

The data was obtained using a 128-channel data acquisition system. Data under stiffness and strength loading was measured at a rate of 10 readings per second. For fatigue testing, the scan rate was 100 readings per second.

6.4 Test Setup

Figure 6-23 shows the full-scale bridge test setup. A 146-kip hydraulic actuator was used to apply point loads at the midspan on girder A (Fig 6-23a) with 11-in. offset form the specimen centerline. The load was applied on a 1.5 in. by 10 in. by 20-in. steel plate, which was seated above a plaster (Fig. 6-23b). The plate area represents the truck tire

loading area. Water dams (Fig. 6-24) were formed above the rehabilitated longitudinal joint to identifying cracking.

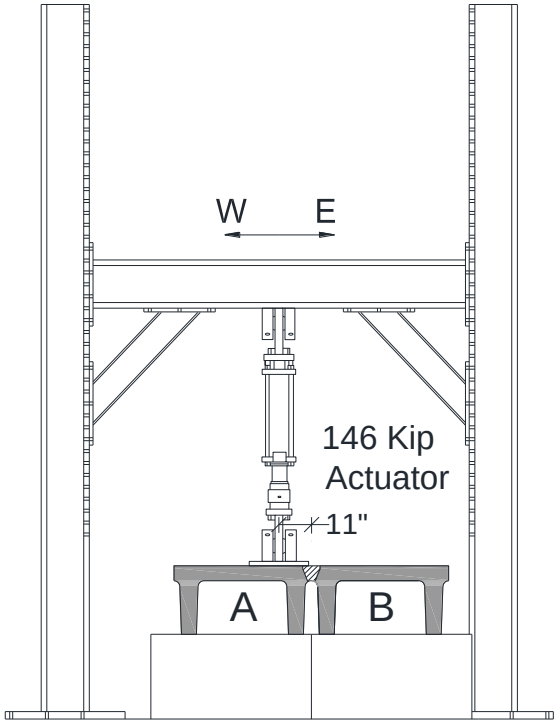

a. Cross-Section View of Test Setup

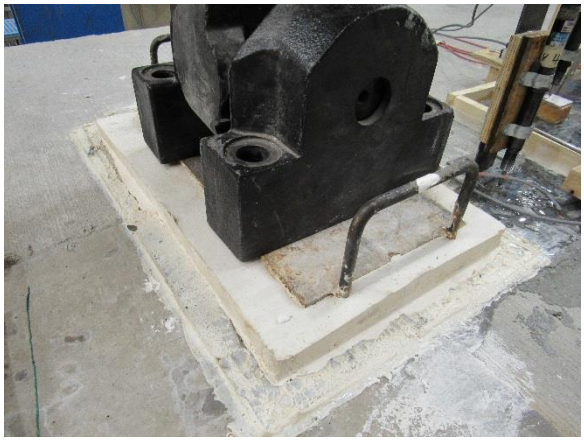

b. Actuator Head with Load Plate

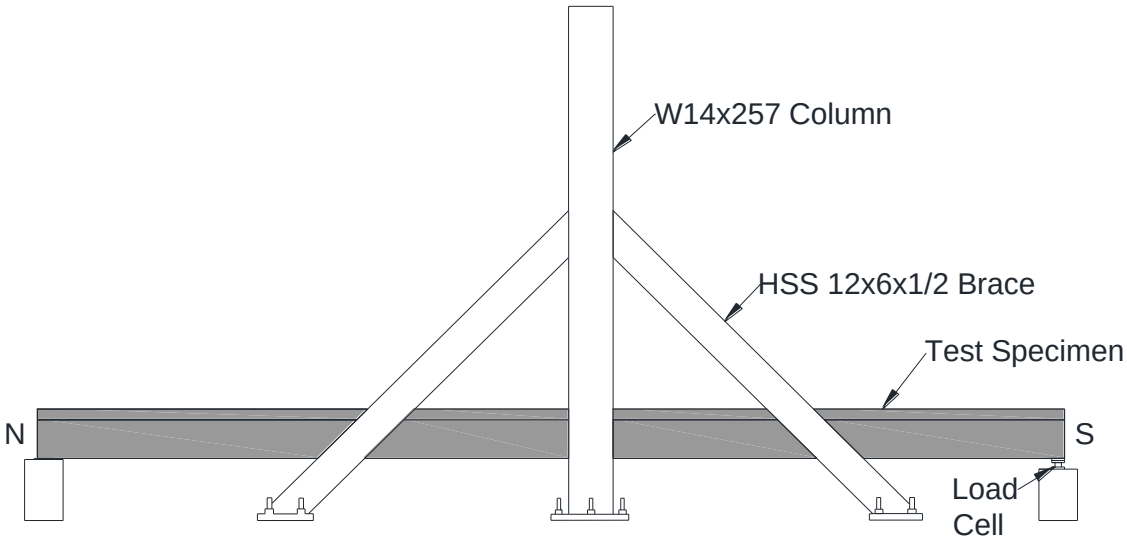

c. Profile View of Test Setup

Figure 6-23. Full-Scale Double-Tee Bridge Test Setup

Figure 6-24. Water Dams on Rehabilitated Joint

6.5 Loading Protocol

Table 6-2 presents the loading protocol for the bridge test specimen. Both conventional and rehabilitated specimens were tested under fatigue loading. The conventional bridge specimen was first tested under fatigue loading then under a monotonic loading to damage the longitudinal joint prior to rehabilitation. Ultimate (strength) testing was performed on the rehabilitated specimen to determine the capacities of the bridge. Figure 6-25 shows the location and the area of the applied load for all testing phases.

Table 6-2. Full-Scale Bridge Loading Matrix

Testing Phase	Bridge Model	Load Type	Load Amplitude	No. of Cycles
I	Conventional Specimen	Cyclic Fatigue	21 kip	250,000
II	Conventional Specimen	Monotonic	50 kip	-
III	Rehabilitated Specimen	Cyclic Fatigue II	21 kip	500,000
IV	Rehabilitated Specimen	Cyclic Fatigue I	42 kip	100,000
V	Rehabilitated Specimen	Monotonic	Failure	-

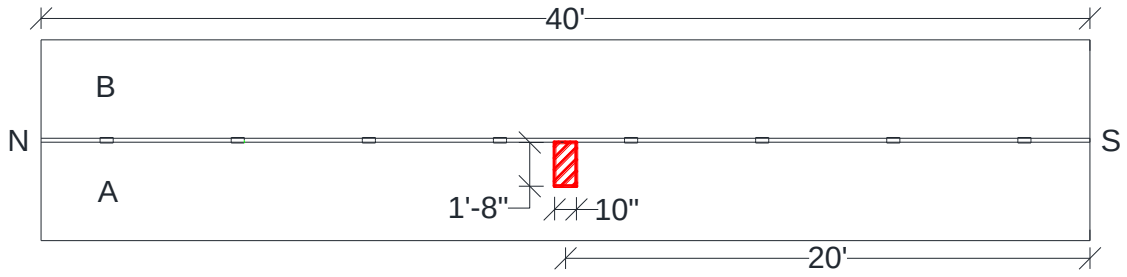

a. Plan View for Conventional Specimen

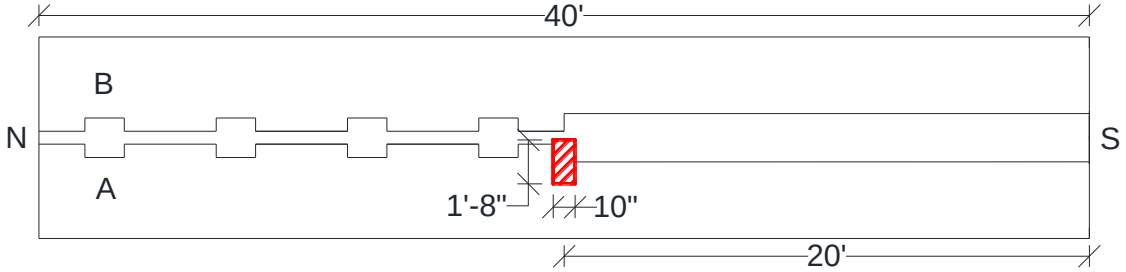

b. Plan View for Rehabilitated Specimen

Figure 6-25. Applied Load Configuration and Location

6.5.1 Fatigue and Stiffness Testing

According to the AASHTO LRFD (2013), the Fatigue II limit state loading was sufficient to evaluate the performance of this bridge for the 75 years of the service life. However, the bridge was tested under both Fatigue I and II loads to maximize the demand on the rehabilitated joint. The fatigue II limit state loading consisted of a sinusoidal 21-kip load applied with a frequency of one cycle per second (Fig. 6-26), which was applied to both conventional and rehabilitated specimens (Table 6-2). The fatigue I limit state loading consisted of a sinusoidal 42-kip load applied with a frequency of 0.7 cycles per second. The magnitude of the loads was determined using the moment envelope from the AASHTO fatigue I and II limit states for a two-lane 40-ft bridge (Appendix A). The load frequency was based on the test setup limitations.

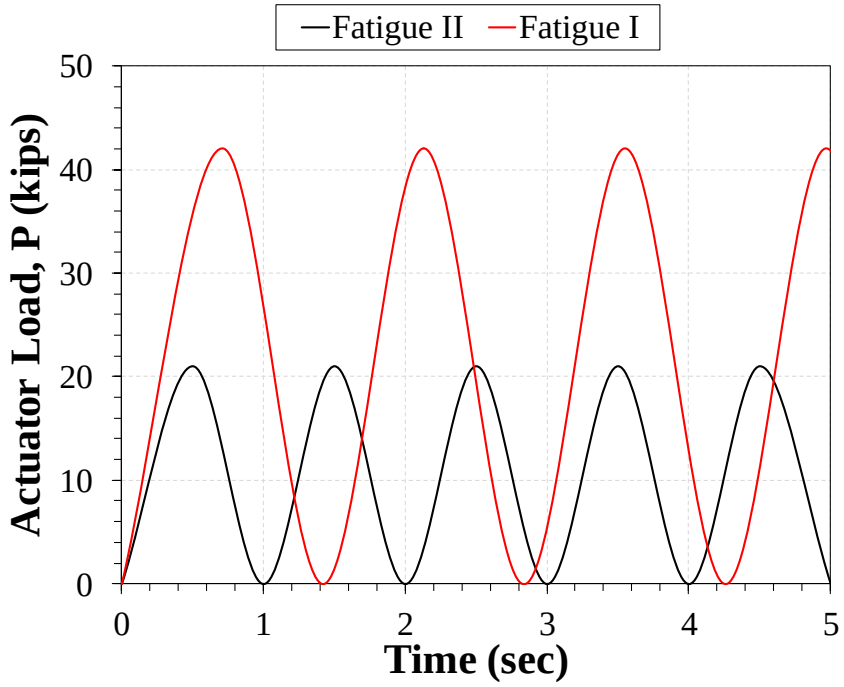

Figure 6-26. Fatigue Testing Loading Protocol

The average daily truck traffic (ADDT) for local roads in South Dakota was assumed to be 15 trucks per day. For the 75-year design life, 410,625 trucks would pass the bridge. The conventional bridge specimen was tested under 250,000 load cycles. The rehabilitated bridge specimen was first tested under 500,000 Fatigue II load cycles (surpassing the required 75-year design life) followed by 100,000 Fatigue I load cycles to maximize the joint load demands.

Stiffness test was carried out at intermediate load cycles to measure bridge stiffness. The stiffness of the conventional test specimen was measured every 10,000 cycles up to 100,000 load cycles. It was then performed every 25,000 cycles to the end of fatigue testing. The stiffness of the rehabilitated test specimen under the Fatigue II and Fatigue I loading was measured every 50,000 and 10,000 load cycles, respectively.

6.5.2 Strength (Ultimate) Testing

The conventional test specimen was monotonically loaded to 50 kips to crack the longitudinal joint prior to rehabilitation. The rehabilitated test bridge was monotonically loaded to failure using a displacement-based controlled point load at the midspan (Fig. 6-26) with a load increment of 0.1 in. and a displacement rate of 0.007 in. per second.

7. Full-Scale Double-Tee Bridge Testing Results

This chapter includes the results of experimental studies on both conventional and rehabilitated full-scale double-tee bridge test specimens discussed in the previous chapter. The measured material properties and performance of both bridge test specimens under fatigue and strength loading are discussed herein.

7.1 Materials Properties

Many different cementitious and steel materials were incorporated in different components of the bridge test specimens. This section presents the material properties for concrete used in the precast bridge girders, non-shrink grout used in the conventional longitudinal girder-to-girder joint, ultra-high performance concrete (UHPC) used in the rehabilitated longitudinal joint pockets, and latex modified concrete (LMC) used in the rehabilitated continuous longitudinal joint, and the steel reinforcement utilized in the precast bridge girders as well as the rehabilitated longitudinal joints.

7.1.1 Properties of Cementitious Materials

This section presents the properties of fresh concrete and the compressive strength of precast concrete, non-shrink grout, UHPC, and LMC.

7.1.1.1 Precast Concrete

The properties of fresh concrete incorporated in the precast double-tee bridge girders measured in accordance to ASTM C143 (2015) and C231 (2016) are presented in Table

7-1. The requirements based on the manufacturer mix design (see Appendix C) for fresh concrete were 6% (+1.5%, -1.0%) air content and a slump between 4 to 6 in. It can be seen that the girder concrete met the requirements.

Table 7-1. Properties of Precast Girder Fresh Concrete

Temperature (^{0} F)	Air Content (%)	Unit Weight (lb/ft^3)	Slump (in.)
70	5.5	143.6	5

Standard 6-in. diameter cylinders were used for concrete sampling. The cylinders were steam cured for 12 hours onsite with the girders, then the cylinders were sealed and stored in the structures lab. The concrete compressive strength was measured in accordance to ASTM C39 (2016) procedures. Tests were performed after 1 day, 7 days, 28 days of casting, and the day of fatigue and strength testing. Table 7-2 presents the compressive strength for concrete used in the girders. The manufacturer 28-day compressive strength requirement (see Appendix C) was 6,000 psi, which was met.

Table 7-2. Compressive Strength of Girder Concrete

Time (Day)	f'_c (psi)
1	5,698
7	7,192
28	7,636
Fatigue Test (Phase I)	8,783
Fatigue Test (Phase III)	9,230
Strength Test (Phase V)	9,512

7.1.1.2 Non-Shrink Grout

Standard 2-in. cube molds were used for sampling the non-shrink grout. The samples were stored and cured in a moist room. The compressive strength was measured in accordance to ASTM C109 (2016) procedures. Compressive tests were performed at 3, 28, and girder fatigue testing days. Table 7-3 presents the compressive strength for the non-shrink grout used in the longitudinal joint of the conventional test specimen. The

South Dakota Depart of Transportation (SDDOT) specifies a minimum 28-day compressive strength of 4,500 (SDDOT, 2004) for non-shrink grout, which was met.

Table 7-3. Compressive Strength of Non-Shrink Grout

Time (Day)	f'_c (psi)
3	5,853
28	8,519
Fatigue Test (Phase I)	5,853

7.1.1.3 Ultra-High Performance Concrete (UHPC)

Three-inch diameter cylinders were used for sampling UHPC. The samples were sealed and stored in the structures lab. Compressive strength tests were carried out in accordance to ASTM C39 (2016) as well as the procedure specified by the UHPC provider. The samples were prepared by saw-cutting the surface to avoid any point load and were tested without bearing pads since pads cannot be used for materials stronger than 11,000 psi. Compressive tests were performed at 7, 14, fatigue, and strength testing days. Table 7-4 presents the compressive strength for UHPC used in the longitudinal joint of the rehabilitated test specimen. According to FHWA-HRT-11-023, the minimum field compressive strength for UHPC is 18 ksi, which was met.

Table 7-4. Compressive Strength of UHPC

Time (Day)	f'_c (psi)
7	11,480
14	19,716
Fatigue Test (Phase III)	19,716
Fatigue Test (Phase IV)	20,835
Strength Test (Phase V)	21,167

7.1.1.4 Latex Modified Concrete (LMC)

Standard 2-in. cube molds were used for sampling LMC. The samples were stored and cured in a moist room. The compressive strength was measured in accordance to

ASTM C109 (2016) procedures. Compressive tests were performed after 3 hours, 7 days, and 14 days of casting as well as the days of fatigue and strength testing. Table 7-5 presents the compressive strength for LMC used in the longitudinal joint of the rehabilitated test specimen. The longitudinal joint incorporating LMC was casted in two stages, seven days apart.

Table 7-5. Compressive Strength of LMC

Time (Day)	Phase I, f'_c (psi)	Phase II, f'_c (psi)
0.125 (3 Hours)	5,457	N/A
7	N/A	7,204
14	7,585	N/A
Fatigue Test (Phase III)	7,742	6,992
Fatigue Test (Phase IV)	8,103	7,283
Strength Test (Phase V)	7,571	7,494

7.1.2 Properties of Prestressing Strands

The prestressing strands used in the girders were seven-wire, Grade 270, 0.5-in. diameter low-relaxation strands, A_s=0.153 in^2. Table 7-6 presents the measured mechanical properties for the prestressing strands.

Table 7-6. Tensile Properties of Prestressing Strands

Properties	0.5-in. Strands (ASTM A416)
Yield Strength, fy (ksi)	258.4
Ultimate Strength, fu (ksi)	285.2
Strain at Break, ε_r	7.4%
Modulus of Elasticity, E (ksi)	29,000

7.1.3 Properties of Steel Reinforcement

This section presents the mechanical properties of steel wires used in welded mesh and deformed reinforcing steel bars used in the joints. The mechanical properties were measured in accordance to ASTM E8 (2016) procedures.

7.1.3.1 Reinforcing Steel Wires

The continuous joint was reinforced with ASTM A497 Grade 70, 4 in. by 4 in., D8/D8 weld wire mesh. The same type of wire was used in the girder flanges. Table 7-7 presents the measured mechanical properties for the steel wire.

Table 7-7. Tensile Properties of Steel Wires Used in Joints and Girders

Properties	D8 Wire (ASTM A497)
Yield Strength, fy (ksi)	117
Ultimate Strength, fu (ksi)	123
Strain at Peak Stress, ε_u	2.9%
Strain at Break, ε_r	19%

7.1.3.2 Reinforcing Steel Bars

Table 7-8 presents the measured mechanical properties of ASTM A615 Grade 60 No. 4 steel bars used in the UHPC pockets of the rehabilitated bridge.

Table 7-8. Tensile Properties of Reinforcing Steel Bars Used in UHPC Pockets

Properties	No.4 Bars (ASTM A615)
Yield Strength, fy (ksi)	74
Ultimate Strength, fu (ksi)	107
Strain at Peak Stress, ε_u	10%
Strain at Break, ε_r	16%

7.1.4 Properties of Elastomeric Neoprene Bearing Pads

Mingo (2016) tested a 6 in. by 6 in. by 3/8-in. elastomeric neoprene bearing pad in compression to determine the force-displacement relationship of the bearing pads used at the supports (Fig 7-1). The same neoprene pads were used in this study. The stiffness of the linear region of the force-displacement relationship was 1,128 kip/in.

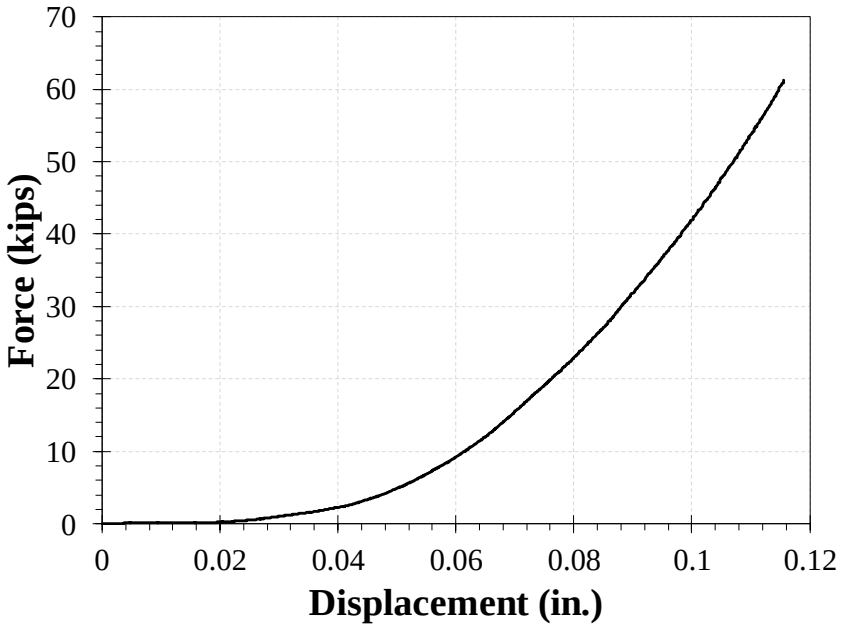

Figure 7-1. Measured Force-Displacement of Elastomeric Neoprene Bearing Pad (Mingo, 2016)

7.2 Bridge Test Results

This section presents the results of the conventional and rehabilitated bridge specimens tested under fatigue and strength loading.

7.2.1 Conventional Double-Tee Bridge Test Specimen

The conventional double-tee bridge specimen (in which the girder-to-girder connection detailing was the same as that currently used in practice) was first tested under 250,000 cycles of the Fatigue II loading (Phase I) applied as a point load at the midspan. The point load was offset from the longitudinal centerline of the bridge to apply the force on only one girder and to maximize the shear load demand transferred between the girders. After the fatigue loading, the conventional bridge specimen was monotonically loaded as Phase II of the testing to damage the longitudinal girder-to-girder joint prior to rehabilitation. The results of experimental testing of the conventional double-tee bridge specimen is discussed herein.

7.2.1.1 Phase I: Fatigue II Testing of Conventional Double-Tee Bridge

Cyclic loads with an amplitude of 21 kips were applied at the midspan of the bridge at a frequency of one cycle per second for a total of 250,000 cycles. The stiffness of the bridge was initially measured at 10,000 load cycle intervals up to 100,000 load cycles. However, the specimen did not degrade as expected, thus the stiffness was measured at an interval of 25,000 load cycles, thereafter. The stiffness test was performed by monotonically loading the specimen up a peak force of 21 kips.

Figure 7-2 shows the measured stiffness versus the number of the load cycles during the AASHTO Fatigue II testing. The stiffness of the specimen was defined as the slope of the measured load-displacement relationship. The net midspan deflection (subtracting the total deflection and the compression of the bearing pads) of only girder A was used for stiffness calculation since it was the loaded girder. It can be seen that the bridge stiffness essentially remained constant during the fatigue II testing. Furthermore, no damage of the longitudinal joint or any other members of the bridge throughout 250,000 cycles of loading was observed.

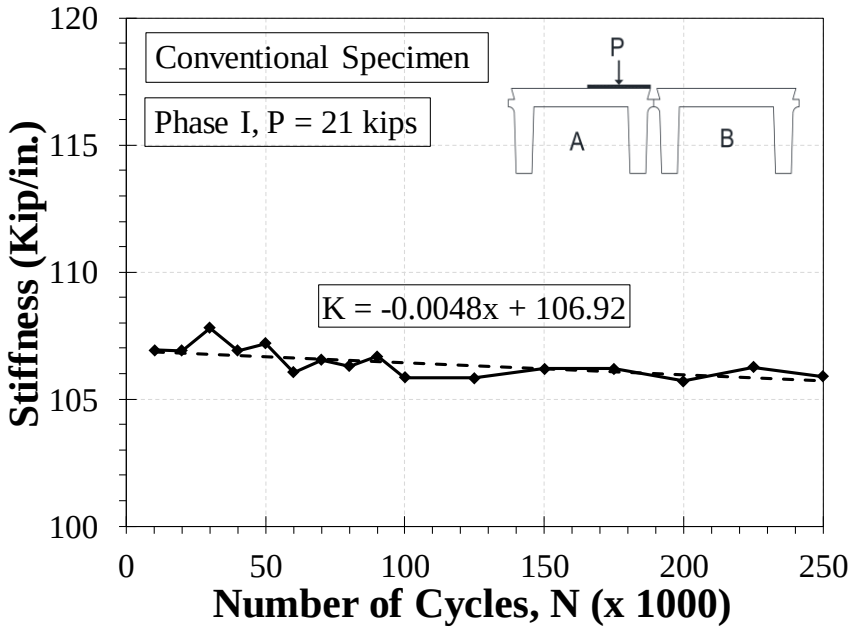

Figure 7-2. Stiffness Degradation during Fatigue II Testing of Conventional Double-Tee Bridge Specimen

Girder-to-girder joint relative vertical displacements were measured 2.0 ft away from the midspan (Fig. 7-3). It can be seen that the measured joint relative displacements were negligible throughout the fatigue testing indicating no girder-to-girder joint damage.

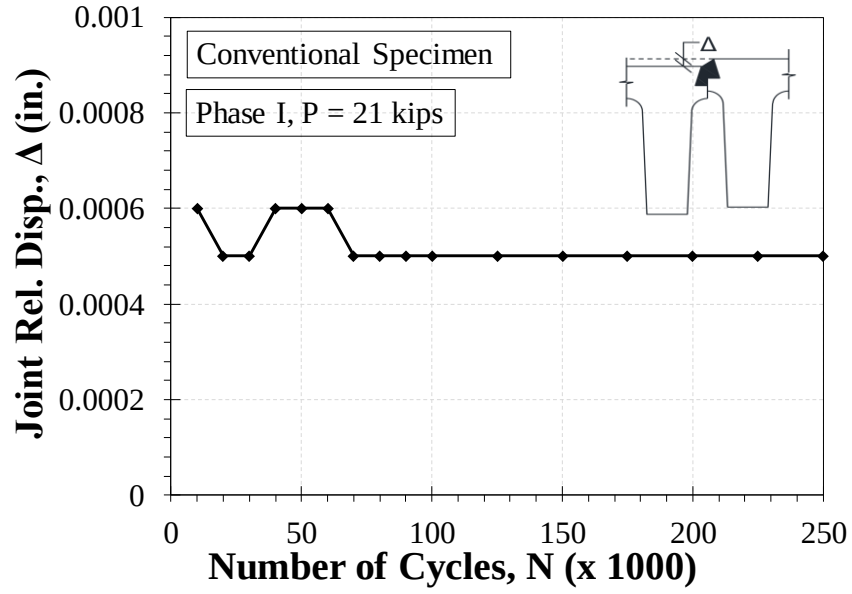

Figure 7-3. Longitudinal Joint Relative Displacement for Conventional Double-Tee Bridge Specimen during Fatigue II Testing

Girder-to-girder joint rotations (Fig. 7-4) in the transverse direction of the bridge were also measured 1.5 ft away from the midspan. The rotations were measured using two LVDTs: one was installed at the top of deck (LVDT TR-1) and another was installed at the bottom of stems (LVDT TR-2). It can be seen that the measured joint rotations were negligible throughout fatigue testing indicating the girder-girder joint did not degrade at this level of loading.

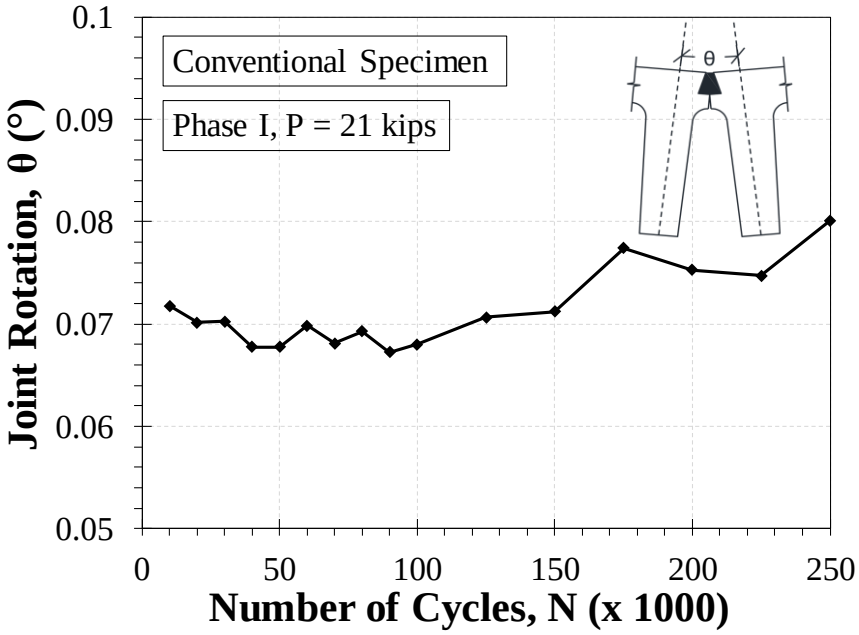

Figure 7-4. Girder-to-Girder Joint Rotation for Conventional Double-Tee Bridge Specimen during Fatigue II Testing

7.2.1.2 Phase II: Joint Crack Strength Testing of Conventional Double-Tee Bridge

After the fatigue II testing, the bridge specimen was monotonically loaded under a displacement controlled loading regime to 48.5 kips, where the girder-to-girder joint was cracked. The goal of this test was to damage the joint prior to rehabilitation without cracking the girders.

The first crack in the joint was observed in the longitudinal direction of the bridge at the midspan at a load of 44 kips (Fig. 7-5). More cracks were observed at the peak load of 48.5 kips, where the test was stopped to avoid girder cracking.

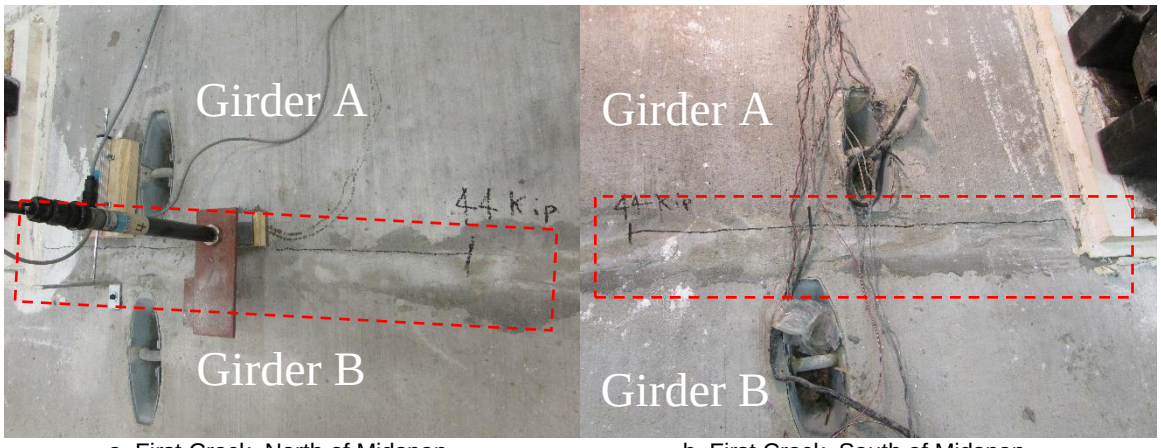

a. First Crack, North of Midspan b. First Crack, South of Midspan

Figure 7-5. Girder-to-Girder Joint Cracking of Conventional Double-Tee Bridge Specimen

Figure 7-6 shows the force-displacement relationship for both girders (A and B) at the midspan up to 48.5 kips at which the deflection of girder A and B was 0.48 and 0.39 in., respectively. Based on the measured strains as well as the joint relative displacement data (discussed later in this section), the load at the first joint cracking was estimated to be 38.7 kips. The first joint cracking was observed at 44 kips. Therefore, it can be concluded that the joint cracking occurred before reaching the AASHTO Service I limit state, which was equivalent to a midspan point load of 51 kips. This indicates that the

current girder-to-girder joint detailing for double-tee bridges is not sufficient even for the service I load.

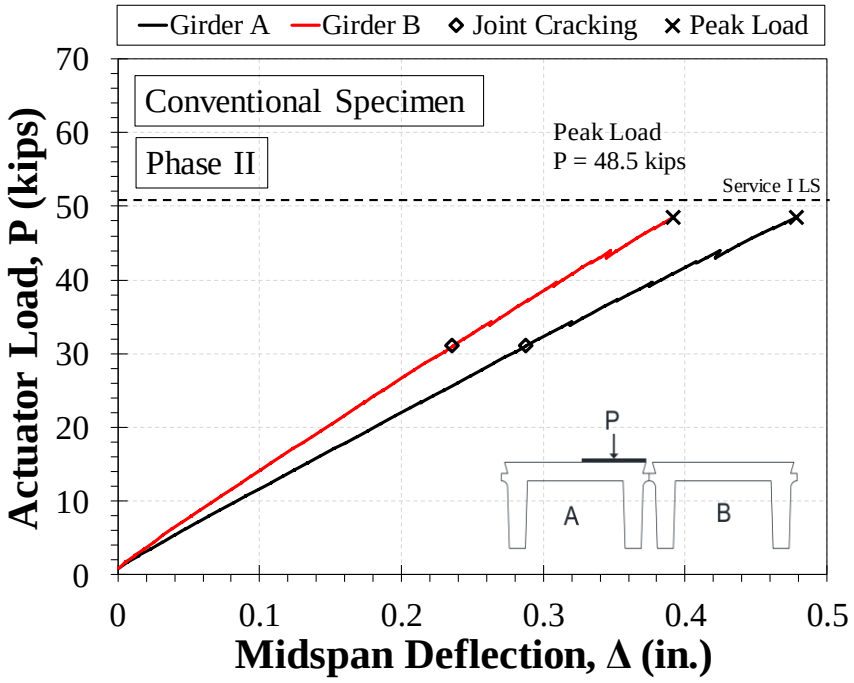

Figure 7-6. Force-Displacement Relationship for Conventional Double-Tee Bridge Specimen during Joint Crack Strength Testing

Load cells were used to measure south end reactions of the girders, one load cell per stem. The reactions were used to determine the girder load distribution based on a percentage of the applied load (P/2 per girder end). The girder end reactions at the beginning of the fatigue testing, after the fatigue testing, and at the joint cracking were compared in Fig. 7-7. It can be seen that the load distribution slightly changed during the fatigue testing but the change was significant when the longitudinal girder-to-girder joint cracked. In this case, stem D did not resist any force resulting in an increase in forces of other stems. This change in load transfer mechanism may crack the stems at higher loads or in the field.

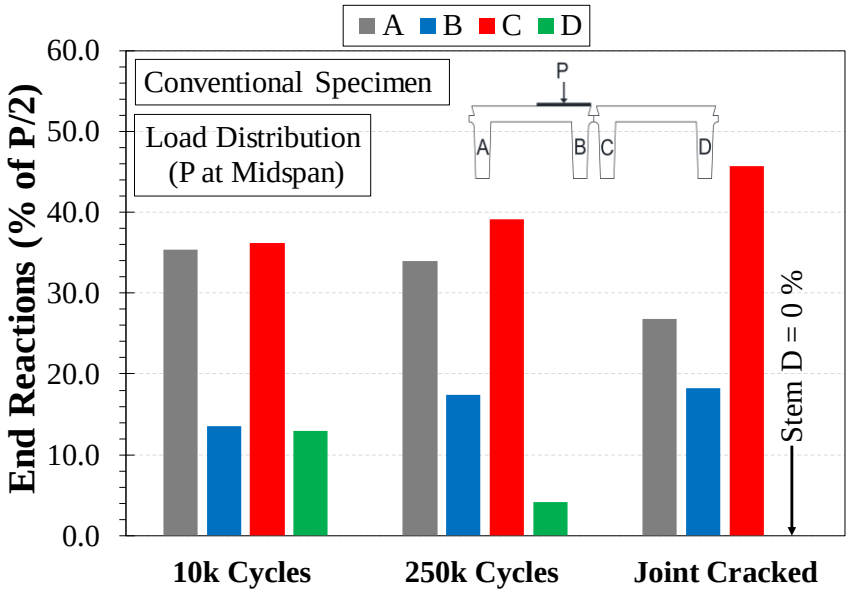

Figure 7-7. Girder Load Distribution for Conventional Double-Tee Bridge Specimen

Figure 7-8 shows the strains of the prestressing strands and concrete in the flange of the loaded girder (A) during the phase II testing. The maximum tensile strain at the extreme strand of the interior stem at the peak load of 48.5 kips was 462 micro-strain (prestressing strains are not included in the graph). The estimated initial strain without any losses from 31-kip pretensioning is 7109 micro-strain from structural mechanics. The yield strain of Grade 270 strands is 8,772 micro-strain. The summation of the strain demand and the prestressing strains suggested that the strands did not yield. The maximum compressive strain in the girder flange concrete was 92.1 micro-strain at the peak load of 48.5 kips. The embedded concrete strain gauges were located 3.5 in. below the girder surface.

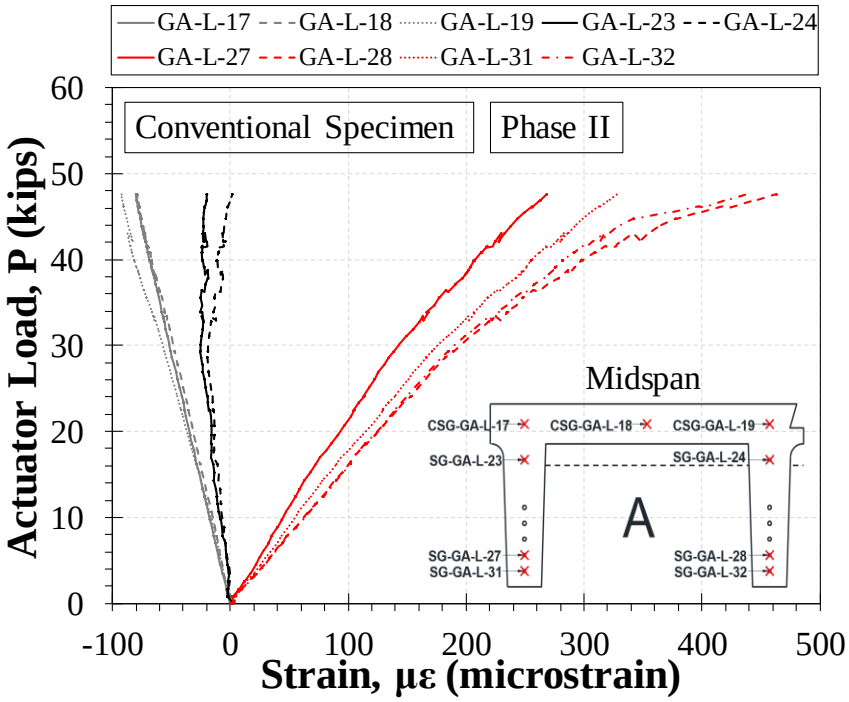

Figure 7-8. Measured Strains of Loaded Girder in Conventional Double-Tee Bridge Specimen during Joint Crack Strength Testing

Figure 7-9 shows the strain of girder B during the phase II testing. It can be seen that the maximum tendon tensile strain in girder B is 29% less than that in girder A, which was the loaded girder. The maximum strain in the extreme strand of girder B at the peak load of 48.5 kips was 329 micro-strain, which was less than the yield strain even after adding the initial prestressing strains. The maximum compressive strain in the girder flange concrete was 80.4 micro-strain at the peak load of 48.5 kips. Similar to girder A, the embedded concrete strain gauges were located 3.5 in. below the girder surface.

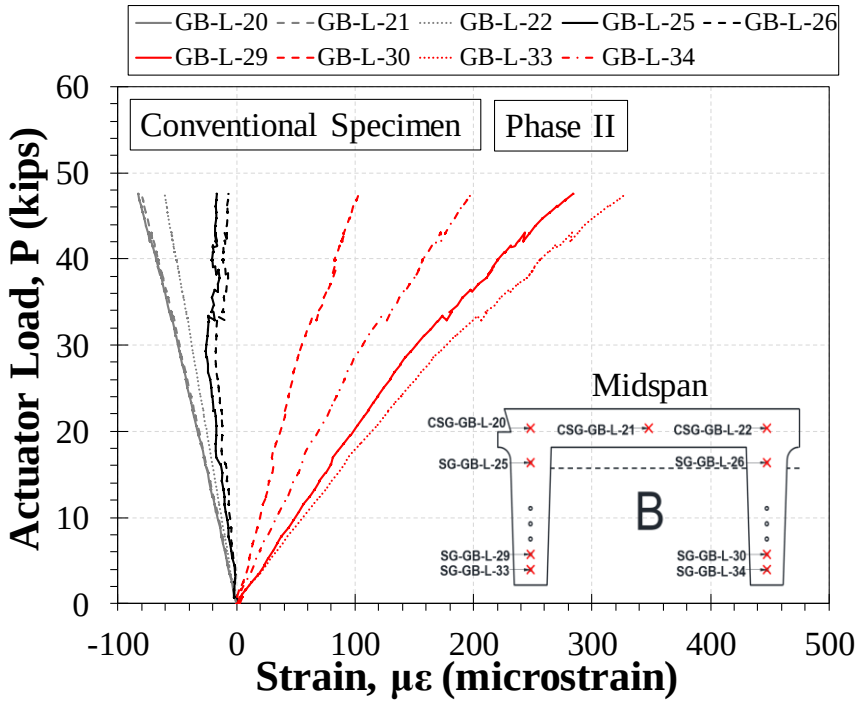

Figure 7-9. Measured Strains of Girder B in Conventional Double-Tee Bridge Specimen during Joint Crack Strength Testing

Girder-to-girder joint relative vertical displacements were measured 2 ft away from the midspan. The measured joint relative vertical displacement was 0.001 in. at the peak load of 48.5 kips (Fig. 7-10), which was insignificant. Furthermore, it can be seen that the joint relative displacement decreased at 38.7 kips and higher loads, which can be attributed to the cracking of the joint.

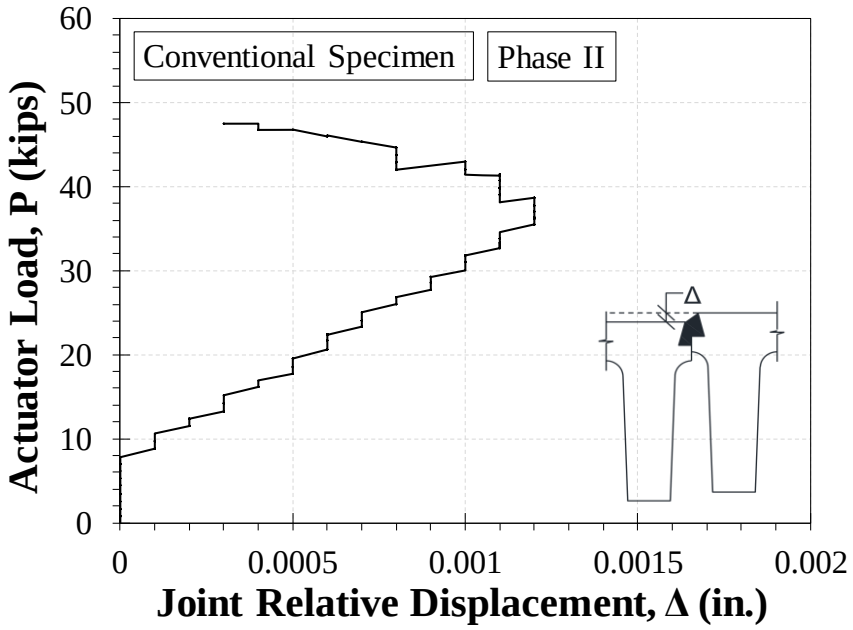

Figure 7-10. Longitudinal Joint Relative Displacement for Conventional Double-Tee Bridge Specimen during Joint Crack Strength Testing

Girder-to-girder joint rotations (Fig. 7-11) in the transverse direction of the bridge were measured 1.5 ft away from the midspan as discussed in Sec. 7.2.1.1. The measured joint rotation was 0.24 degrees at the peak load of 48.5 kips, which was significant compared to that of fatigue loading confirming that the joint cracked. If the test was continued by applying larger loads, the rotation would have been increased significantly in a nonlinearly manner. However, the test was stopped to perform the rehabilitation.

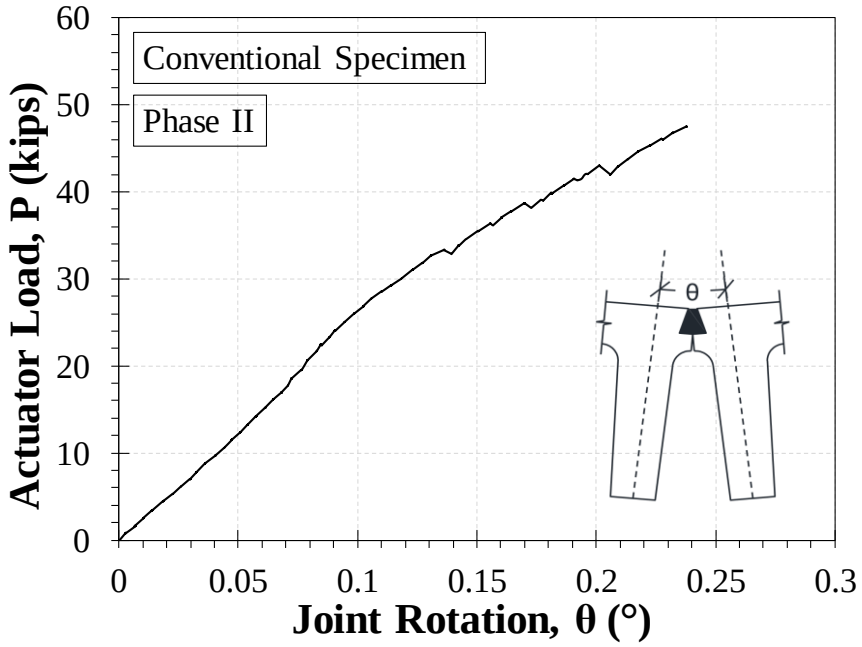

Figure 7-11. Girder-to-Girder Joint Rotation for Conventional Double-Tee Bridge Specimen during Joint Crack Strength Testing

7.2.2 Rehabilitated Double-Tee Bridge Test Specimen

After completion of the tests on the conventional double-tee bridge specimen, the bridge girder-to-girder longitudinal joint was rehabilitated using two methods discussed in the previous chapters. The longitudinal joint for the half length of the bridge was rehabilitated using the UHPC pocket detailing and the other half with the continuous LMC detailing.

The rehabilitated bridge specimen was initially tested under 500,000 cycles of the AASHTO Fatigue II loading, which is referred to as "Phase III" hereafter, followed by additional 100,000 cycles of the AASHTO Fatigue I loading as Phase IV. Finally, the rehabilitated bridge was monotonically loaded to failure in Phase V.

7.2.2.1 Cracks of Rehabilitated Double-Tee Bridge Prior to Testing

Several cracks were observed in the transverse direction of the bridge in LMC of the continuous joint prior to testing (Fig. 7-12). The cracks were spaced 12-in. apart along the length of the continuous joint. The LMC cracks may be due to the expansion of the grout during the high-temperature rapid curing and restrained boundaries (adjacent girders) causing induced stresses at the time of cooling.

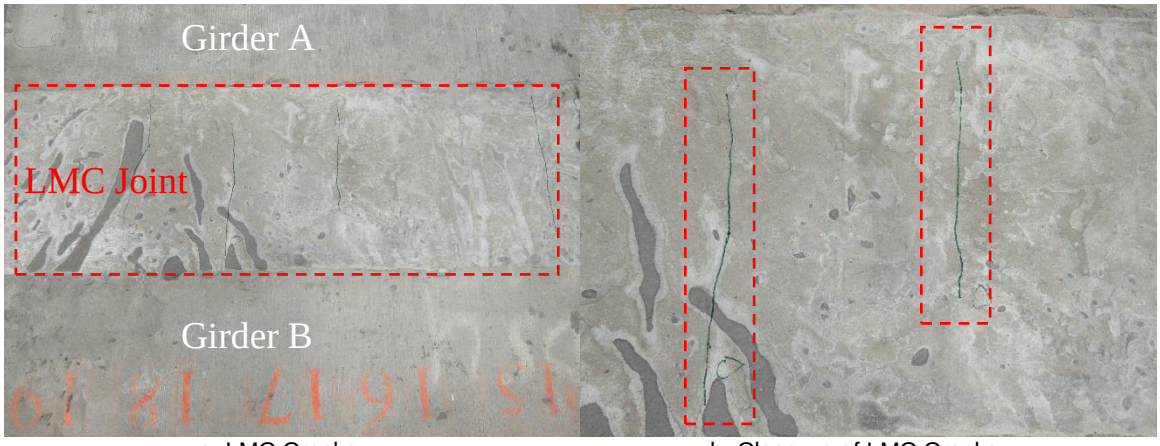

a. LMC Cracks b. Close-up of LMC Cracks

Figure 7-12. Transverse Cracks in the Continuous Joint of Rehabilitated Double-Tee Bridge Specimen Prior to Testing

7.2.2.2 Phase III: Fatigue II Testing of Rehabilitated Double-Tee Bridge

The fatigue II testing was carried out by applying 500,000 cycles of 21-kip load at the midspan of the bridge with a frequency of one cycle per second. Stiffness tests were performed every 50,000 cycles. The stiffness test was performed by monotonically loading the specimen up a force of 21 kips.

Water was seeping through the aforementioned cracks before the initiation of the fatigue II testing (Fig. 7-13a). The water seepage beneath the joint reduced through 500,000 cycles (Fig. 7-13b) maybe because of the rehydration of LMC when water penetrated. No additional leaks or any other damage was observed during the fatigue

testing. Furthermore, the pocket joints filled with UHPC did not damage or leak during the entire 500,000 cycles of the fatigue II testing (Fig. 7-14a and b).

a. Leak in LMC Before Testing

b. Leak in LMC After Testing

c. Before Testing – Top of Bridge

d. After Testing – Top of Bridge

Figure 7-13. Damage of Continuous Joint of Rehabilitated Double-Tee Bridge Specimen during Fatigue II Testing

a. Before Testing – Underneath of Bridge b. After Testing – Underneath of Bridge

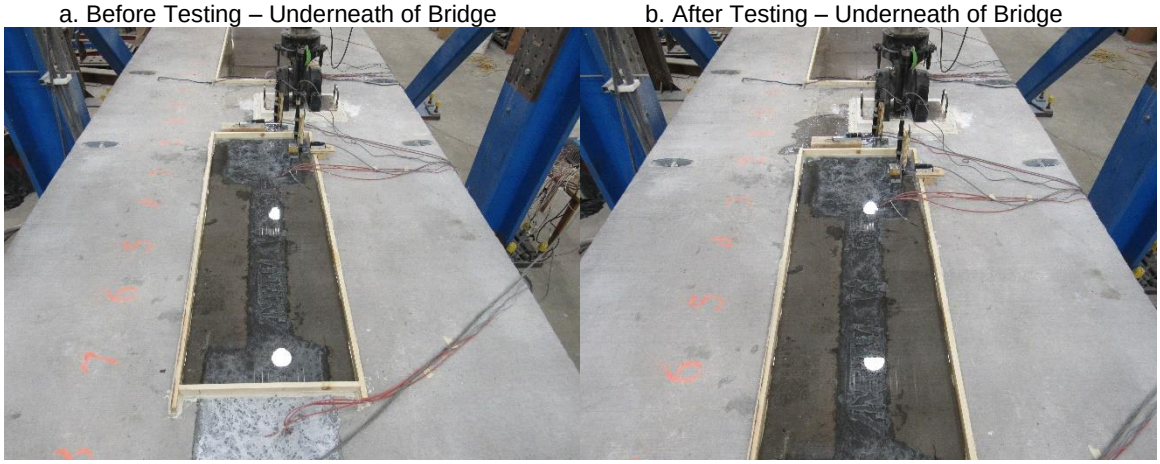

c. Before Testing – Top of Bridge d. After Testing – Top of Bridge

Figure 7-14. Damage of UHPC Pocket Joints of Rehabilitated Double-Tee Bridge Specimen during Fatigue II Testing

Figure 7-15 shows the measured stiffness versus the number of the load cycles during the Fatigue II testing. The stiffness of the specimen was determined as explained in section 7.2.1.1. It can be seen that the bridge stiffness essentially remained constant during the fatigue II testing. Furthermore, no damage of the pocket joint, continuous joint, or any other members of the bridge through 500,000 cycles of loading was observed.

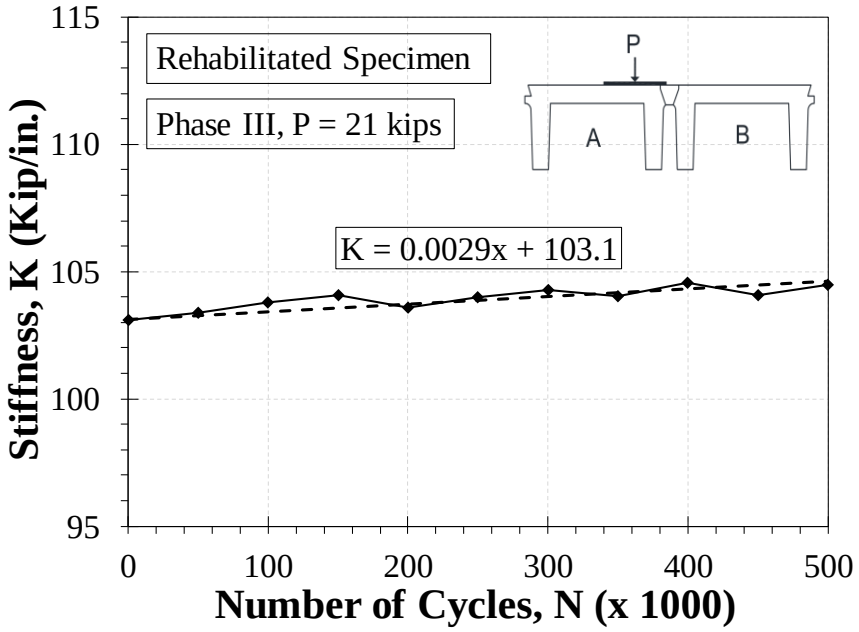

Figure 7-15. Stiffness Degradation during Fatigue II Testing of Rehabilitated Double-Tee Bridge Specimen

Girder-to-girder joint relative vertical and horizontal displacements were measured as shown in Figure 7-16. It can be seen that the measured joint relative displacements were negligible throughout the Fatigue II testing indicating no girder-to-girder joint damage.

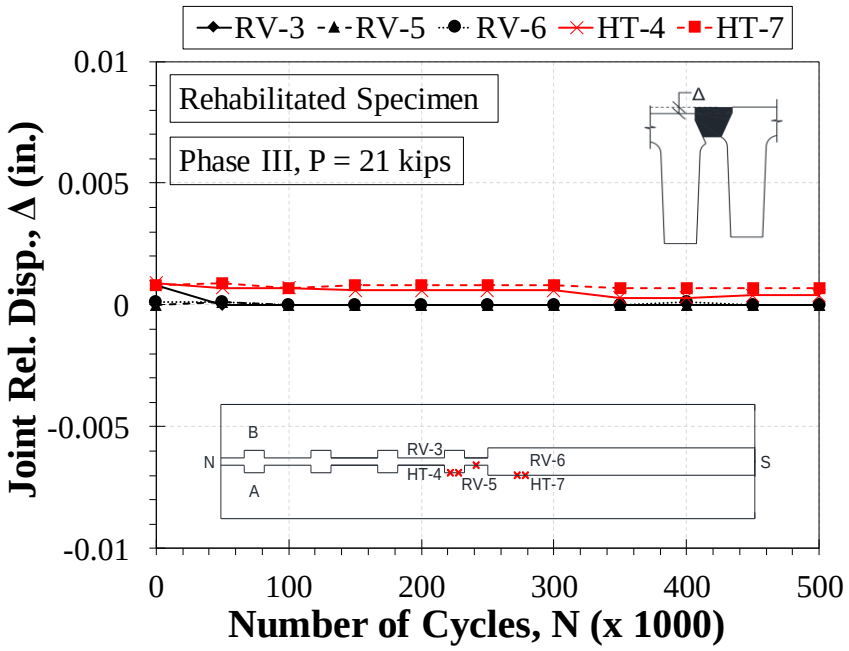

Figure 7-16. Longitudinal Joint Relative Displacement for Rehabilitated Double-Tee Bridge Specimen during Fatigue II Testing

Girder-to-girder joint rotations (Fig. 7-17) in the transverse direction of the bridge were also measured 1.5 ft away from the midspan. The rotations were measured as explained in section 7.2.1.1. It can be seen that the measured joint rotations were negligible throughout the Fatigue II testing indicating the girder-girder joint did not degrade.

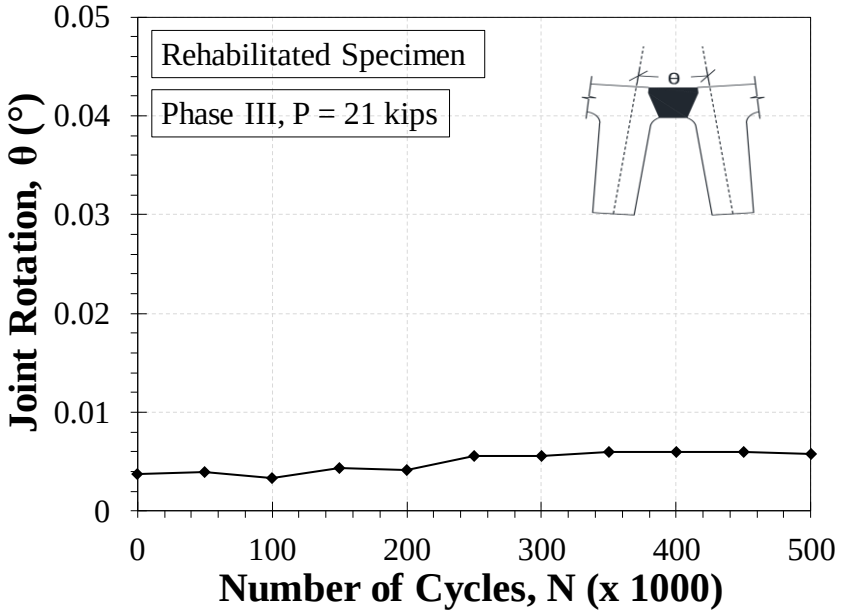

Figure 7-17. Girder-to-Girder Joint Rotation for Rehabilitated Double-Tee Bridge Specimen during Fatigue II Testing

7.2.2.3 Phase IV: Fatigue I Testing of Rehabilitated Double-Tee Bridge

The AASHTO fatigue I loading consisted of a 42-kip load cyclically applied at the midspan of the bridge with a frequency of one cycle per second for a total of 100,000 cycles. Stiffness tests were initially performed after every 25,000 cycles up to 50,000 cycles then at every 10,000 cycles for the remaining cycles to better monitor the bridge performance. The stiffness test was performed by monotonically loading the specimen up a force of 21 kips.

Figure 7-18 shows the joint condition after the fatigue I testing. No new damage or leaks beyond the LMC prior to testing cracks discussed in section 7.2.2.1 were observed in LMC continuous joint or the UHPC pocket joints throughout 100,000 cycles of the Fatigue I testing.

a. LMC Continuous Joint - underneath of Bridge

b. UHPC Pocket Joint - underneath of Bridge

c. LMC Continuous Joint – Top of Bridge

d. UHPC Pocket Joint – Top of Bridge

Figure 7-18. Damage of Rehabilitated Double-Tee Bridge Specimen after Fatigue I Testing

Figure 7-19 shows the measured stiffness versus the number of the load cycles during the Fatigue I testing. The stiffness of the specimen was determined as explained in section 7.2.1.1. It can be seen that the bridge stiffness essentially remained constant during the fatigue I testing.

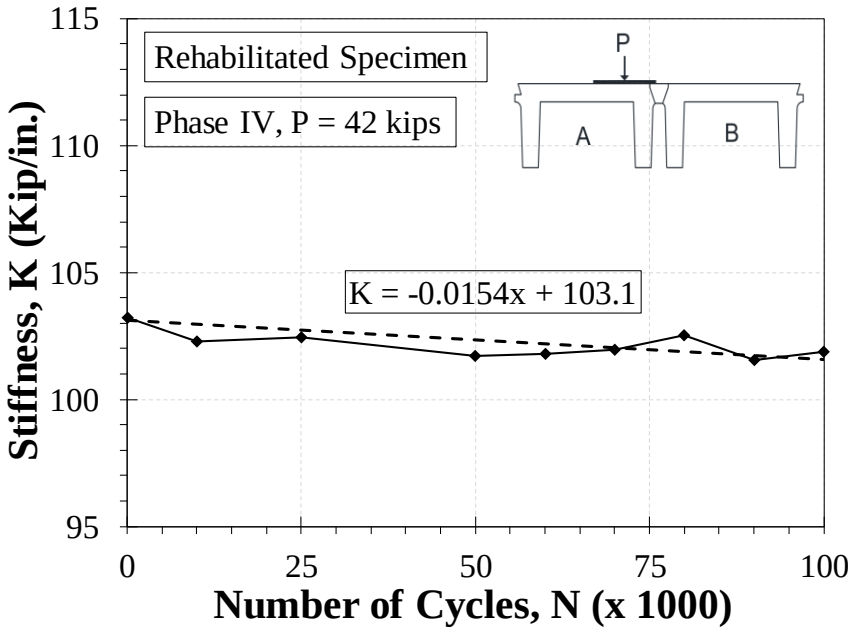

Figure 7-19. Stiffness Degradation for Rehabilitated Double-Tee Bridge Specimen during Fatigue I Testing

Figure 7-20 shows the girder-to-girder joint relative vertical and horizontal displacements. It can be seen that the measured joint relative displacements were negligible throughout the Fatigue I testing indicating no girder-to-girder joint damage.

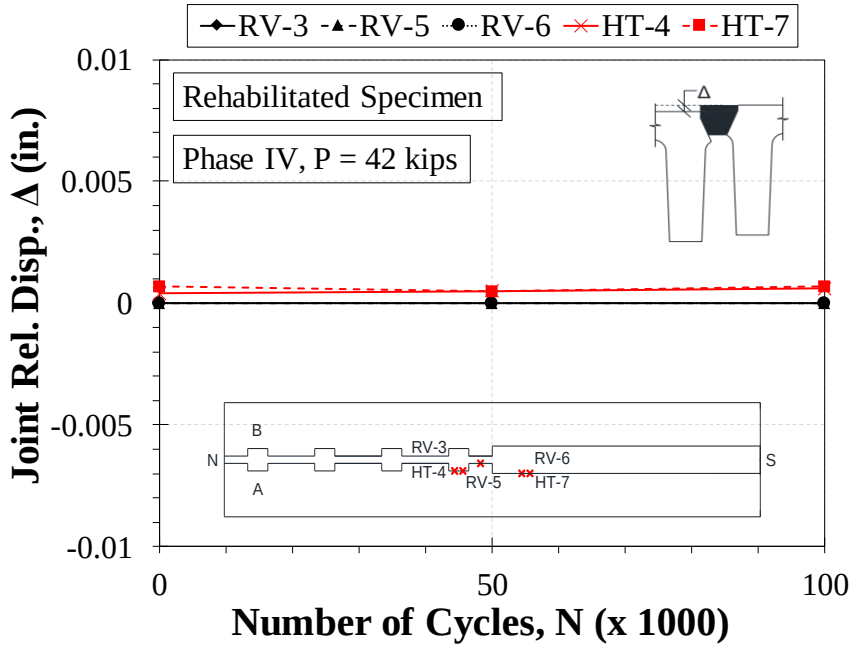

Figure 7-20. Longitudinal Joint Relative Displacement for Rehabilitated Double-Tee Bridge Specimen during Fatigue I Testing

Girder-to-girder joint rotations (Fig. 7-21) in the transverse direction of the bridge were also measured 1.5 ft away from the midspan. The rotations were measured as explained in section 7.2.1.1. It can be seen that the measured joint rotations were negligible throughout the Fatigue I testing indicating the girder-girder joint did not degrade.

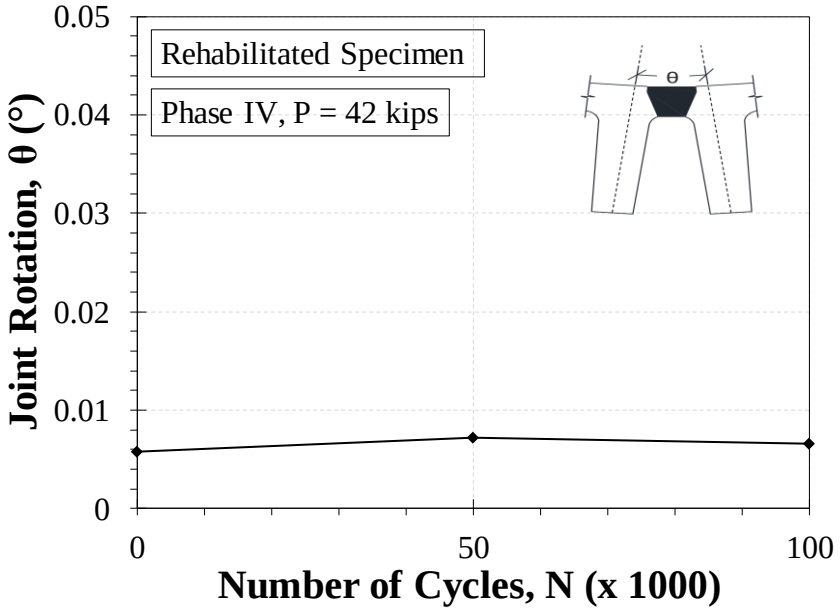

Figure 7-21. Girder-to-Girder Joint Rotation for Rehabilitated Double-Tee Bridge Specimen during Fatigue I Testing

7.2.2.4 Phase V: Strength (Ultimate) Testing of Rehabilitated Double-Tee Bridge

The rehabilitated specimen was monotonically loaded at the midspan of the bridge under a displacement controlled loading protocol to failure (Fig. 7-22). The mode of failure of the bridge was compression failure of the concrete at the girder top flange in a ductile manner indicating that the both rehabilitated joints were sufficiently strong to avoid connection failure and to make the bridge behaves monolithically. The first crack was observed in the west stem of girder A (loaded girder) at the midspan during loading to 60 kips (Fig.7-22a). New cracks formed, extended, and widened on the stems of the

both girders at higher displacement demands (Fig. 7-22b). Both girders exhibited ductile failure with a displacement capacity of 9.5 in. (Fig. 7-22c and d). No new damage beyond the LMC prior to testing cracks discussed in section 7.2.2.1 was observed in the LMC continuous joint or the UHPC pocket joints at the bridge failure (Fig. 7-22e and f).

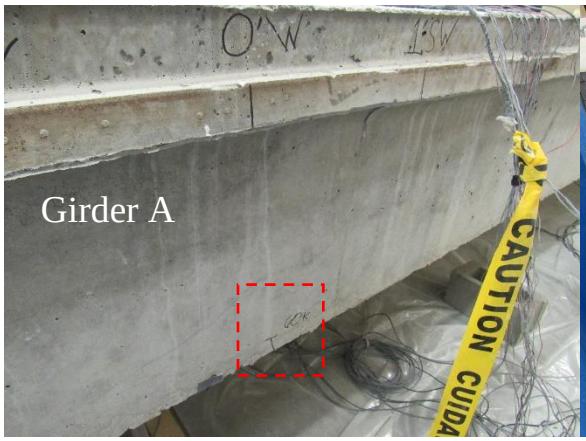

a. First Crack during loading to 60 kips on West Girder

b. East Side of Girder B Damage at 1.5-in. Deflection

c. Compressive Failure of Concrete at 9.5-in. Deflection

d. Bridge Condition at Failure

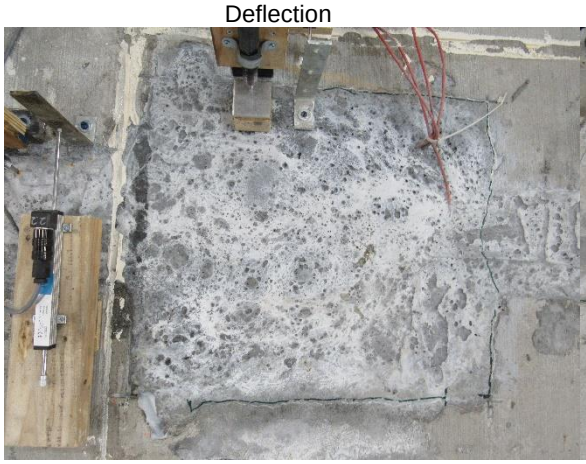

e. UHPC Pocket Joint after Testing

f. LMC Continuous Joint after Testing

Figure 7-22. Damage of Rehabilitated Double-Tee Bridge Specimen during Strength Testing

Figure 7-23 shows the force-displacement relationship for each girder (A and B) measured at the midspan. It can be seen that both girders acted similarly in a ductile fashion indicating monolithic behavior for the rehabilitated joints. The girders reached the AASHTO Service I limit state without cracking and surpassed the AASHTO Strength I limit state indicating sufficient structural performance. At the peak load of 113.9 kips, the deflection of girder A and B was 7.56 and 7.14 in., respectively. The bridge failed at the girder A displacement of 9.55 in. and the actuator load of 111.1 kips. The first girder crack was observed during loading the bridge to 60 kips. The load amplitude at which the girders cracked based on the strain data (discussed later, Fig. 7-25) was estimated to be 53.8 kips. Overall, both rehabilitation methods found to be structurally viable.

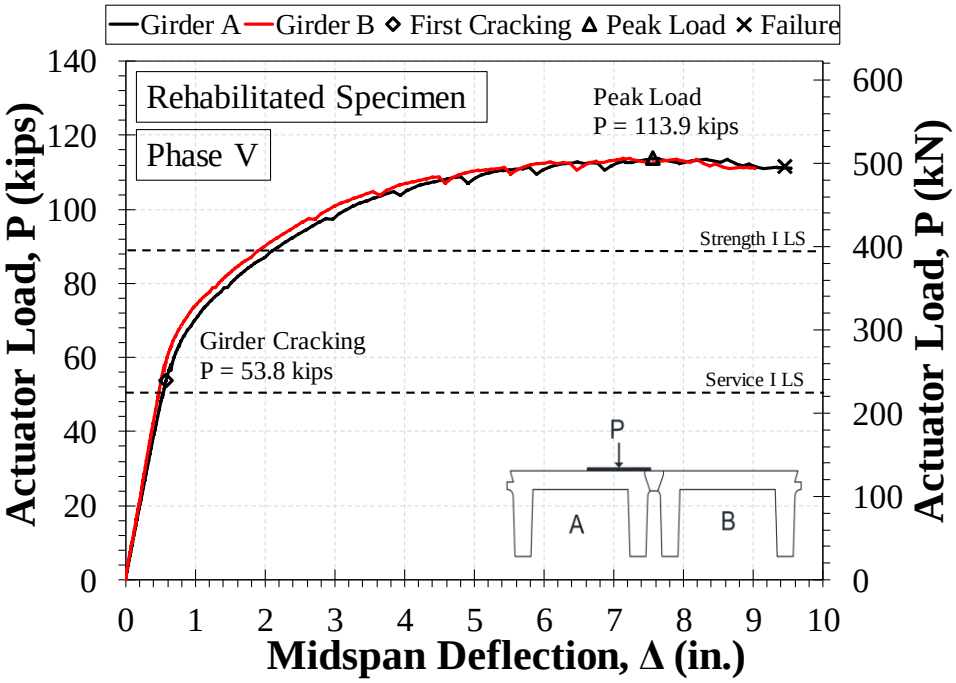

Figure 7-23. Force-Displacement Relationship for Rehabilitated Double-Tee Bridge Specimen during Strength Testing

Load cells were used to measure south end reactions of the girders, one load cell per stem. The reactions were used to determine the girder load distribution based on a percentage of the applied load (P/2 per girder end). The girder end reactions at the beginning of the fatigue testing, after the fatigue II and fatigue I testing, and at the AASHTO service I and strength I limit states were compared in Fig. 7-24. It can be seen that the load distribution remained approximately the same throughout all phases of testing indicating sufficient girder-to-girder performance for the rehabilitated joints.

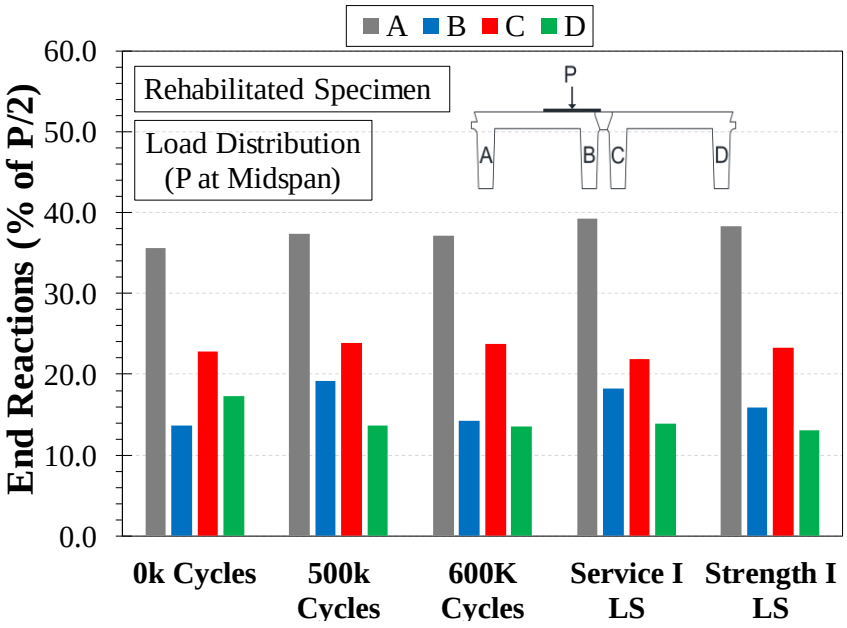

Figure 7-24. Girder Load Distribution for Rehabilitated Double-Tee Bridge Specimen

Figure 7-25 shows the strains of the prestressing strands and concrete in the flange of the loaded girder (A) during the strength testing. Cracking of girders can be identified using strain data where there is a sudden increase in reinforcement strains. From Fig. 7-25, it can be concluded that that first girder cracking occurred at an actuator load of 53.8 kips. Prestressing losses were not measured in this project. The estimated initial strain from 31-kip pretensioning was 7,109 micro-strain from structural mechanics. The yield strain of Grade 270 tendons is 8,772 micro-strain. Based on these assumptions, the yield

strain of the extreme tendon was estimated to be 1,663 micro-strain, which corresponds to an actuator load of 71.2 kips. The maximum strain in the extreme tendon in the right stem of girder A at the peak load of 113.9 kips was 22,317 micro-strain. The maximum measured tendon strain at the girder failure was 30,601 micro-strain. The maximum compressive strain in the concrete was -114.4 micro-strain at a load of 60.2 kips. The neutral axis of the section shifted upward when load increased. For example, the neutral axis at a load of 79 kips was at a depth of 3.5 in. from the top of the girder where the embedded concrete strain gauges were installed. The unloaded section neutral axis was at a depth of 7.75 in. from the top of the girder.

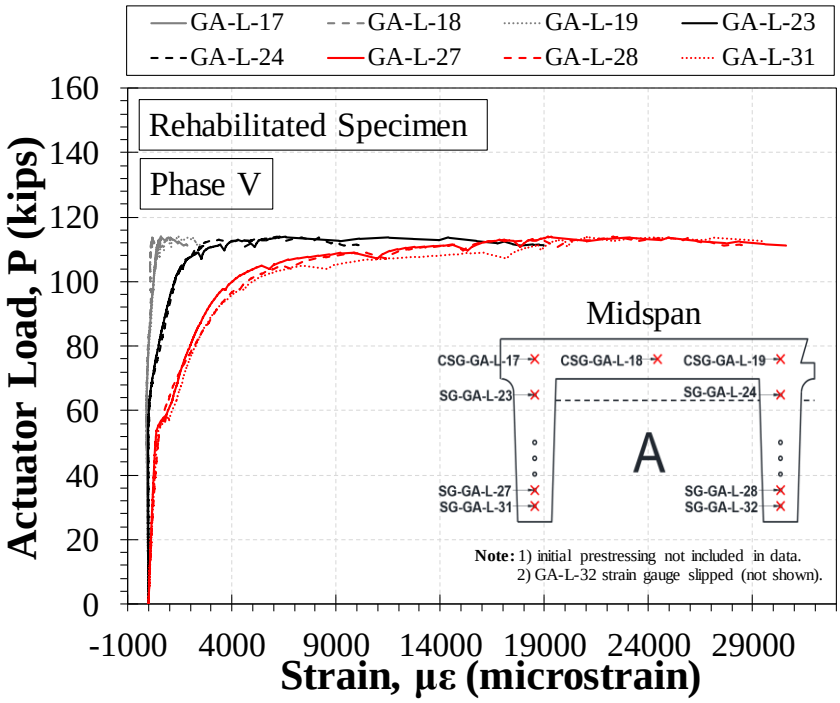

Figure 7-25. Measured Strains of Loaded Girder in Rehabilitated Double-Tee Bridge Specimen during Strength Testing

Figure 7-26 shows the strains of the prestressing strands and concrete in the flange of girder B during the strength testing. From Fig. 7-25, it can be concluded that the first

girder cracking occurred at an actuator load of 55.4 kips. The yield strain of the extreme tendon was estimated to be 1,663 micro-strain, which corresponds to an actuator load of 75.6 kips. The maximum strain in the extreme tendon in the left stem of girder B at the peak load of 113.9 kips was 23,552 micro-strain. The maximum measured tendon strain at the girder failure was 31,478 micro-strain. The maximum compressive strain in the concrete was -122.6 micro-strain at a load of 68.6 kips. The neutral axis of the section shifted upward to 3.5-in. depth (location of embedded concrete strain gauges) from the top of the girder at a load of 92.5 kips. It can be seen that the maximum tendon tensile strain in girder B is 3% more than that in girder A, and the load at first cracking in girder B is 3% higher than that in Girder A. Overall, both girders behaved monolithically and the difference is insignificant.

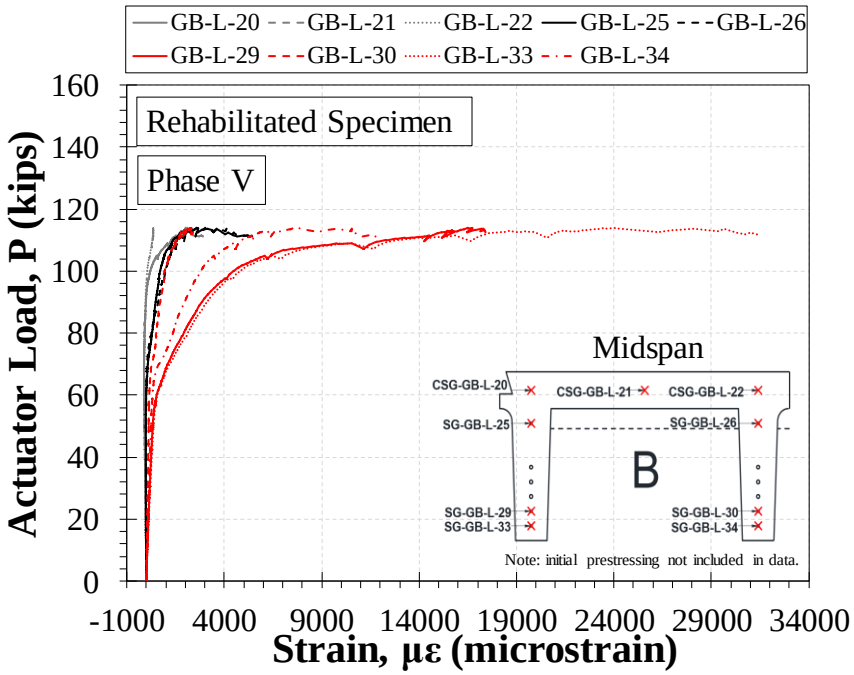

Figure 7-26. Measured Strains of Girder B in Rehabilitated Double-Tee Bridge Specimen during Strength Testing

Several strain gauges were also installed on the reinforcement of the rehabilitated joints. Figure 7-27 shows the strains of the transverse reinforcement in the UHPC

pockets of the rehabilitated bridge during the strength testing. The reinforcement strains were higher in pocket P4 compared to the other pockets. The maximum pocket reinforcement strain at the girder failure was 1,839 micro-strain for the girder exposed steel D8 wires and 1,471 micro-strain for the pocket new No.4 steel bars. For pocket P3, the maximum reinforcement strain at the girder failure was 132 micro-strain in the exposed D8 wires and 767 micro-strain in the No.4 bars. The theoretical yield strain of a Grade 70 steel wire and a Grade 60 steel bars is 2,414 and 2,069 micro-strain, respectively. Therefore, it can be concluded that none of the UHPC pocket reinforcement yielded even at the girder failure indicating sufficient capacity-protected performance of the joint.

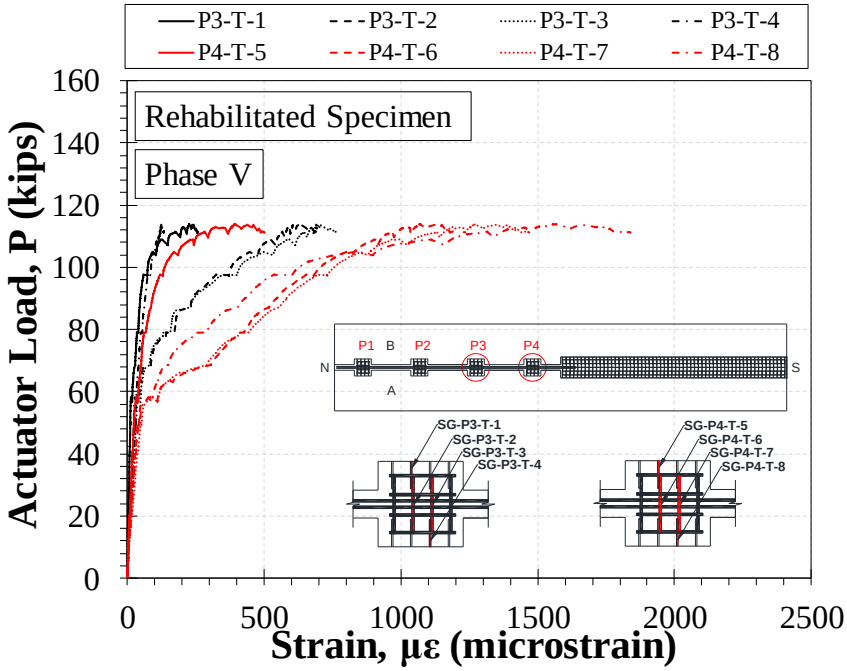

Figure 7-27. Measured Strains of Transverse Reinforcement in UHPC Pockets of Rehabilitated Double-Tee Bridge Specimen during Strength Testing

Figure 7-28 shows the strains in the transverse reinforcement of the LMC continuous joint during the strength testing. The strains of one of the steel wires located under the

applied load were higher than the others mainly due to stress concentration. The strain of this wire at the girder failure was 2,949 micro-strain, which was 20% higher than the wire yield strain. The strain of another wire located 12 in. away from the point load at the girder failure was 1,272 micro-strain, which was 50% lower than the wire yielding. Therefore, reinforcing steel wires in the rehabilitated continuous joints of double-tee bridges are not expected to yield even under the AASHTO strength I limit state.

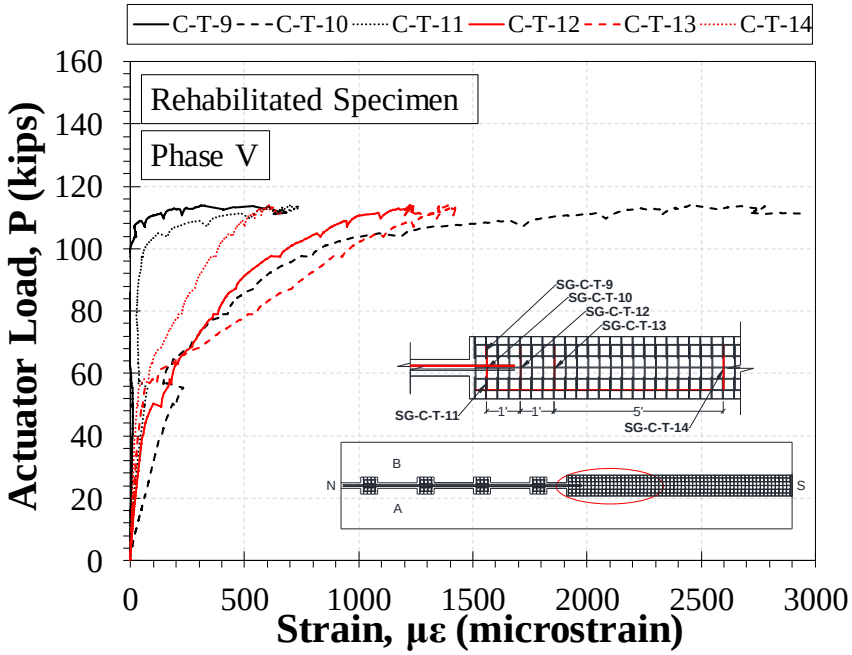

Figure 7-28. Measured Strains of Transverse Reinforcement in LMC Continuous Joint of Rehabilitated Double-Tee Bridge Specimen during Strength Testing

Figure 7-29 shows the strain in the longitudinal reinforcement in both the pocket and continuous joints of the rehabilitated bridge during the strength testing. The reinforcement strains were all compressive. The maximum measured compressive strain at the girder failure was -777 micro-strain, which is in the linear-elastic range.

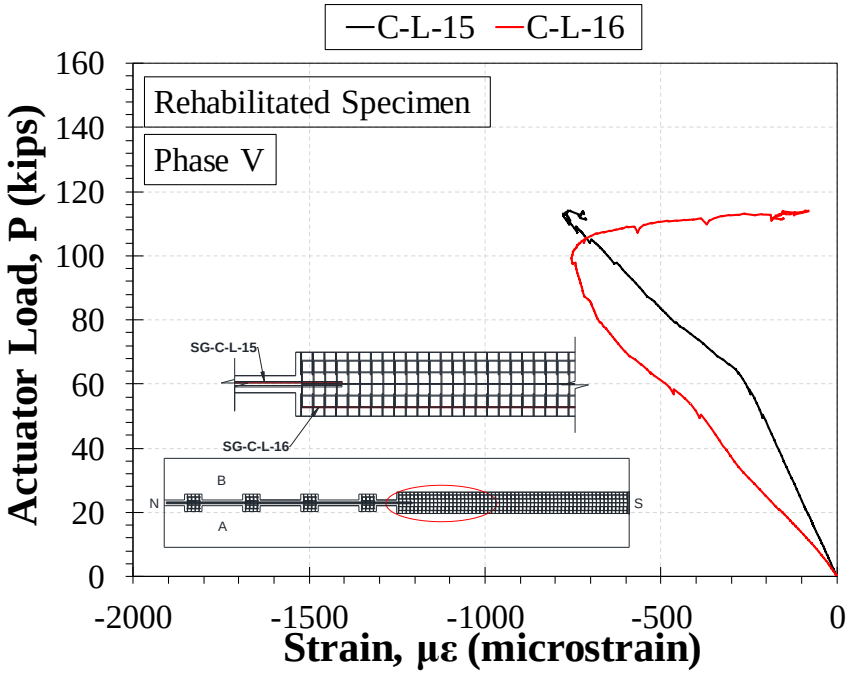

Figure 7-29. Measured Strains of Joint Longitudinal Reinforcement in Rehabilitated Double-Tee Bridge Specimen during Strength Testing

Figure 7-30 shows the girder-to-girder joint relative displacements during strength testing. The girder-to-girder relative vertical displacement closest to the applied point (RV-5) at the girder failure was 0.0062 in. Based on the measured data, it can be inferred that the UHPC joint under the applied load and between the two UHPC pockets cracked at an actuator load of 56.8 kips, which was higher than the AASHTO Service I limit state of 51 kips. Note that no crack was observed for the UHPC joint at this load level. Therefore, the relative joint displacement was considered insignificant. The joint relative vertical displacement at other locations of at the pocket and continuous joints were negligible.

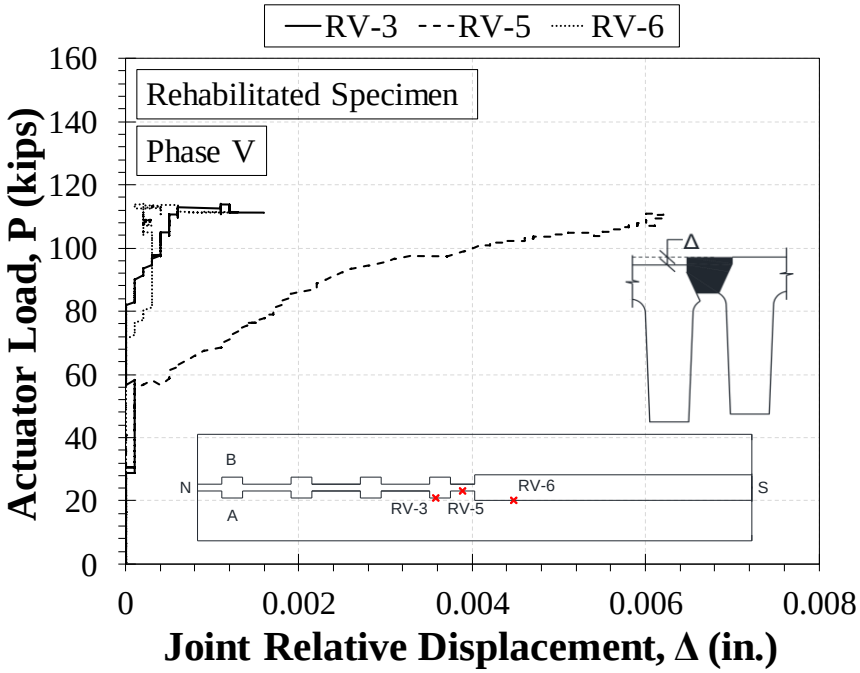

Figure 7-30. Girder-to-Girder Joint Relative Displacement for Rehabilitated Double-Tee Bridge Specimen during Strength Testing

Girder-to-girder joint rotations (Fig. 7-31) in the transverse direction of the bridge were measured 1.5 ft away from the midspan as discussed in Sec. 7.2.1.1. The measured joint rotation was 0.009 degrees at the girder failure, which was negligible.

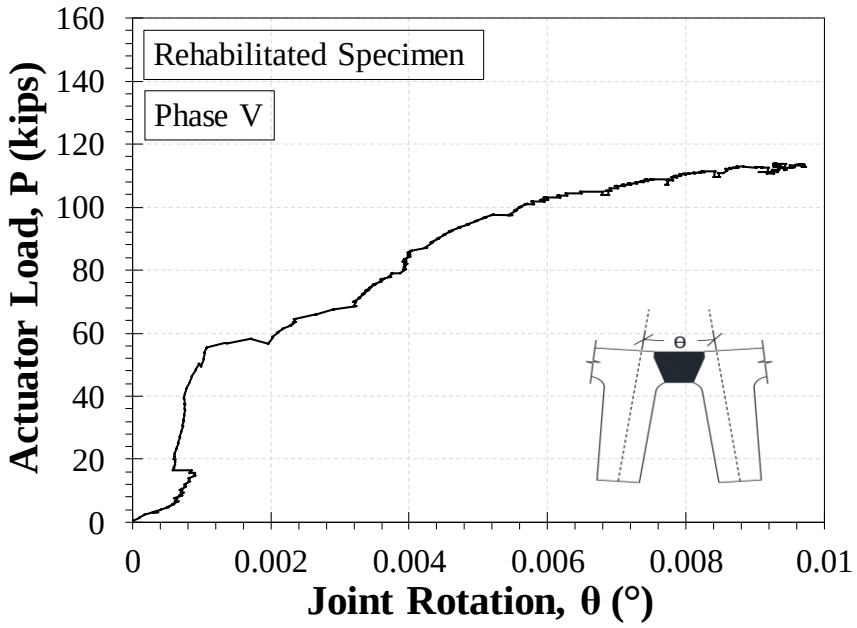

Figure 7-31. Girder-to-Girder Joint Rotation for Rehabilitated Double-Tee Bridge Specimen during Strength Testing

8. Evaluation of Double-Tee Longitudinal Joint Rehabilitation Methods

This chapter includes the evaluation of conventional and rehabilitated double-tee bridges in terms of structural performance and suitability of rehabilitated longitudinal girder-to-girder joints. The performance under the service, fatigue, and strength limit states, the constructability, and the cost of the proposed rehabilitation methods are discussed herein.

8.1 Performance of Double-Tee Bridges under Different Limit States

8.1.1 Double-Tee Bridge Test Specimens

A full-scale 40-ft long double-tee bridge incorporating the conventional girder-to-girder joint detailing was first tested to damage the joints. Subsequently, the bridge joint was rehabilitated using two methods. The rehabilitated bridge was then tested under the AASHTO Fatigue II, Fatigue I, Service, and Strength limit states to investigate the performance of the rehabilitated bridge and to comment on the suitability of the proposed joint detailing.

The response of the rehabilitated bridge tested in the present study was compared with that of two double-tee bridges each incorporating either a conventional or a continuous girder-to-girder detailing (Wehbe et al., 2016). The conventional girder-to-girder joint detailing consisted of discrete steel plates welded to embedded anchors in a shear key, which was then filled with a non-shrink grout. The continuous joint detailing

(suited for new construction not rehabilitation) consisted of extending the wire mesh outside the double-tee girders and lap-splicing the extended wire mesh along the entire length of the bridge then filling the joint with a non-shrink grout. Wehbe et al. (2016) evaluated the performance of both the conventional girder-to-girder detailing of a double-tee bridge and the new continuous joint detailing through full-scale testing of double-tee bridges. The geometry, detailing, material properties, and testing procedures of the bridges tested by Wehbe et al. (2016) were the same as those for the rehabilitated bridge tested in the present study.

8.1.2 Observed Damage

Transverse cracks were observed in latex modified concrete (LMC) utilized in the continuous joint of the rehabilitated bridge prior to testing the bridge (Fig. 8-1). The cracks were spread along the entire length of the continuous joint and spaced at 12 inches. The cracks were deep allowing water to penetrate through the joint. These cracks had no effect on the structural performance of the continuous joint. Nevertheless, LMC is not recommended for this project since it is not durable when used in the continuous rehabilitation joint detailing. No cracks or leaks were observed in ultra-high performance concrete (UHPC) incorporated in the pocket joint prior or during all phases of the testing. UHPC was found to be a durable and structurally viable material for this project. Therefore, the filler material in either the pocket or continuous rehabilitation detailing shall be only UHPC for field applications.

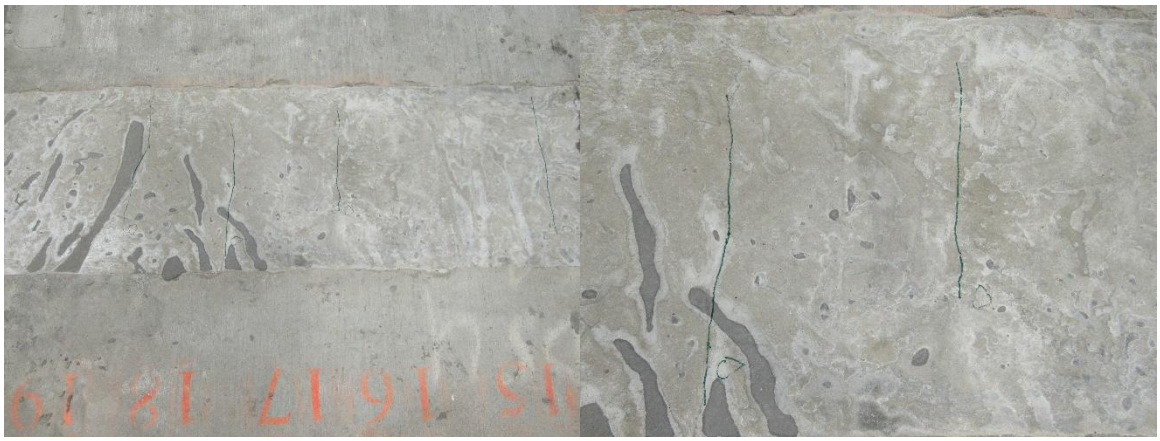

a. LMC Cracks b. Close-up of LMC Cracks

Figure 8-1. Transverse Cracks of Continuous Joint in Rehabilitated Double-Tee Bridge

Wehbe et al. (2016) observed no cracks or leaks in the longitudinal joint of the continuous double-tee specimen throughout fatigue and strength testing. The longitudinal joint of the conventional specimen started leaking at 19,500 load cycles, grout spalled at 43,000 load cycles, and the connection failed at a load cycle of 62,000 during the AASHTO fatigue I testing. The conventional joint failed during the strength testing by headed-stud pullout before reaching the AASHTO strength limit state requirements.

8.1.3 Fatigue Performance

Approximately 411,000 trucks will pass a bridge located on South Dakota (SD) local roads for a 75-year design life based on an average daily truck traffic (ADTT) of 15. The rehabilitated test bridge was subjected to 500,000 cycles of the AASHTO Fatigue II loading at the midspan followed by an additional 100,000 cycles of the AASHTO Fatigue I loading. The point load applied at the midspan was equivalent to the maximum moment that two interior double-tee girders would experience under truck loading for limit states specified in AASHTO (2013). The rehabilitated bridge specimen experienced no stiffness degradation throughout the fatigue testing (Fig. 8-2 and 8-3). The total of

600,000 fatigue cycles is equivalent to 110 years of service for a bridge local bridge in SD. No damage beyond those discussed for LMC was observed in the fatigue testing indicating sufficient structural performance for the rehabilitated bridge.

The bridge with the conventional longitudinal joint (Wehbe et al, 2016) degraded significantly under 100,000 cycles of the AASHTO Fatigue II loading (Fig. 8-2) and 60,000 cycles of the AASHTO Fatigue I loading (Fig. 8-3) confirming that the conventional longitudinal joint detailing is not structurally adequate for long-term performance. The double-tee bridge specimens with either rehabilitated or continuous girder-to-girder detailing performed sufficiently under fatigue loading and are suitable for field applications.

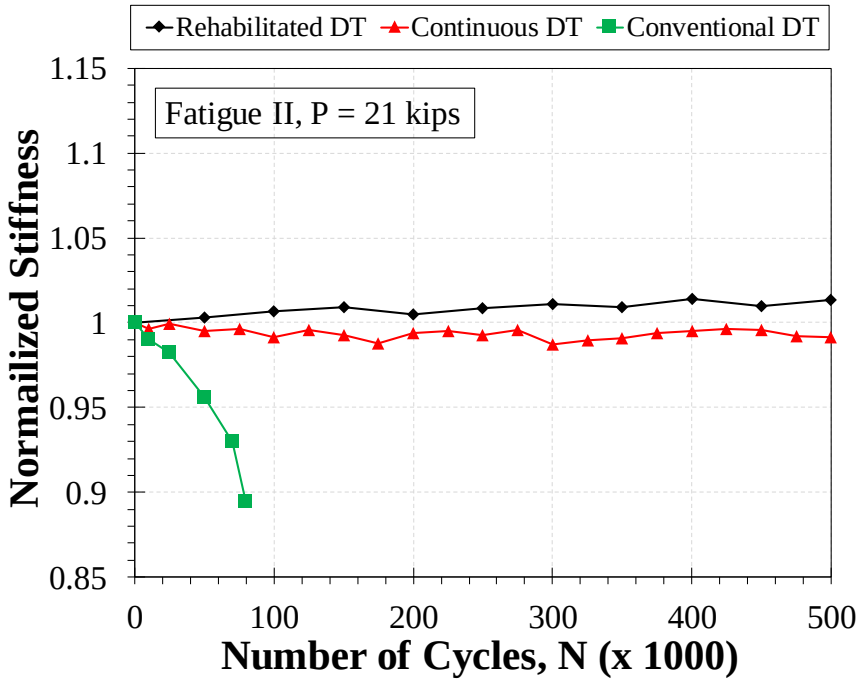

Figure 8-2. Stiffness Degradation for Different Double-Tee Bridges under AASHTO Fatigue II Loading

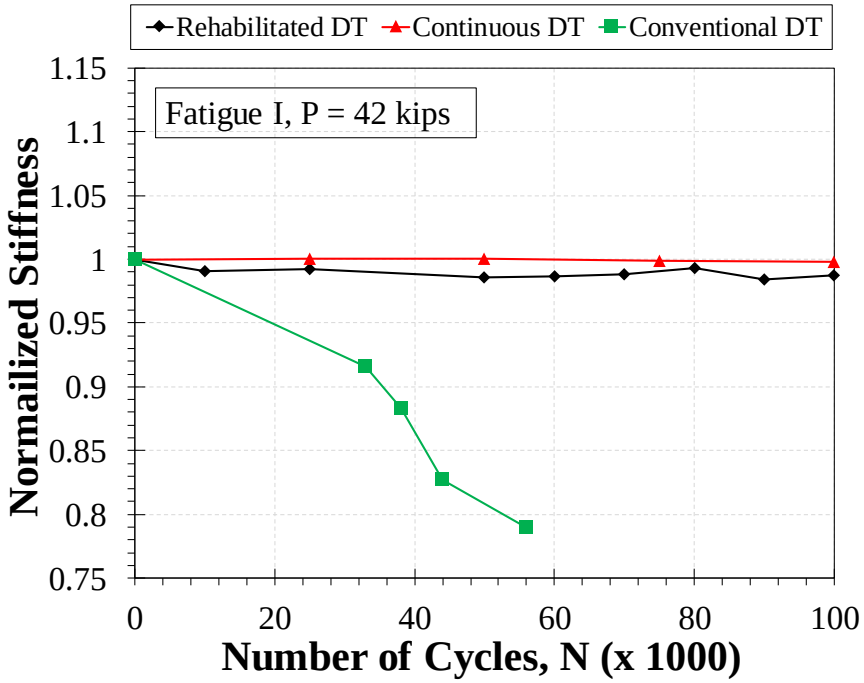

Figure 8-3. Stiffness Degradation for Different Double-Tee Bridges under AASHTO Fatigue I Loading

8.1.4 Force-Displacement Relationships

Figure 8-4 shows the force-displacement relationships for the rehabilitated double-tee bridge, the conventional double-tee bridge, and the double-tee bridge with continuous joint detailing. The AASHTO Service I and Strength I limit states are also included in the figure. The rehabilitated specimen did not crack under the Service I limit state. The first crack of the girders of the rehabilitated bridge was at a force of 53.8 kips. The load carrying capacity of the rehabilitated bridge was 113.9 kips, which was 28% higher than the Strength I limit state indicating sufficient performance. The failure mode of the rehabilitated bridge was compressive failure of the girder flange concrete at 9.55 in. of displacement in a ductile manner.

The bridge with the continuous detailing (Wehbe et al., 2016) performed similarly to the rehabilitation bridge in terms of force-displacement response (Fig. 8-4). The force-

displacement relationship was approximately the same as that for the rehabilitated specimen with 113-kip load capacity and 9 in. of displacement capacity. However, the conventional bridge was insufficient since it did not meet the AASHTO limit state requirements. The girders of the conventional double-tee specimen cracked at 40 kips prior to the Service I limit state of 51 kips. The girder-to-girder joint failed at a load equivalent to 70% of the Strength I limit state where the headed studs of the embedded steel plates pulled out from the girder concrete.

Overall, the performance of the rehabilitated bridge was found to be acceptable since the rehabilitated bridge behaved as a monolithic cast-in-place bridge. Both rehabilitation methods, pocket and continuous joints, are structurally viable, but UHPC should only be used as filled material due to improved durability.

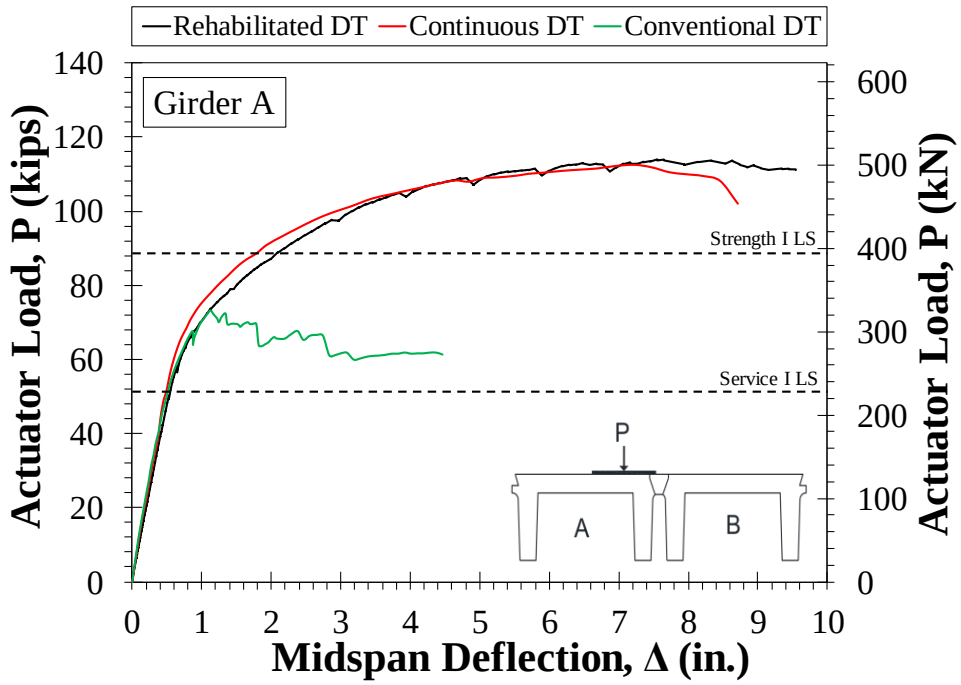

Figure 8-4. Force-Displacement Relationship for Loaded Girders of Different Double-Tee Bridges

8.2 Constructability of Proposed Joint Rehabilitation Methods

This section discusses the constructability of the pocket and continuous joint rehabilitation methods.

8.2.1 Method of Demolishing

The perimeters of the pocket and continuous joint were saw-cut using a portable gas powered diamond-blade concrete saw. This process was very easy. The longitudinal joint was demolished using hammer-chipping at a 45-degree inclination. The hammer-chipping was somewhat tedious since the girders were new and relatively undamaged and built with concrete with a compressive strength of 9,000 psi. The hammer-chipping was more effective when using a 30-lb pneumatic hammer-chipper. However, 30-lb pneumatic hammer-chippers should not be used when exposing the reinforcement and finishing the joint. Some minor spalling of the concrete stem was noticed during demolishing (Fig. 8-5a). The disturbed areas were patched with the filler material using a formwork consisting of Styrofoam and plywood (Fig. 8-5b). The formwork was installed from the top and removed relatively easily from the bottom of the bridge. A significant amount of concrete debris fell through the joint during demolition. If debris is not allowed to fall underneath the bridge, a catcher could be placed underneath of the bridge. Overall, the hammer-chipping demolition process was found to be a viable method for field applications for the both continuous and pocket joints.

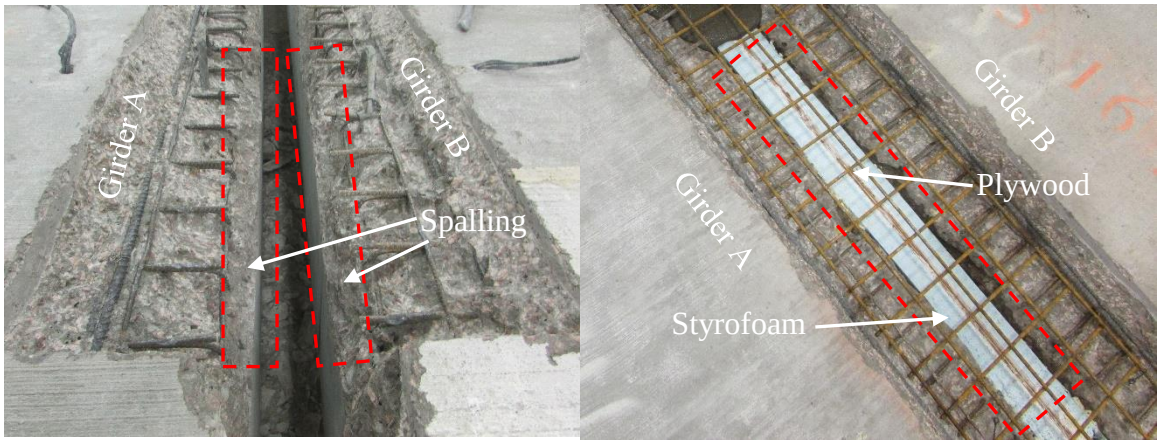

a. Girder Concrete Spalling b. Formwork Placement

Figure 8-5. Joint Preparation for Rehabilitation

8.2.2 Construction of Continuous Joint

The girder concrete was hammer-chipped in two stages each on a 25% of the length of the bridge to form the continuous joint. This was done to improve the overall stability of the bridge by avoiding stem-to-deck connection failure. The wire mesh installation was easy and relatively fast. The time to demolish and prepare the continuous joint was 2.5 times longer than that for the pocket joint.

Premix latex modified concrete (LMC) was used in the continuous joint as the filler material. The mix was simple and fast since the premix LMC just requires water. The set time of LMC was only 30 minutes, which requires advanced planning and proper management of workforce in the field.

8.2.3 Construction of Pocket Joints

The girder concrete was hammer-chipped to form the pockets. Preparation of the pocket joints was easier and 2.5 times faster than the continuous joint. The installation of the new reinforcing steel bars was relatively easy and fast.

Premix ultra-high performance concrete (UHPC) was used to fill the pockets. The UHPC mix is more involved and time consuming compared to conventional grout or LMC since it requires adding premix powder, steel fibers, plasticizer, and water. Mortar mixers are required for mixing UHPC, and each batch of UHPC can take up to 20 minutes depending on the size of the mixer. Multiple or large mortar mixers should be used in field applications for batching UHPC. Unlike LMC, UHPC has a long working time. Static flow of the UHPC should be checked before placement.

8.3 Cost of Rehabilitation

The cost of both the pocket and continuous joint rehabilitation methods was compared to the cost of the superstructure replacement for a 40-ft long by 30.66-ft wide double-tee girder bridge.

The material and fabrication cost provided by the South Dakota Department of Transportation (SDDOT) for a 46-in. wide and 23-in. deep double-tee girder is approximately $247 per linear foot. For a 30.66-ft wide bridge having eight girders and seven longitudinal joints, the total material and fabrication cost is $79,040. Furthermore, crane mobilization, superstructure demolition and removal, and onsite activity costs should be included as presented in Table 8-1.

Costs of double-tee bridge girder-to-girder joint rehabilitation were estimated by a contractor. The cost of the filler material was assumed to be $88/ft^3. The rehabilitation cost does not include mobilization. The approximate cost of the “pocket” and “continuous” joint rehabilitation detailing for a 40-ft long and 30.7-ft wide bridge with eight double-tee girders was respectively $31,685 and $64,856, which are respectively 28% and 57% of the cost of bridge superstructure replacement.

Overall, it can be concluded that the pocket rehabilitation alternative is the cheapest solution to preserve in-service double-tee bridges compared to the continuous joint rehabilitation method as well as the superstructure replacement. Both methods of rehabilitations are structurally viable and are feasible in the field.

Table 8-1. Rehabilitation vs. Replacement Cost for 40-ft Double-Tee Bridges

Type	Item	Cost
Replacement	Girder Material and Fabrication	$79, 040
	Girder Demolition, Removal, and Construction	$15,000
	Crane Mobilization	$20,000
	Total	**$114,040**
Rehabilitation	Pocket Joint	$31,685 (or 28% of Replacement)
	Continuous Joint	$64,856 (or 57% of Replacement)

9. Proposed Construction Specifications for Rehabilitation of Double-Tee Bridge Longitudinal Joints

This chapter includes the proposed construction specifications for the rehabilitation of double-tee bridge girder-to-girder longitudinal joints.

9.1 Preparation for Double-Tee Longitudinal Joint Rehabilitation

The general requirements for the demolition and preparation of double-tee bridge girder-to-girder longitudinal joints for field applications are:

1. A maximum 1-in. deep saw-cut shall be allowed around the perimeter of the joint for ease of demolishing.
2. Hammer-chipping should be allowed for existing concrete demolishing if meeting all of the following requirements:
    a. For pocket joint rehabilitation, concrete shall be chipped with a slope of 45°. Concrete of the intermediate shear keys between the pockets shall be chipped with a minimum of 20° with respect to a vertical line.
    b. For continuous joint rehabilitation, concrete shall be chipped with a slope of 45°.
    c. The use of either 15-lb or 30-lb pneumatic hammer chippers shall be allowed. However, 30-lb hammer chippers shall not be used for demolishing of double-tee flange existing concrete deeper than 2.5 in.

from the surface of the girder. In this case or in the vicinity of the girder reinforcement, only 15-lb hammer chippers shall be used.

3. The use of hydro-demolition shall be allowed to remove the existing concrete of the double-tee girder flange and to form the joint.
4. After forming the joint and exposing the existing reinforcement, the joint surface shall be sand-blasted and pre-wetted with burlap for at least 24 hours prior to pouring.
5. Formwork shall be water tight and may be installed from the top of the bridge. Nets shall be installed underneath the bridge to catch falling debris.

9.2 Proposed Rehabilitation Methods for Double-Tee Longitudinal Joints

Feasibility and performance of two rehabilitation methods were investigated in the present study: (1) discrete pockets filled with ultra-high performance concrete (UHPC) and reinforced with steel bars, and (2) continuous joints filled with latex modified concrete (LMC) and reinforced with wire mesh. Of the two method, only the UHPC pocket joint was found to be both structurally viable and durable. Even though LMC continuous joint was structurally viable, it showed shrinkage cracks, which may cause serious durability issues in field applications. Therefore, only the UHPC filled pocket joint detailing shall be used for the rehabilitation of double-tee bridge longitudinal joints. Continuous joint detailing may be accepted for field applications if the joint is filled with UHPC or a new material which does not shrink when used in large volumes.

9.2.1 Pocket Detailing for Rehabilitation of Double-Tee Bridge Longitudinal Joints

Rehabilitation of girder-to-girder joints of double-tee bridges using the pocket detailing shall be performed meeting the following requirements:

1. Square pockets each with a minimum side dimension of 18 in. shall be formed meeting the preparation requirements. The pocket spacing shall not exceed 5 ft (Fig. 9-1) center-to-center. Pockets shall be placed at the midspan of the bridge and no more than 24 in. away from the ends of the bridge (Fig. 9-1c). The pocket shall be filled with ultra-high performance concrete (UHPC) with a minimum 28-day compressive strength of 18 ksi.
2. A continuous shear key with a minimum width of 5.5 in. shall be formed meeting the preparation requirements then be filled with UHPC. The UHPC intermediate keys shall be longitudinally reinforced with two ASTM A706 (or A615) Grade 60 No. 4 bars (Fig. 9-2a) for the entire length of the bridge. A minimum of 2.5 in. clear cover shall be provided for the longitudinal reinforcement.
3. Square pockets shall be reinforced with four ASTM A706 (or A615) Grade 60 No. 4 reinforcing steel bars in both the longitudinal and transverse directions of the bridge (Fig. 9-2b and c).
4. A minimum of 3-in. lap-splice between the pocket reinforcement and the deck existing wires shall be provided to ensure the full development (Fig. 9-2b and c).

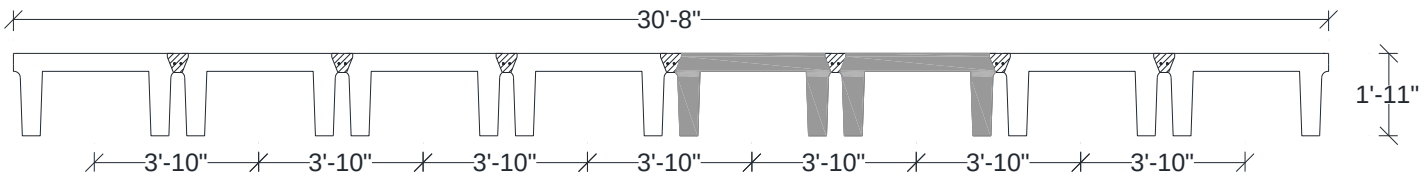

a. Cross-section of Two-Lane Double-Tee Bridges with Pocket Joints

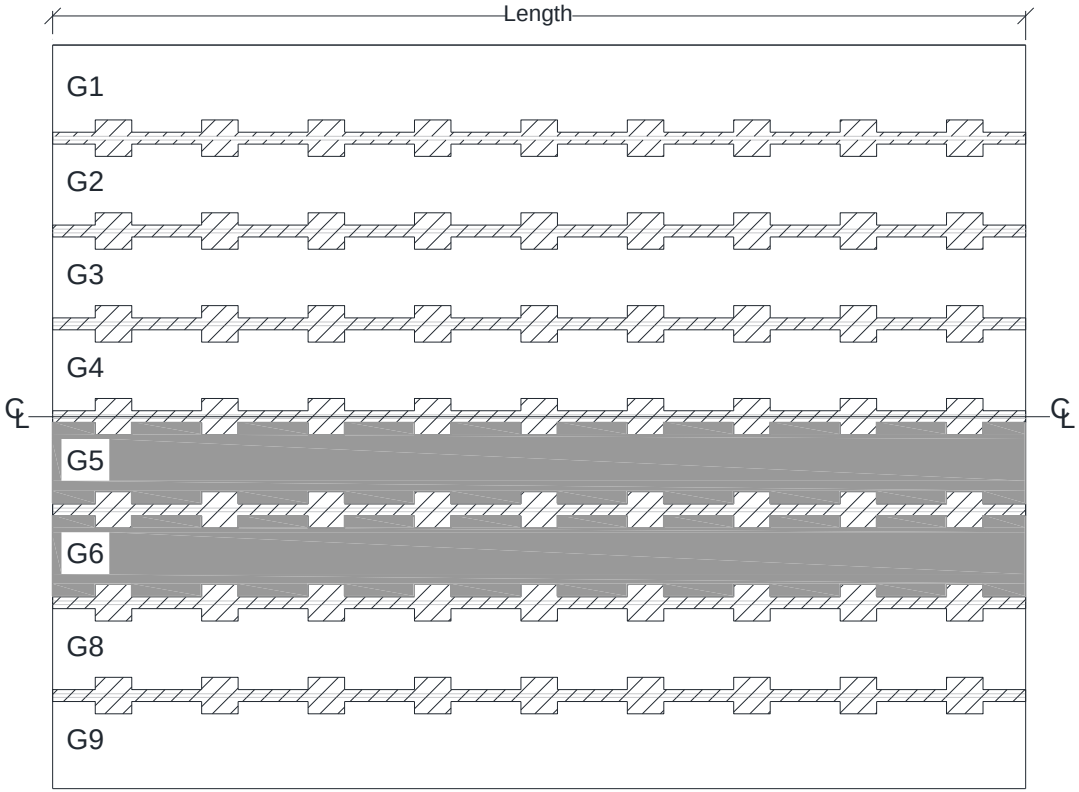

b. Plan view of Rehabilitated Double-Tee Bridges

Figure 9-1. Geometry Requirements for Proposed UHPC Pocket Joint Rehabilation Method

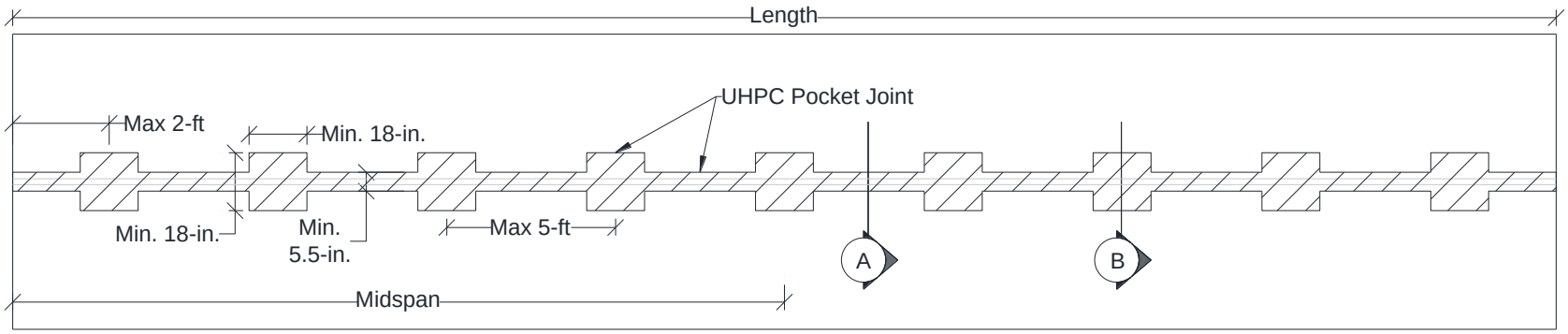

c. Dimentions for Rehabilitated Longitudinal Pocket Joint Detailing

Figure 9-1. Continued

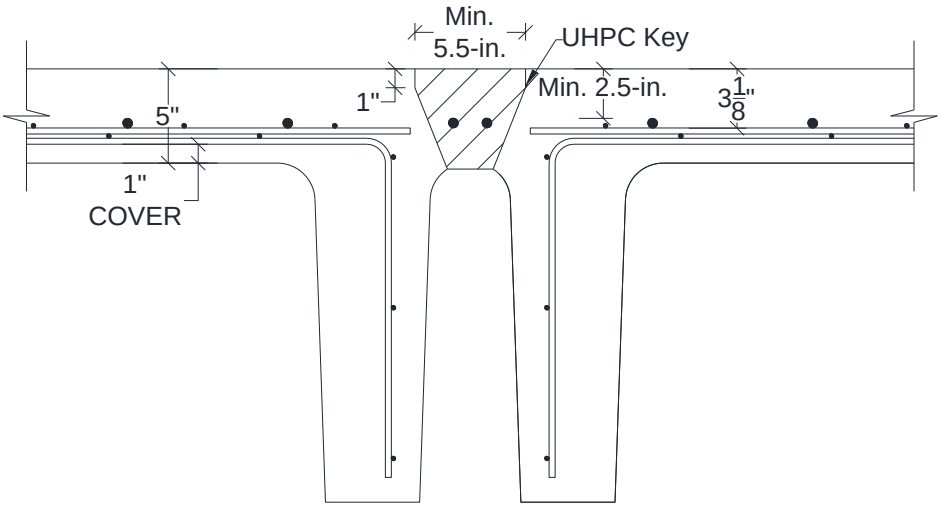

a. Section A - Intermediate Pocket Joint Detailing

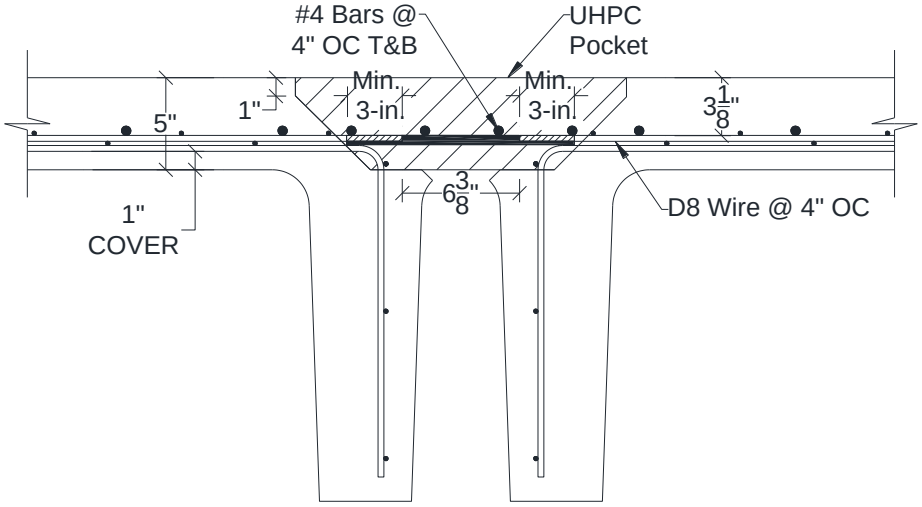

b. Section B - Pocket Joint Detailing

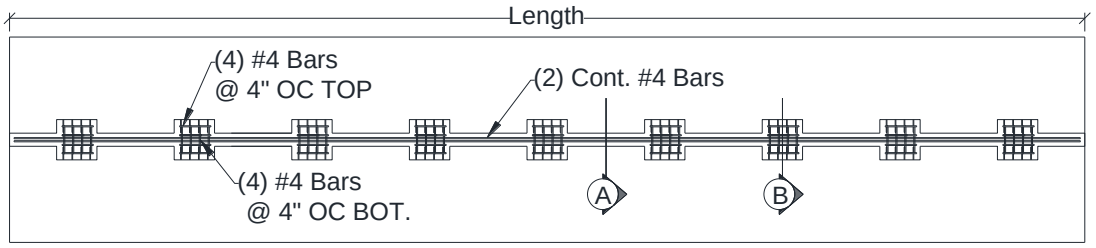

c. Pocket and Shear Key Reinforcement – Plan View

Figure 9-2. Detailing for Proposed UHPC Pocket Joint Rehabilitation Method

9.2.2 Continuous Detailing for Rehabilitation of Double-Tee Bridge Longitudinal Joints

Rehabilitation of girder-to-girder joints of double-tee bridges using the continuous detailing shall be performed meeting the following requirements:

1. Demolition and construction for each longitudinal joint of the bridge using the "continuous" detailing shall be performed using segmental construction with quarter-span increments per joint. Two adjacent joints shall not be demolished and rehabilitated at the same time. None of the joints shall not be rehabilitated along the length of the bridge all at once.
2. A continuous opening with a minimum width of 22 in. shall be formed meeting the preparation requirements (Fig. 9-3). The joint shall be filled with ultra-high performance concrete (UHPC) with a minimum 28-day compressive strength of 18 ksi.
3. Other filler materials such as non-shrink grout, latex modified concrete, and fiber reinforcement concrete shall not be used for the continuous joints due to cracking resulted from initial shrinkage. New materials with improved durability suitable for a large pour may be used depending bridge owner approval.
4. Continuous joint shall be reinforced with ASTM A497 Grade 70, 4 in. by 4 in. D8/D8 welded wire mesh (Fig. 9-4a and b).
5. A minimum of 5-in. lap-splice between the new and existing reinforcement shall be provided to ensure full development of the wires (Fig. 9-4a and b).

6. If wire meshes must be spliced over the length of the bridge, five No. 4 ASTM A706 (or A615) Grade 60 reinforcing steel bars shall be used to splice the wires with a minimum splice length of 12 in. as shown in Fig. 9-4c.

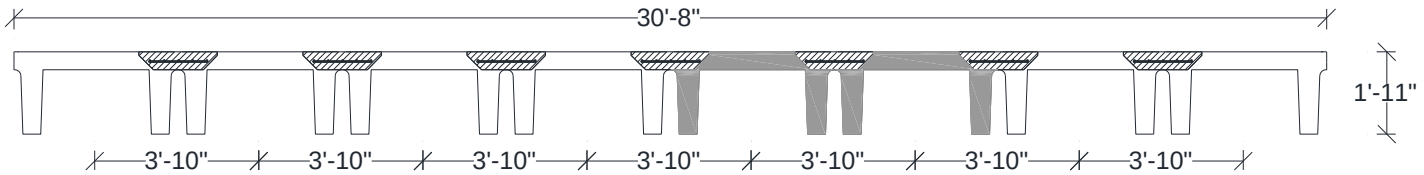

a. Cross-section of Two-Lane Double-Tee Bridges with Continous Joints

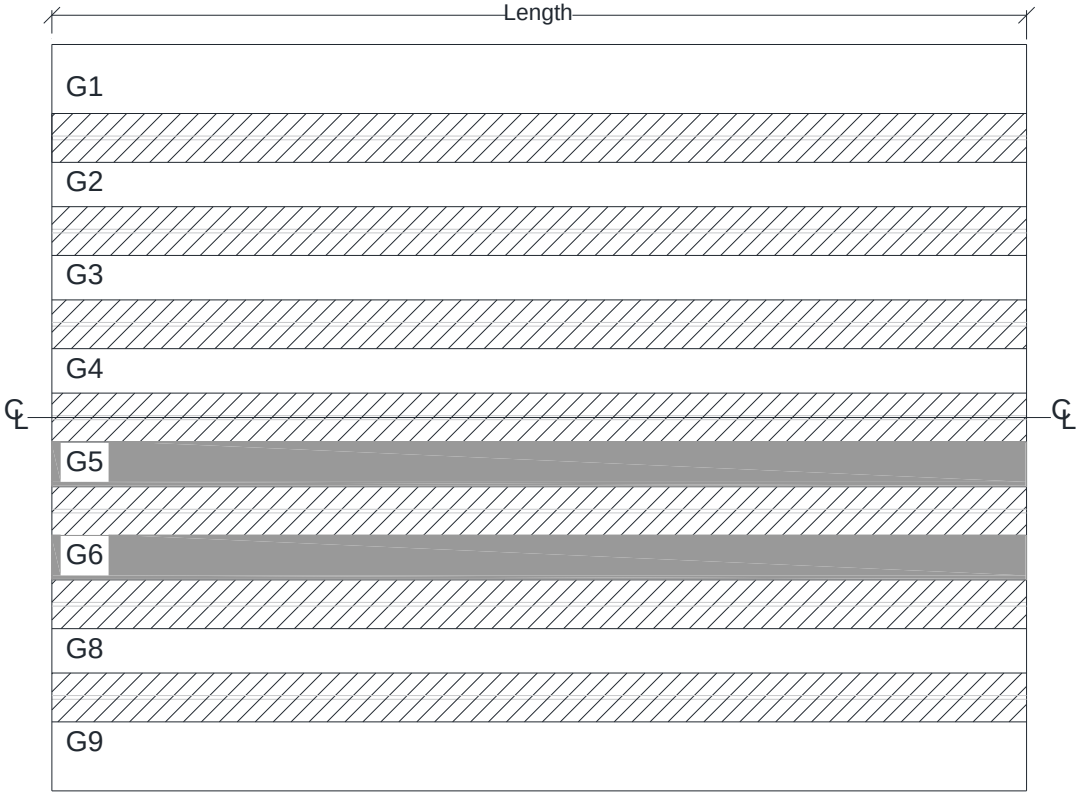

b. Plan view of Rehabilitated Double-Tee Bridges

Figure 9-3. Geometry Requirements for Proposed Continuous Joint Rehabilation Method

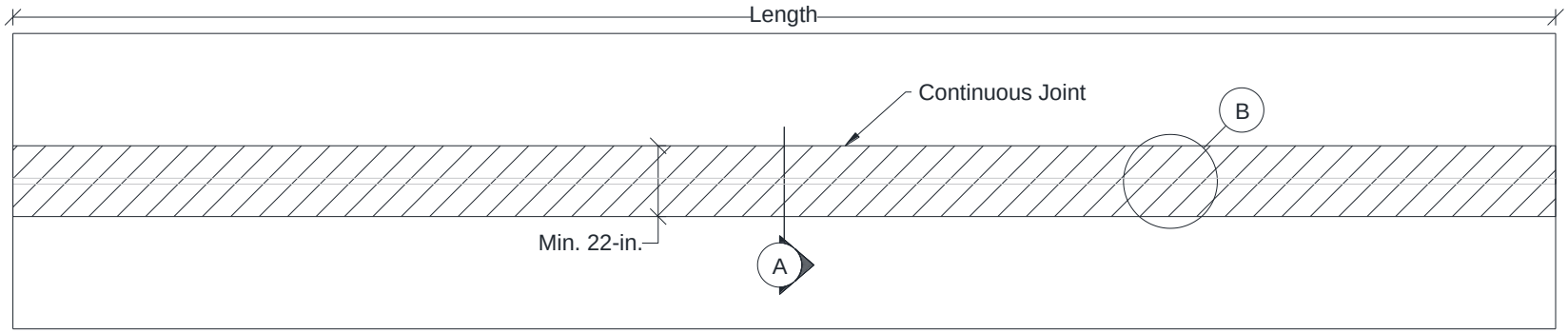

c. Dimentions for Rehabilitated Longitudinal Joint Detailing

Figure 9-3. Continued

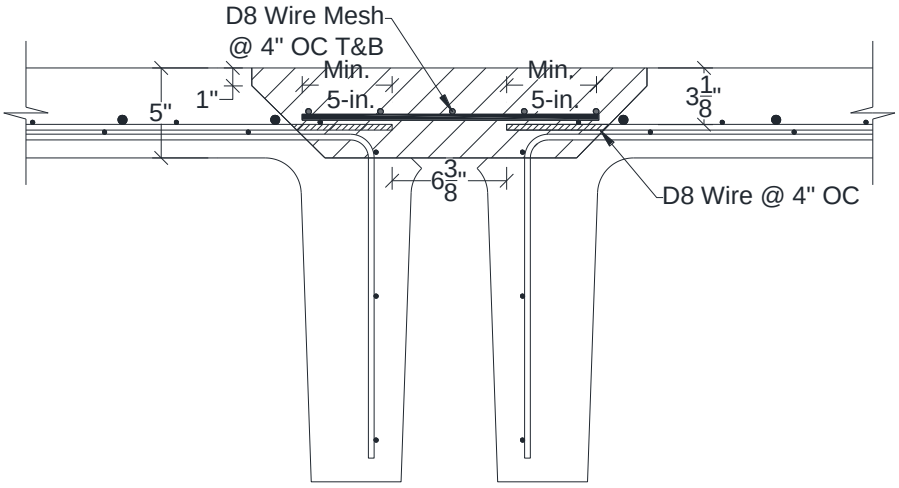

a. Section A – Continuous Joint Detail

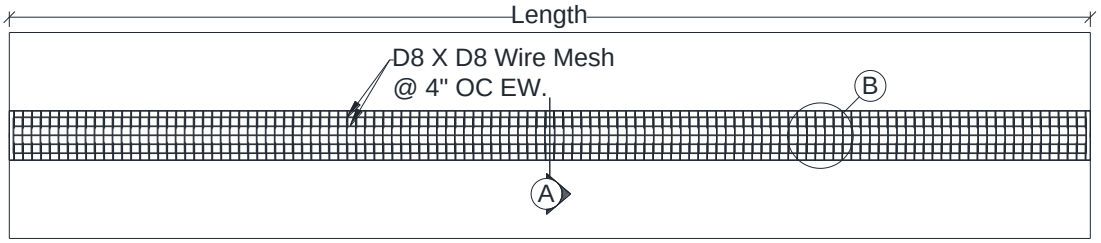

b. Continuous Joint Reinforcement – Plan View

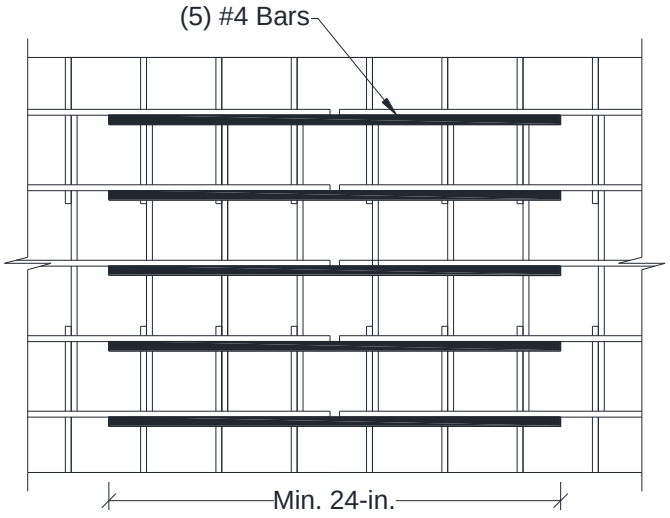

c. Section B – Wire Mesh Splice Detailing

Figure 9-4. Detailing for Proposed Continuous Joint Rehabilitation Method

10. Summary and Conclusions

The girder-to-girder joints of double-tee bridges, which are the most common type of bridges on South Dakota load roads, are deteriorating due to insufficient detailing. Analytical and experimental studies were carried out in the present study to investigate the feasibility and performance of two rehabilitation methods for longitudinal joints in double-tee bridges. A summary of the project and conclusions are presented herein.

10.1 Summary

Twenty joint detailing alternatives for the rehabilitation of the longitudinal joint of double-tee girder bridges were proposed in the present study. Of the 20 alternatives, continuous joint details were selected for further study since they offer minimal durability issues. The proposed continuous joint rehabilitation details consisted of exposing the transverse reinforcement of the deck, lap-slicing the reinforcement, and using a filler material to replace the removed concrete. Ultra-high performance concrete (UHPC) and latex modified concrete (LMC) were selected as the filler materials because of their improved strength and durability.

A rating system was developed to identify the best rehabilitation alternative. The results from the rating system showed that four of the 20 alternatives were favorable for further testing. Thirteen large-scale beam tests were carried out to investigate the performance of the selected joint rehabilitation details and to select the best for large-scale testing. Subsequently, two joint concepts, “pocket” and “continuous”, were

developed and analytically investigated using linear finite element analyses to optimize the selected joint detailing.

A full-scale 40-ft long double-tee bridge consisting of two interior girders was constructed using the conventional longitudinal joint detailing then tested under 250,000 cycles of the AASHTO Fatigue II loading using a point load applied at the midspan. The point load was offset in the transverse direction to maximize the joint shear demand. Furthermore, the conventional specimen was monotonically loaded to crack the longitudinal girder-to-girder joint. Subsequently, the bridge was rehabilitated using the two proposed details, "pocket" joint and "continuous" each incorporated on half the length of the bridge. The "pocket" joint consisted of discrete pockets reinforced with steel bars and filled with ultra-high performance concrete (UHPC). A UHPC keyway was used to connect the pockets. The "continuous" joint was reinforced with wire mesh and filled with latex modified concrete (LMC).

The rehabilitated specimen was tested under fatigue and strength loading to evaluate the performance of the bridge and to comment on the suitability of the proposed joint rehabilitation alternatives. The specimen was first tested under 500,000 cycles of AASHTO Fatigue II loading. Next, the joint was tested under additional 100,000 cycles of the AASHTO Fatigue I loading. Stiffness tests were performed to monitor the degradation of the bridge. Finally, the specimen was monotonically tested to failure.

10.2 Conclusions

Based on the analytical and experimental studies, the following conclusions can be derived:

- Of 20 rehabilitation alternatives, those with continuous detailing were found to be more durable.
- UHPC and LMC were found to be durable materials and was selected for beam testing.
- Thirteen beam tests showed that at least a 3-in. lap-splice is needed for joints with UHPC to fully develop the reinforcement. The minimum splice length for joints with LMC was found to be 5 in. In these cases, the new reinforcement of the joint fractured. UHPC and LMC were then selected as filler materials for the rehabilitation of double-tee longitudinal joints.
- The conventional non-shrink grout used in the conventional longitudinal joint detailing cracked below the AASHTO Service I limit state of 51 kips. Therefore, current double-tee joint detailing is inadequate.
- Finite element analyses showed that the use of discrete pockets is feasible for the bridge rehabilitation and the joint forces were determined.
- Hammer-chipping was found to be a viable demolition method.
- Shrinkage cracks and water leaks were observed in LMC of the continuous joint of the full-scale bridge before testing. The shrinkage cracks had no effect on the structural performance of the bridge but it will cause durability issues if this material is utilized in the field. More durable filler materials such as UHPC may be used for the continuous detailing. No shrinkage cracks were observed for UHPC.
- Both proposed longitudinal joint details did not show any signs of deterioration or water leakage through 500,000 cycles of the AASHTO Fatigue II loading and

100,000 cycles of the AASHTO Fatigue I loading. The test specimen was subjected to a total of 110 years of service loads. The stiffness of the loaded girder remained constant throughout the fatigue testing.

- The first flexural crack in the stem of the loaded girder of the rehabilitated bridge was observed at 53.8 kips, which was higher than the Service I limit state of 51 kips.
- The rehabilitated bridge load carrying capacity of 113.9 kips was higher than the AASHTO Strength I limit state of 89 kips indicating sufficient performance. The strength capacity of the rehabilitated specimen was 1.5 times higher than a conventional reference bridge test specimen.
- The force-displacement relationship of both girders of the rehabilitated bridge was essentially the same throughout strength testing indicating monolithic behavior.
- No structural damage or yielding of the reinforcement was observed in both joint rehabilitation details during the strength testing.
- The failure mode of the bridge was crushing of concrete in the deck of both girders at 9.55 in. of displacement in a ductile manner.
- The rehabilitation cost of the pocket and continuous joint detailing for a 40-ft long, 30.6 ft wide double-tee bridge is respectively only 28% and 57% of the replacement cost of the same bridge.

Overall, both proposed rehabilitation methods are structurally viable. However, the UHPC pocket alternative is the cheapest and the most durable solution to extend the service life of existing double-tee bridges for another 75 years.

11. References

American Association of State Highway and Transportation Officials (AASHTO) (2013). "AASHTO-LRFD Bridge Design Specifications, 2012 Edition." Washington, DC.

ASTM A416 / A416M-16 (2016). "Standard Specification for Low-Relaxation, Seven-Wire Steel Strand for Prestressed Concrete." ASTM International, West Conshohocken, PA.

ASTM A497 / A497M-07 (2007). "Standard Specification for Steel Welded Wire Reinforcement, Deformed, for Concrete." ASTM International, West Conshohocken, PA.

ASTM A615 / A615M-16 (2016). "Standard Specification for Deformed and Plain Carbon-Steel Bars for Concrete Reinforcement." ASTM International, West Conshohocken, PA.

ASTM A706 / A706M-16 (2016). "Standard Specification for Deformed and Plain Low-Alloy Steel Bars for Concrete Reinforcement." ASTM International, West Conshohocken, PA.

ASTM C39 / C39M-16 (2016). "Standard Test Method for Compressive Strength of Cylindrical Concrete Specimens." ASTM International, West Conshohocken, PA.

ASTM C109 / C109M-16a (2016). "Standard Test Method for Compressive Strength of Hydraulic Cement Mortars (Using 2-in. or [50-mm] Cube Specimens)." ASTM International, West Conshohocken, PA.

ASTM C143 / C143M-15a (2015). “Standard Test Method for Slump of Hydraulic-Cement Concrete.” ASTM International, West Conshohocken, PA.

ASTM C231 / C231M-16 (2016) “Standard Test Method for Air Content of Freshly Mixed Concrete by the Pressure Method.” ASTM International, West Conshohocken, PA.

ASTM E8 / E8M-16a (2016). “Standard Test Methods for Tension Testing of Metallic Materials.” ASTM International, West Conshohocken, PA, 2016.

Baer, C. (2013). “Investigation of Longitudinal Joints Between Precast Prestressed Deck Bulb Tee Girders Using Latex Modified Concrete.” University of South Carolina - Columbia, Department of Civil Engineering, Columbia, SC.

Barde, A., Parameswaran, S., Chariton, T., Weiss, J., Cohen, M., & Newbolds, S. (2006). “Evaluation of Rapid Setting Cement-Based Materials for Patching and Repair.” Report No. FHWA/IN/JTRP/2006-11, Purdue University, School of Civil Engineering, West Lafayette, IN.

BASF Corporation (2011). “Placement of Latex Modified Concrete.” Charlotte, NC.

Beckemeyer, C. and McPeak, T. (1995). “Rural Road Design, Maintenance, and Rehabilitation Guide.” Report No. SD95-16-G2, SD Department of Transportation Office of Research, Pierre, SD.

Champa, J., Gulyas, R., & Wirthlin, G. (1995). “Evaluation of Keyway Grout Test Methods for Precast Concrete Bridges.” PCI Journal, Cleveland, OH.

Computers and Structures, Inc. (2016). “SAP2000, Version 18.” Berkeley, CA.

Dayton Superior Corporation (2015). “Technical Data Sheet: HD-50.” Miamisburg, OH.

Five Star Products, Inc (2015). "Technical Data Sheet: Highway Patch FR." Fairfield, CT.

French, C., Shield, C., Klaseus, D., Smith, M., Ericksson, W., Ma, Z., et al. (2011). "Cast-in-Place Concrete Connection for Precast Deck Systems." NCHRP Project No. 173, University of Minnesota; University of Tennessee, Minneapolis, Mn; Knoxville, TN.

Graybeal, B. (2010). "Behavior of Field-Cast Ultra-High Performance Concrete Bridge Deck Connections Under Cyclic and Static Structural Loading." FHWA Publication No. FHWA-HRT-11-023, Office of Infrastructure Research & Development Federal Highway Administration, Mclean, VA.

Graybeal, B. (2014). "Design and Construction of Field-Cast UHPC Connections." FHWA Publication No. FHWA-HRT-14-084, Office of Infrastructure Research & Development Federal Highway Administration, Mclean, VA.

Haber, Z. and Graybeal, B. (2014). "Experimental Evaluation of Prefabricated Deck Panel Connections." Office of Infrastructure Research & Development Federal Highway Administration, Mclean, VA.

Headed Reinforcement Corporation (2014), "HRC 555 Headed Reinforcing Bars." International Code Council – Evaluation Service Report No. ESR-2935, Fountain Valley, CA.

Jones, H. (2001). "Lateral Connections for Double Tee Bridges." Report No. FHWA/TX-01/1856-2, Texas Trasportation Institute, Texas A&M University, Austin, TX.

Jones, J., Ryan, K., & Saiidi, M. (2015). "Toward Successful Implementation of Prefabricated Deck Panels to Accelerated the Bridge Construction Process." University of Nevada-Reno, Department of Civil and Enviromental Engineering, Reno, NV.

Keegan, M. (2015). "Price Quote." Construction Products and Consultants, Inc., Sioux Falls, SD.

Konrad, M. (2014). "Precast Bridge Girder for Improved Performance." South Dakota State University, Department of Civil and Enviromental Engineering, Brookings, SD.

Li, Z. and Rangaraju, R. (2016). "Effect of Surface Roughness on the Bond Between Ultrahigh-Performance and Precast Concrete in Bridge Deck Connections." *Journal of the Transportation Board, No. 2577,* Transportation Research Board, Washington, D.C, pp. 88-96.

Marsh, M., Wernli, M., Garrett, B., Stanton, J., Eberhard, M., & Weinert, M. (2011). "Application of Accelerated Bridge Construction Connection in Moderate-to-High Seismic Regions." NCHRP Report No. 698, Bergerabam; University of Washington, Seattle, WA.

Mingo, M. (2016). "Precast Full-Depth Panels on Inverted Bulb-tee Bridge Girders." South Dakota State University, Department of Civil Engineering, Brookings, SD.

Pierce, L., Uhlmeyer, J., Weston, J., Lovejoy, J., & Mahoney, J. (2002). "Ten-Year Performance of Dowel Bar Retrofit - Application, Performance, and Lessons Learned." Washington State Department of Transportation, Olympia, WA.

South Dakota Department of Transportation (SDDOT) (2004). "Standard Specifications for Roads and Bridges." SDDOT, Pierre, SD.

Swenty, M., & Graybeal, B. (2013). "Material Characterization of Field-Cast Connection Grouts." Report No. FHWA-HRT-13-041, Office of Infrastructure Research & Development Federal Highway Administration, Mclean, VA.

Wehbe, N., Konrad, M., and Breyfogle, A. (2016). "Joint Detailing Between Double Tee Bridge Girders for Improved Serviceability and Strength." *Transportation Journal of the Transportation Research Board, No. 2592,* Transportation Research Board, Washington, D.C, pp. 13.

Wenzlick, J. (2002). "Hydrodemolition and Repair of Bridge Decks." Report No. RDT02-002, Missouri Department of Transportation, Jefferson City, MO.

Wenzlick, J. (2006). "Evaluation of Very High Strength Latex Modified Concrete Overlays." Report No. OR06-004, Missouri Department of Transportation, Jefferson City, MO.

Appendix A. Design Calculations

A.1 Girder Distribution Factor

Distribution of Live Loads for Moment in Interior Beams:

Applicable Cross-Section from AASHTO Table 4.6.2.2.1-1

h

or:

If connected only enough to prevent relative vertical displacement at

the Interface: g, i, j

Regardless of Number of Loaded Lanes

$$LLDF = \frac{S}{D} \qquad \text{Eq. A-1}$$

where:

$$C = K\left(\frac{W}{L}\right) \leq K \qquad \text{Eq. A-2}$$

when $C \leq 5$ Eq. A-3

$$D = 11.5 - N_L + 1.4N_L(1 - 0.2C)^2$$

when $C > 5$ Eq. A-4

$$D = 11.5 - N_L$$

$$K = \sqrt{\frac{(1+\mu)I}{J}} \qquad \text{Eq. A-5}$$

S = 3.86 ft, L = 40 ft, W = 30.67 ft,. μ = 0.2, I = 18,640 in.^{4}, J = 6,670

in.^{4}

$$K = \sqrt{\frac{(1+0.2)18{,}640}{6{,}670}} = 1.83 \qquad \text{Eq. A-5}$$

$$C = 1.83\left(\frac{30.67}{40}\right) = 1.4 \leq 1.83 \quad \text{Eq. A-2}$$

$$D = 11.5 - \ 2 + 1.4 * 2(1 - 0.2 * 1.4)^2 = 10.95 \quad \text{Eq. A-3}$$

$$LLDF = \frac{3.86}{10.95} = 0.35 \quad \text{Eq. A-1}$$

Range of Applicability

Skew $\leq 45^0$

$N_L \leq 6$

Definitions:

D = width of distribution per lane (ft)

S = spacing of beams or webs (ft)

C = stiffness parameter

W = edge-to-edge width of bridge (ft)

L = span of beam (ft)

K = constant for different types of construction

N_L = number of design lanes

μ = Poisson's ratio

I = moment of inertia of beam ($in.^4$)

J = St. Venant's torsional inertia ($in.^4$)

A.2 Service I Limit State Loading

Case I: Tandem Truck

Maximum moment: Tandem, 451.3 k-ft**, Lane Load**, 128 k-ft

$$Scale\ Factor = \gamma\ (1 + \frac{IM}{100}) \quad \text{Eq. A-6}$$

IM = 33% for Service I Limit State

γ = 1.0 for Service I Limit State

$$Factored\ Moment = 1\left(1 + \frac{33}{100}\right) * 451.3 + 128 = 728.2\ k - ft \quad \text{Eq. A-7}$$

Equivalent Moment based on Point Load at Midspan

$$P = 4 * N_g * LLDF * M/L \quad \text{Eq. A-8}$$

$$P = 4 * 2 * 728.2 * \frac{0.35}{40} = 51.0\ kips \quad \text{Eq. A-8}$$

Case II: HL-93 Truck

Maximum moment: HL-93, 447.4 k-ft**, Lane Load**, 128 k-ft

$$Scale\ Factor = \gamma\ (1 + \frac{IM}{100}) \quad \text{Eq. A-6}$$

IM = 33% for Service I Limit State

γ = 1.0 for Service I Limit State

$$Factored\ Moment = 1\left(1 + \frac{33}{100}\right) * 447.4 + 1.0 * 128 = 723\ k - ft \quad \text{Eq. A-7}$$

Equivalent Moment based on Point Load at Midspan

$$P = 4 * N_g * LLDF * M/L \quad \text{Eq. A-8}$$

$$P = 4 * 2 * 723 * \frac{0.35}{40} = 50.6\ kips \quad \text{Eq. A-8}$$

A.3 Fatigue I Limit State Loading

HL-93 Truck (rear-axles spaced at 30 ft)

Maximum moment: 346 k-ft

$$Scale\ Factor = \gamma\ (1 + \frac{IM}{100}) \quad \text{Eq. A-6}$$

IM = 15% for Fatigue I Limit State

γ = 1.5 for Fatigue I Limit State

$$Factored\ Moment = 1.5\left(1 + \frac{15}{100}\right) * 346 = 596.9\ k - ft \quad \text{Eq. A-7}$$

Equivalent Moment based on Point Load at Midspan

$$P = 4 * N_g * LLDF * M/L \quad \text{Eq. A-8}$$

$$P = 4 * 2 * 596.9 * \frac{0.35}{40} = 41.8\ kips \quad \text{Eq. A-8}$$

A.4 Fatigue II Limit State Loading

HL-93 Truck (rear-axles spaced at 30 ft)

Maximum moment: 346 k-ft

$$Scale\ Factor = \gamma\ (1 + \frac{IM}{100}) \quad \text{Eq. A-6}$$

IM = 15% for Fatigue II Limit State

γ = 0.75 for Fatigue II Limit State

$$Factored\ Moment = 0.75\left(1 + \frac{15}{100}\right) * 346 = 298.4\ k - ft \quad \text{Eq. A-7}$$

Equivalent Moment based on Point Load at Midspan

$$P = 4 * N_g * LLDF * M/L \quad \text{Eq. A-8}$$

$$P = 4 * 2 * 298.4 * \frac{0.35}{40} = 20.9\ kips$$ Eq. A-8

A.5 Strength I Limit State Loading

Tandem Truck Case (Controlling Case)

Maximum moment: Tandem, 451.3 k-ft**, Lane Load**, 128 k-ft

$$Scale\ Factor = \gamma\ (1 + \frac{IM}{100})$$ Eq. A-6

IM = 33% for Service I Limit State

γ = 1.75 for Service I Limit State

$$Factored\ Moment = 1.75\left(1 + \frac{33}{100}\right) * 451.3 + 1.75 * 128$$ Eq. A-7

$$= 1{,}274.4\ k - ft$$

Equivalent Moment based on Point Load at Midspan

$$P = 4 * N_g * LLDF * M/L$$ Eq. A-8

$$P = 4 * 2 * 1{,}274.4 * \frac{0.35}{40} = 89.2\ kips$$ Eq. A-8

A.6 Strength I Limit State Loading for Connection Design

Tandem Truck Case (Controlling Case)

Maximum moment: Tandem, 451.3 k-ft**, Lane Load**, 128 k-ft

$$Scale\ Factor = \gamma\ (1 + \frac{IM}{100})$$ Eq. A-6

IM = 75% for Strength I Limit State (connection)

γ = 1.75 for Strength I Limit State

$$Factored\ Moment = 1.75\left(1 + \frac{75}{100}\right) * 451.3 + 1.75 * 128 \qquad \text{Eq. A-7}$$

$$= 1{,}606.1\ k - ft$$

Equivalent Moment based on Point Load at Midspan

$$P = 4 * N_g * LLDF * M/L \qquad \text{Eq. A-8}$$

$$P = 4 * 2 * 1{,}606.1 * \frac{0.35}{40} = 112.4\ kips \qquad \text{Eq. A-8}$$

Appendix B. Shop Drawings

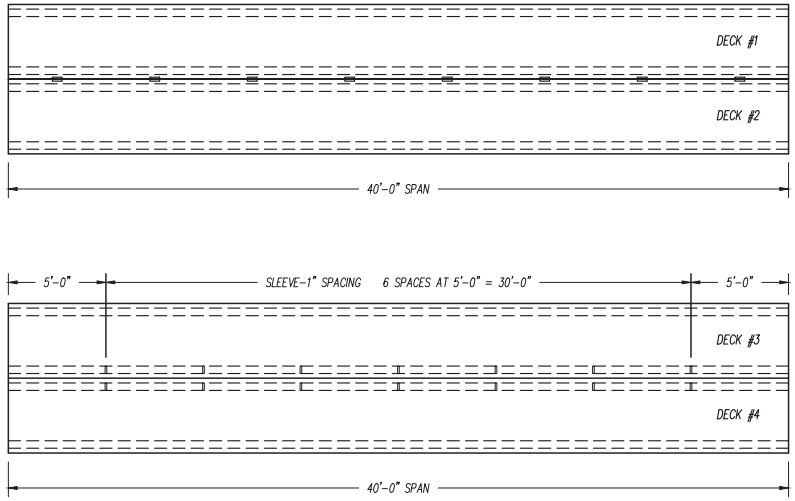

23" X 3'-10" X 40'-0" DTEE (0° SKEW)

19,300 LBS EACH

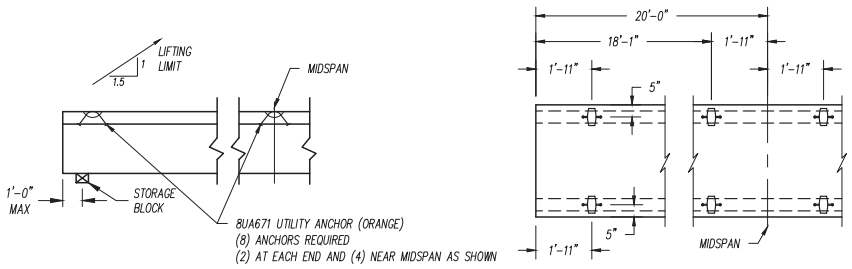

LIFTING & STORAGE DETAIL

MISCELLANEOUS ITEMS	
8	4" x 15" x 1/2" Loose Bearing Pads
8	Weld Plates
14	Sleeve-1"

REV:	DESCRIPTION:	DATE:	BY:
1	UPDATED RS#, STENCIL, & TITLE BLOCK	05/31/16	JWB

PROJECT INFORMATION	
PLACE OF FABRICATION	MITCHELL
PROJECT #	N/A
STRUCTURE #	N/A
COUNTY	N/A
FORTERRA PROJECT #	9016167BR1
ENGINEER	N/A
CONTRACTOR	SDSU
STATE INSPECTION REQ'D	NO

SECTION INFORMATION	
BEAM TYPE	23" DTEE – NO SKEW
CONCRETE	TYPE I-II LA
f'ci (DETENTION)	5,000 psi
f'c (28 DAY)	6,000 psi
PS STRAND	1/2" DIA. X 270K LOW RELAXATION STRAND PER ASTM A-416
INITIAL TENSION	30,980 lbs
RE-BAR	ASTM A-615 GRADE 60
RE-MESH	ASTM A-497

1. STENCIL EACH DECK WITH THE INFORMATION LISTED BELOW. PLACE STENCIL ON EXTERIOR FACE OF INTERIOR BEAMS – INSIDE FACE OF EXTERIOR BEAMS. CENTER STENCIL VERTICALLY ON LEG 4'-0" FROM END OF BEAM.

DATE OF MANUFACTURE
FORTERRA™
MITCHELL, SD
HL-93 LOADING
SDSU TEST BEAMS
DECK # 1 2 3 4

2. THE TOP SURFACE SHALL BE ROUGHED BY BROOMING IN THE TRANSVERSE DIRECTION. THE AREA UNDER EACH RAILPOST SHALL BE FINISHED TO A SMOOTH AND UNIFORM SURFACE TO ASSURE PROPER FIT.

3. CONTRACTOR TO GROUT DEPRESSION AROUND LIFT ANCHORS IN FIELD (TYP.) – GROUT NOT PROVIDED.

FORTERRA™
Rapid City, South Dakota
2046 Samco Road, Suite 2
Rapid City, SD 57702
(605) 718-4111

SCALE: NONE	PROJECT: 23" X 40'-0" DTEE (0° SKEW) SDSU TEST BEAMS BROOKINGS, SD
DATE: 05/20/14	
OR#: 9016167BR1	
DR'N BY: BSJ	CUSTOMER: SDSU
CHK'D BY: –	DWG NAME: 9016167BR1-01

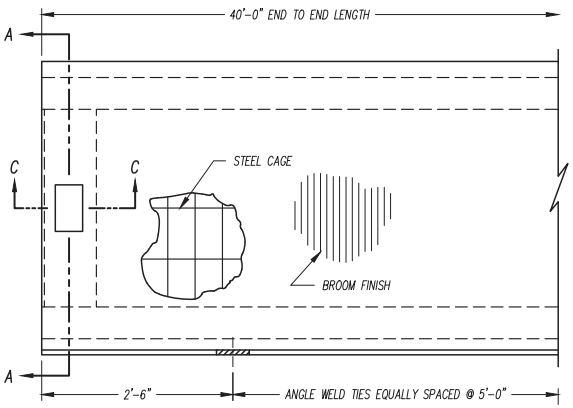

TOP VIEW

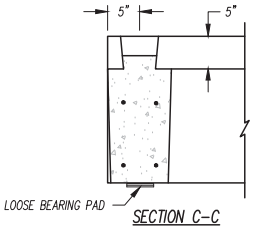

SECTION C-C

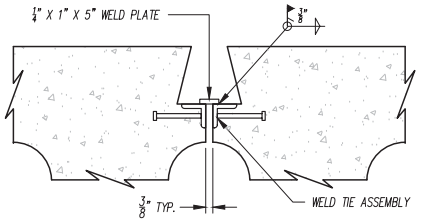

ANGLE WELD TIE CONNECTION DETAIL FOR BEAMS 414151-01 AND 414151-02 ONLY

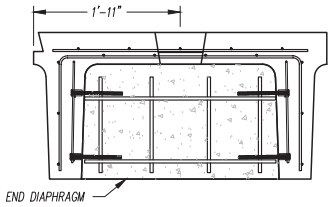

SECTION A-A FOR DECK #1 AND DECK #2 ONLY

SEE DIAPHRAGM DETAILS ON FOLLOWING PAGES

STRESSING INFORMATION

GAUGE PRESSURE = 3165 ELONGATION = 10 3/4"

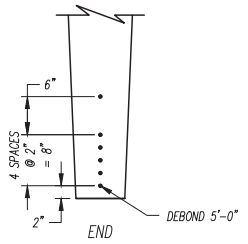

STRAND PATTERN

PRESTRESSING STRAND CONFORMS TO AASHTO M203, SUPPLEMENT 1 (LOW LAX STRAND)

CONCRETE STRENGTH = 5000 AT DETENSION
6000 AT 28 DAYS

REV:	DESCRIPTION:	DATE:	BY:
1	UPDATED RS#, & TITLE BLOCK	05/31/16	JWB

FORTERRA

Rapid City, South Dakota
2046 Samco Road, Suite 2
Rapid City, SD 57702
(605) 718-4111

SCALE: NONE	PROJECT: CASTING DETAILS 23" X 40'-0" DTEE (0° SKEW) SDSU TEST BEAMS
DATE: 05/20/14	
OR#: 9016167BR1	
DR'N BY: BSJ	CUSTOMER: SDSU
CHK'D BY: –	DWG NAME: 9016167BR1-02

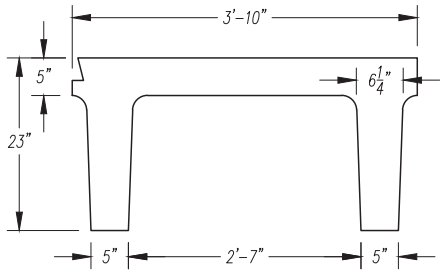

TYPICAL SECTION VIEW

23" DEEP PRESTRESSED CONCRETE CHANNEL

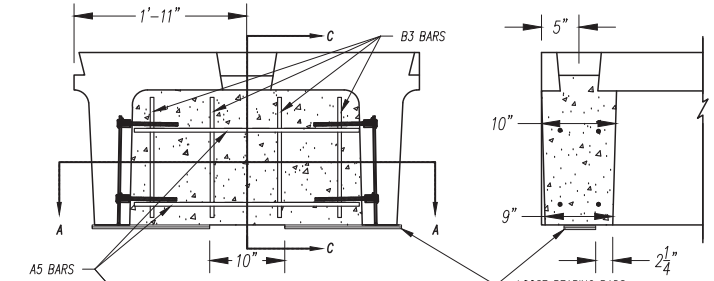

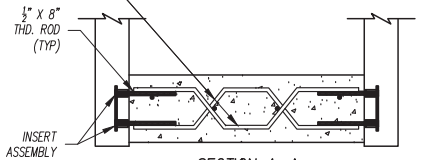

SECTION A-A

END DIAPHRAGM

FORTERRA

Rapid City, South Dakota
2046 Samco Road, Suite 2
Rapid City, SD 57702
(605) 718-4111

SCALE: NONE	PROJECT: RAIL POST & DIAPHRAGM DETAILS 23" X 40'-0" DTEE (0° SKEW) SDSU TEST BEAMS
DATE: 05/21/14	
OR#: 9016167BR1	
DR'N BY: BJS	CUSTOMER: SDSU
CHK'D BY: –	DWG NAME: 9016167BR1-03

REV:	DESCRIPTION:	DATE:	BY:
1	UPDATED RS#, & TITLE BLOCK	05/31/16	JWB

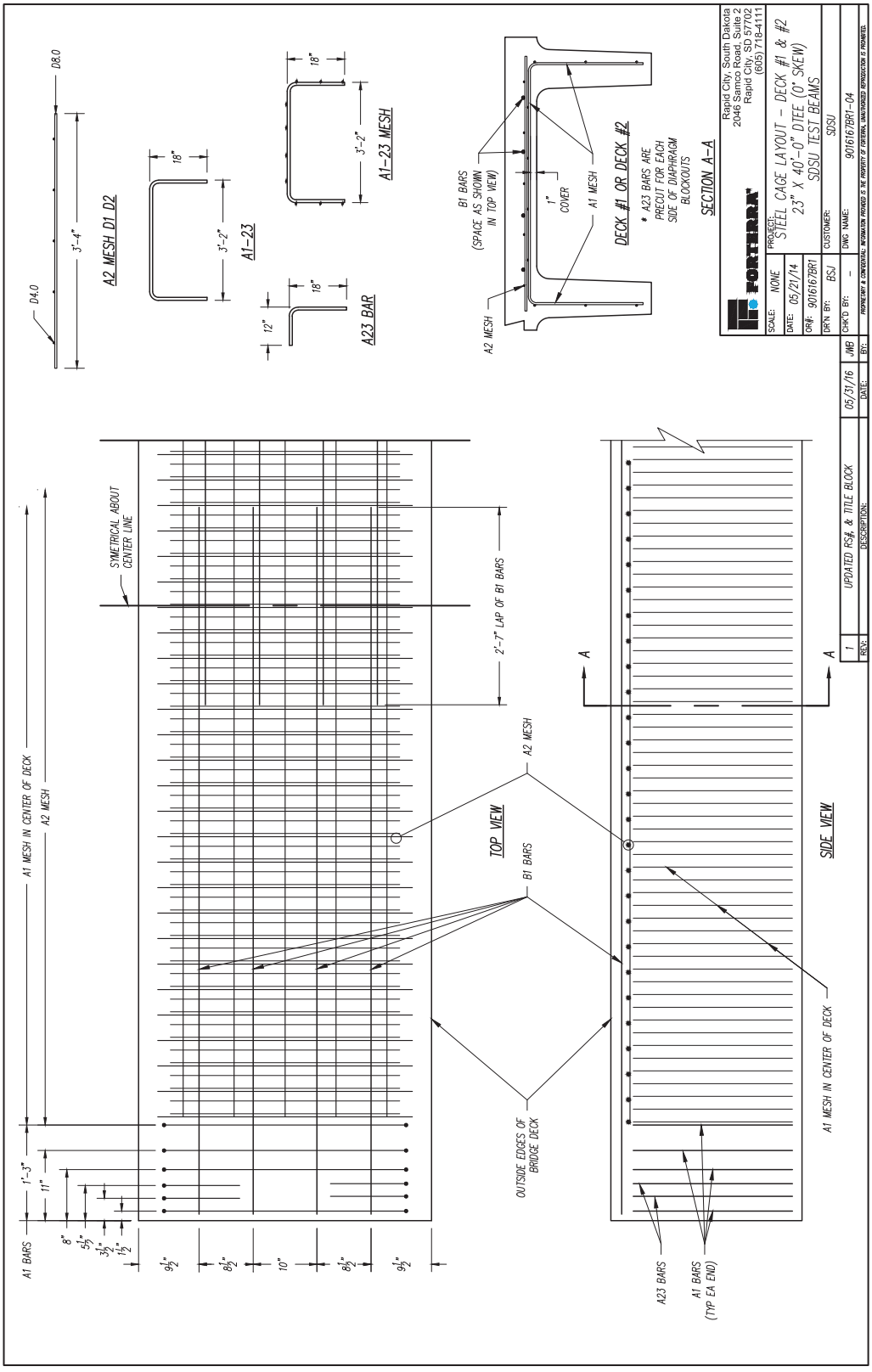
A2 MESH D1 D2
D4.0
D8.0
3'-4"
A1-23
18"
3'-2"
A1-23 MESH
A23 BAR
12"
B1 BARS
(SPACE AS SHOWN
IN TOP VIEW)
A2 MESH
1"
COVER
A1 MESH
DECK #1 OR DECK #2
* A23 BARS ARE
PRECUT FOR EACH
SIDE OF DIAPHRAGM
BLOCKOUTS
SECTION A-A
Rapid City, South Dakota
2046 Samco Road, Suite 2
Rapid City, SD 57702
(605) 718-4111
FORTERRA
PROJECT:
STEEL CAGE LAYOUT - DECK #1 & #2
23" X 40'-0" DTEE (0° SKEW)
SDSU TEST BEAMS
SCALE: NONE
DATE: 05/21/14
DWG#: 901616?BR1
DR'N BY: BSJ
CUSTOMER: SDSU
CHK'D BY: -
DWG NAME: 901616?BR1-04
PROPRIETARY & CONFIDENTIAL INFORMATION PROVIDED IS THE PROPERTY OF FORTERRA, UNAUTHORIZED REPRODUCTION IS PROHIBITED.
REV: 1
DESCRIPTION: UPDATED RS#, & TITLE BLOCK
DATE: 05/31/16
BY: JMB
SYMETRICAL ABOUT
CENTER LINE
A1 MESH IN CENTER OF DECK
A2 MESH
1'-3"
11"
8"
5½"
3½"
1½"
A1 BARS
9½"
8½"
10"
8½"
9½"
2'-7" LAP OF B1 BARS
TOP VIEW
A2 MESH
B1 BARS
OUTSIDE EDGES OF
BRIDGE DECK
A
A
SIDE VIEW
A1 MESH IN CENTER OF DECK
A23 BARS
A1 BARS
(TYP EA END)

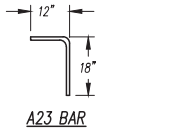

A23 BAR

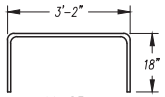

A1-23

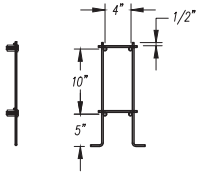

INSERT ASSEMBLY

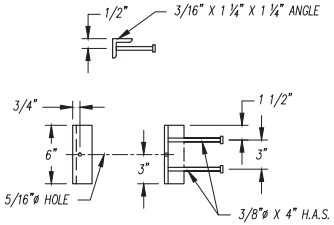

ANGLE WELD TIE

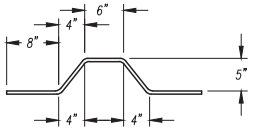

A5

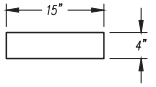

1/2" BEARING PAD - 70 DUROMETER

BEARING PAD DETAIL

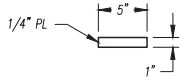

WELD PLATE

MARK	# / DECK INT/EXT	SHAPE	SIZE	LENGTH	TOTAL
A1-23 BAR	8		4	6'-2"	32
A1-23 MESH	5		8.0/4.0	6'-2"	20
A2 MESH D1 D2	5	STR.	8.0/4.0	3'-4"	10
A2 MESH D3 D4	5	STR.	8.0/4.0	4'-2"	10
A5	8		4	2'-10"	32
A23	8		4	2'-6"	32
B1-15	8	STR	4	15'-0"	32
B3	8	STR	3	1'-4"	32
SLEEVE-1"	7			1" X 5"	14
ANG. W/ TIE	0/8				16
INSERT ASMBLY	4				16
WELD PLATE	8		1/4" PL	1" X 5"	8
BOLT-$\frac{3}{4}$"	7			$\frac{3}{4}$" X 2'-0"	7
NUT-$\frac{3}{4}$"	7			$\frac{3}{4}$" dia. NUT	7
WASHER-$\frac{3}{4}$"	14			$\frac{3}{4}$" dia. WASHER	14
THD. ROD	16		1/2" X 8"		64
BRG. PAD	4	70 DURO	1/2" X 4"	15"	8
BUA671	8				32

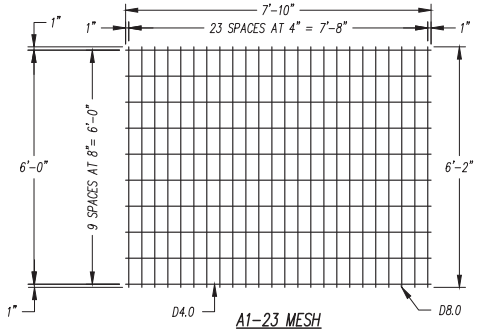

A1-23 MESH

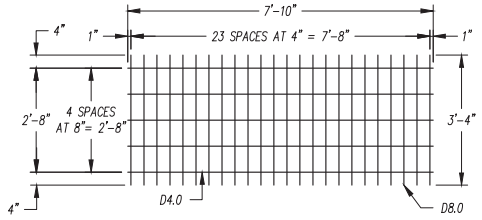

A2 MESH D1 D2

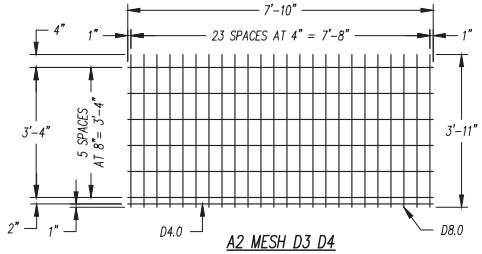

A2 MESH D3 D4

NOTE:
1) Reinforcing steel dimensions are out to out.
2) Reinforcing steel as per ASTM A-615 Grade 60.
3) Structural steel as per ASTM A-36.
4) BOLT-$\frac{3}{4}$" shall be A307 bolt with 6" thread.
5) NUT-$\frac{3}{4}$" shall be A563A.
6) WASHER-$\frac{3}{4}$" shall be F844.
7) SLEEVE-1" shall be PVC Schedule 40.

FORTERRA
Rapid City, South Dakota
2046 Samco Road, Suite 2
Rapid City, SD 57702
(605) 718-4111

SCALE: NONE	PROJECT: MATERIALS LIST 23" X 40'-0" DTEE (0° SKEW) SDSU TEST BEAMS
DATE: 05/27/14	
OR#: 9016167BR1	
DR'N BY: BSJ	CUSTOMER: SDSU
CHK'D BY: -	DWG NAME: 9016167BR1-06

REV:	DESCRIPTION:	DATE:	BY:
1	UPDATED RS#, & TITLE BLOCK	05/31/16	JWB

Appendix C. Concrete Mix Design

Cretex Concrete Products

Concrete Mix Design Data for Mitchell

Mix Designation	Targets (psi)		Date
6000 PS	1 Day:	3000	1/13/2015
	28 Day:	6000	

	Material	Cubic Yard Quantity		Specific Gravity	Cubic Yard Volume	
Cement	Cement, Type I-II	700	lbs	3.150	3.56	ft³
Cementitious Materials						
Aggregates	Coarse Aggregate, 3/4" CA	1805	lbs	2.653	10.90	ft³
	Fine Aggregate, Washed Sand	1203	lbs	2.604	7.40	ft³
Chemical Admixtures	Air Entrainer	0.7	oz/CWT	1.050	4.9	oz
	HRWR SN	16.4	oz/CWT	1.200	114.8	oz
Water	Water	212	lbs	1.000	3.40	ft³
Air	Air Content, %	6.0%	+ -	1.5% 1.0%	1.62	ft³
				Total Volume	**27.00**	ft³
Batch Properties	Pozzolans, %	0%		**Yd³ Weight**	**3929**	lbs/yd³
	Total Cementitious	700	lbs	**Unit Weight**	**145.53**	lbs/ft³
	Water Cement Ratio*	0.31				
	Slump	6	in +/-	2	in	

**Water Cement Ratio includes water from liquid admixtures*

Material	Type/Classification	Supplier
Cement	Type I-II	GCC Dakota, Rapid City, SD
Coarse Aggregate	3/4" CA	Spencer Quarries Inc., Spencer, SD
Fine Aggregate	Washed Sand	Bitterman Sand Pit, Delmont. SD
Air Entrainer	Daravair M	WR Grace
HRWR SN	Daracem 19	WR Grace

Appendix D. LMC and Grout Specifications

DAYTON SUPERIOR

HD 50

Horizontal Repair Mortar

TECHNICAL DATA SHEET

DESCRIPTION

HD 50 is a fast setting, fiber reinforced, latex-modified, shrinkage compensated,heavy duty, one component concrete repair material requiring only water to mix and apply. HD 50 is a cement based compound having similar characteristics to normal portland cement mixes and is compatible with portland cement concrete.

USE

HD 50 is designed for the repair of heavy duty surfaces such as concrete highways, bridge decks, parking structures, airport runways, freezer rooms, industrial and warehouse floors, and loading docks. HD 50 is a flowable material that may be poured into place for horizontal applications or into formed vertical and overhead applications.

FEATURES

- Can be opened to use or traffic within 60 minutes
- High compressive strength quickly – over 2,000 psi in one hour
- Resists salt penetration and damage from freeze/thaw cycles
- Contains no chlorides or magnesium phosphate
- Meets ASTM C-928; Specification for Very Rapid Hardening Cementitious Repair Materials
- Non Corrosive
- Compatible with portland cement concrete
- Aggregate extension – Up to 60% on repairs greater than 2 inches (5cm) deep
- Can be coated with epoxy in as little as 4 hours

PROPERTIES

Meets ASTM C-928: As a Type R-3 mortar

Compressive Strength – ASTM C-109 At 73°F (22.8°C)
1 Hour 2000 psi (13.8 MPa)
3 Hours 3500 psi (24.1 MPa)
1 Day 5200 psi (35.9 MPa)
7 Days 6500 psi (44.8 MPa)
28 Days 8100 psi (55.8 MPa)

Slant Shear Bond Strength ASTM C-882 (*modified per ASTM C 928)
1 day 2,000 psi (13.8 MPa)
7 days 2,750 psi (18.9 MPa)

Length Change of Hardened Cement Mortar and Concrete ASTM C 157 (*modified per ASTM C 928)
Length Change @ 28 days
Air Cure -0.11%
Water Cure 0.04%

Scaling Resistance (Freeze/Thaw) - ASTM C-672
Average of 3 specimens
25 cycles 0 (no scaling)
Scaling of oven-dry mass @ 25 cycles 0.0 lbs/ft²

Rapid Freeze/Thaw Test: ASTM C-666
At 300 Cycles - No loss

Initial Set
15-20 minutes
Final Set: 25-30 minutes

Moisture content: <4% in 4hrs when tested in laboratory conditions. (always test in field placements prior to coating as ambient conditions may vary)

Note:
The data shown is typical for controlled laboratory conditions. Reasonable variation from these results can be expected due to interlaboratory precision and bias. When testing the field mixed material, other factors such as variations in mixing, water content, temperature and curing conditions should be considered.

Estimating Guide

Yield: 0.42 cu. ft./50 lb. (0.012 cu m /22.7 kg)
0.60 cu. ft./50 lb. (0.017 cu. m/22.7 kg) bag with 60% extension, 30 lbs. (13.61 kg) with 3/8 in. (1 cm) pea gravel.

Packaging

PRODUCT CODE	PACKAGE	SIZE	
		lbs.	kg
67460	Bag	50	22.67

STORAGE

Shelf life of unopened bags, when stored in a dry facility, is 12 months. Excessive temperature differential and/or high humidity can shorten the shelf life expectancy. Store in a cool, dry area free of direct sunlight.

APPLICATION

Surface Preparation:

The concrete must be sound and free of all foreign material, including oil, grease, dust, laitance, or other surface contaminants. Surface preparation in accord with ICRI Guidelines is recommended. The edges of the patches should be saw-cut perpendicular to the surface to no more than a depth of 1/2 in. (13 mm) to avoid feather edging the repair material. Best results will be obtained by abrasive blasting the area to be repaired, providing uniform depth, a high surface profile and a firm bonding area. All surfaces to be repaired should be in a saturated-surface-dry (SSD) condition with no standing water on the surface.

Water Requirements:

Use 6½ pints (3.07 L) of water /50 lb. (22.7 kg) of powder.

Mixing:

Mix with a low speed drill or, for larger projects a mortar mixer with rubber tipped blades, by adding the water first and then the powder. Mixing time should be two to three minutes and placing should not exceed fifteen minutes. Adequate placing and finishing equipment and material should be available for continuous placement of the material.

DAYTON SUPERIOR

HD 50

Horizontal Repair Mortar

TECHNICAL DATA SHEET

Placement:
Using freshly mixed material, scrub a thin layer onto the SSD substrate with a stiff fiber brush and place the repair mortar before the scrub coat dries. Trowel the repair material onto the surface to a minimum thickness of 1/2 in. (1.3 cm) and a maximum thickness of 2 in. (5.1 cm).

For repairs over 2 in. (5 cm) deep, the material should be extended 60% by weight with clean, SSD, pea gravel with an approximate size of 3/8 in (9.5 mm) and conforming to the requirements of ASTM C 33.

CLEAN UP
Clean tools and equipment immediately with water. Hardened material will require mechanical removal.

CURING
Water cure for a minimum of 1 hour or apply a Dayton Superior ASTM C309 water-based curing compound to the repaired area immediately after placement.

LIMITATIONS

FOR PROFESSIONAL USE ONLY
Prior to coating, moisture content must be measured and comply with the coating manufacture's requirements. Any and all curing material must be removed from the HD50 prior to coating.
When testing the field mixed material, other factors such as variations in mixing, water content, temperature and curing conditions should be considered.
When using less than one bag always drymix the full bag prior to each use. DO NOT apply at temperatures below 40°F (5°C) without following the cold weather concreting procedures outlined in ACI 306. For application in temperatures below 45°F (4°C), best results will be obtained by warming the material and mix water as well as the substrate. Colder temperatures will extend the setting time and warmer temperatures will reduce the setting time. DO NOT featheredge. Do not re-temper the mixed material or use admixtures. Do not use for resurfacing or topping large floor areas. Mixing equipment should be cleaned with water frequently and prior to material hardening.

PRECAUTIONS

READ SDS PRIOR TO USING PRODUCT
- Product contains Crystalline Silica and Portland Cement – Avoid breathing dust – Silica may cause serious lung problems
- Use with adequate ventilation
- Wear protective clothing, gloves and eye protection (goggles, safety glasses and/or face shield)
- Keep out of the reach of children
- Do not take internally
- In case of ingestion, seek medical help immediately
- May cause skin irritation upon contact, especially prolonged or repeated. If skin contact occurs, wash immediately with soap and water and seek medical help as needed.
- If eye contact occurs, flush immediately with clean water and seek medical help as needed
- Dispose of waste material in accordance with federal, state and local requirements

MANUFACTURER
Dayton Superior Corporation
1125 Byers Road
Miamisburg, OH 45342
Customer Service: 888-977-9600
Technical Services: 877-266-7732
Website: www.daytonsuperior.com

WARRANTY
Dayton Superior Corporation ("Dayton") warrants for 12 months from the date of manufacture or for the duration of the published product shelf life, whichever is less, that at the time of shipment by Dayton, the product is free of manufacturing defects and conforms to Dayton's product properties in force on the date of acceptance by Dayton of the order. Dayton shall only be liable under this warranty if the product has been applied, used, and stored in accordance with Dayton's instructions, especially surface preparation and installation, in force on the date of acceptance by Dayton of the order. The purchaser must examine the product when received and promptly notify Dayton in writing of any non-conformity before the product is used and no later than 30 days after such non-conformity is first discovered. If Dayton, in its sole discretion, determines that the product breached the above warranty, it will, in its sole discretion, replace the non-conforming product, refund the purchase price or issue a credit in the amount of the purchase price. This is the sole and exclusive remedy for breach of this warranty. Only a Dayton officer is authorized to modify this warranty. The information in this data sheet supersedes all other sales information received by the customer during the sales process. THE FOREGOING WARRANTY SHALL BE EXCLUSIVE AND IN LIEU OF ANY OTHER WARRANTIES, EXPRESS OR IMPLIED, INCLUDING WARRANTIES OF MERCHANTABILITY AND FITNESS FOR A PARTICULAR PURPOSE, AND ALL OTHER WARRANTIES OTHERWISE ARISING BY OPERATION OF LAW, COURSE OF DEALING, CUSTOM, TRADE OR OTHERWISE.

Dayton shall not be liable in contract or in tort (including, without limitation, negligence, strict liability or otherwise) for loss of sales, revenues or profits; cost of capital or funds; business interruption or cost of downtime, loss of use, damage to or loss of use of other property (real or personal); failure to realize expected savings; frustration of economic or business expectations; claims by third parties (other than for bodily injury), or economic losses of any kind; or for any special, incidental, indirect, consequential, punitive or exemplary damages arising in any way out of the performance of, or failure to perform, its obligations under any contract for sale of product, even if Dayton could foresee or has been advised of the possibility of such damages. The Parties expressly agree that these limitations on damages are allocations of risk constituting, in part, the consideration for this contract, and also that such limitations shall survive the determination of any court of competent jurisdiction that any remedy provided in these terms or available at law fails of its essential purpose.

DAYTON SUPERIOR

1107 Advantage Grout

Cement Based Grout

TECHNICAL DATA SHEET

DESCRIPTION

The 1107 Advantage Grout is a non-shrink, non-metallic, non-corrosive, cementitious grout that is designed to provide a controlled, positive expansion to ensure an excellent bearing area. The 1107 Advantage Grout can be mixed from a fluid to a dry pack consistency.

USE

Exterior grouting of structural column base plates, pump and machinery bases, anchoring bolts, dowels, bearing pads and keyway joints. It finds applications in paper mills, oil refineries, food plants, chemical plants, sewage and water treatment plants etc.

FEATURES

- Controlled, net positive expansion
- Non shrink
- Non metallic/non corrosive
- Pourable, pumpable or dry pack consistency
- Interior/exterior applications

PROPERTIES

Corps of Engineers Specification for non-shrink grout:

CRD-C 621 Grades A, B, C

ASTM C-1107 Grades A, B, C

ASTM C-827 - 1107 Advantage Grout yielded a controlled positive expansion

Expansion - ASTM C-1090:

1 day: 0.10%

3 days: 0.11%

14 days: 0.11%

28 days: 0.11%

Test Results

	@ 1 Day		@ 3 Days		@ 7 Days		@ 28 Days	
Fluidity	PSI	MPa	PSI	MPa	PSI	MPa	PSI	MPa
Dry-Pack	5000	34.5	7000	48.2	9000	62.0	10000	68.9
Flowable	2500	17.2	5000	34.5	6000	41.4	8000	55.1
Fluid	2000	13.8	4000	27.6	5000	34.5	7500	51.7

Note:

The data shown is typical for controlled laboratory conditions. Reasonable variation from these results can be expected due to interlaboratory precision and bias. When testing the field mixed material, other factors such as variations in mixing, water content, temperature and curing conditions should be considered.

Estimating Guide

Yield (Flowable Consistency):
0.43 cu. ft./50 lbs. (0.0122 cu. m/22.7 kg) bag
0.59 cu. ft./50 lbs. (0.017 cu. m/22.7 kg) bag extended with 25 lbs. (11.34 kg) of washed 3/8 in. (1cm) pea gravel

Packaging

PRODUCT CODE	PACKAGE	SIZE	
		lbs	kg
67435	Bag	50	22.67
67437	Supersack	3,000	1,360.78

STORAGE

Store in a cool, dry area free from direct sunlight. Shelf life of unopened bags, when stored in a dry facility, is 12 months. Excessive temperature differential and /or high humidity can shorten the shelf life expectancy.

APPLICATION

Surface Preparation:

Thoroughly clean all contact surfaces. Existing concrete should be strong and sound. Surface should be roughened to insure bond. Metal base plates should be clean and free of oil and other contaminants. Maintain contact areas between 45°F (7°C) and 90°F (32°C) before grouting and during curing period.

Thoroughly wet concrete contact area 24 hours prior to grouting, keep wet and remove all surface water just prior to placement. If 24 hours is not possible, then saturate with water for at least 4 hours. Seal forms to prevent water or grout loss. On the placement side, provide an angle in the form high enough to assist in grouting and to maintain head pressure on the grout during the entire grouting process. Forms should be at least 1 in. (2.5 cm) higher than the bottom of the base plate.

Water Requirements:

Desired Mix Water / 50 lbs. (22.67 kg) Bag
Dry Pack: 5 pints (2.4 L)
Flowable: 8 pints (3.8 L)
Fluid: 9 pints (4.2 L)

Mixing:

A mechanical mixer with rotating blades like a mortar mixer is best. Small quantities can be mixed with a drill and paddle. When mixing less than a full bag, always first agitate the bag thoroughly so that a representative sample is obtained.

DAYTON SUPERIOR

1107 Advantage Grout

Cement Based Grout

TECHNICAL DATA SHEET

Place approximately 3/4 of the anticipated mix water into the mixer and add the grout mix, adding the minimum additional water necessary to achieve desired consistency.
Mix for a total of five minutes ensuring uniform consistency. For placements greater in depth than 3 in. (7.6 cm), up to 25 lbs. (11.34 kg) of washed 3/8 in. (1 cm) pea gravel must be added to each 50 lbs. (22.7 kg) bag of grout. The approximate working time (pot life) is 30 minutes but will vary somewhat with ambient conditions.

For hot weather conditions, greater than 85°F (29°C), mix with cold water approximately 40°F (4°C).
For cold weather conditions, less than 50°F (10°C), mix with warm water, approximately 90°F (29°C). For additional hot and cold weather applications, contact Dayton Superior.

Placement:

Grout should be placed preferably from one side using a grout box to avoid entrapping air. Grout should not be over-worked or over-watered causing segregation or bleeding. Vent holes should be provided where necessary.
When possible, grout bolt holes first. Placement and consolidation should be continuous for any one section of the grout. When nearby equipment causes vibration of the grout, such equipment should be shut down for a period of 24 hours. Forms may be removed when grout is completely self-supporting. For best results, grout should extend downward at a 45 degree angle from the lower edge of the steel base plates or similar structures.

CLEAN UP

Use clean water. Hardened material will require mechanical removal methods.

CURING

Exposed grout surfaces must be cured. Dayton Superior recommends using a Dayton Superior curing compound, cure seal or a wet cure for 3 days. Maintain the temperature of the grout and contact area at 45°F (7°C) to 90°F (32°C) for a minimum of 24 hours.

LIMITATIONS

FOR PROFESSIONAL USE ONLY

Do not re-temper after initial mixing
Do not add other
cements or additives
Setting time for the 1107 Advantage Grout will slow during cooler weather, less than 50°F (10°C) and speed up during hot weather, greater than 80°F (27°C)
Prepackaged material segregates while in the bag, thus when mixing less than a full bag it is recommended to first agitate the bag to assure it is blended prior to sampling.

PRECAUTIONS

READ SDS PRIOR TO USING PRODUCT

- Product contains Crystalline Silica and Portland Cement Avoid breathing dust Silica may cause serious lung problems
- Use with adequate ventilation
  n Wear protective clothing, gloves and eye protection (goggles, safety glasses and/or face shield)
- Keep out of the reach of children
- Do not take internally
- In case of ingestion, seek medical help immediately
- May cause skin irritation upon contact, especially prolonged or repeated. If skin contact occurs, wash immediately with soap and water and seek medical help as needed.
- If eye contact occurs, flush immediately with clean water and seek medical help as needed
- Dispose of waste material in accordance with federal, state and local requirements

MANUFACTURER

Dayton Superior Corporation
1125 Byers Road
Miamisburg, OH 45342
Customer Service: 888-977-9600
Technical Services: 877-266-7732
Website: www.daytonsuperior.com

WARRANTY

Dayton Superior Corporation ("Dayton") warrants for 12 months from the date of manufacture or for the duration of the published product shelf life, whichever is less, that at the time of shipment by Dayton, the product is free of manufacturing defects and conforms to Dayton's product properties in force on the date of acceptance by Dayton of the order. Dayton shall only be liable under this warranty if the product has been applied, used, and stored in accordance with Dayton's instructions, especially surface preparation and installation, in force on the date of acceptance by Dayton of the order. The purchaser must examine the product when received and promptly notify Dayton in writing of any non-conformity before the product is used and no later than 30 days after such non-conformity is first discovered. If Dayton, in its sole discretion, determines that the product breached the above warranty, it will, in its sole discretion, replace the non-conforming product, refund the purchase price or issue a credit in the amount of the purchase price. This is the sole and exclusive remedy for breach of this warranty. Only a Dayton officer is authorized to modify this warranty. The information in this data sheet supersedes all other sales information received by the customer during the sales process. THE FOREGOING WARRANTY SHALL BE EXCLUSIVE AND IN LIEU OF ANY OTHER WARRANTIES, EXPRESS OR IMPLIED, INCLUDING WARRANTIES OF MERCHANTABILITY AND FITNESS FOR A PARTICULAR PURPOSE, AND ALL OTHER WARRANTIES OTHERWISE ARISING BY OPERATION OF LAW, COURSE OF DEALING, CUSTOM, TRADE OR OTHERWISE.

TECHNICAL DATA SHEET

Dayton shall not be liable in contract or in tort (including, without limitation, negligence, strict liability or otherwise) for loss of sales, revenues or profits; cost of capital or funds; business interruption or cost of downtime, loss of use, damage to or loss of use of other property (real or personal); failure to realize expected savings; frustration of economic or business expectations; claims by third parties (other than for bodily injury), or economic losses of any kind; or for any special, incidental, indirect, consequential, punitive or exemplary damages arising in any way out of the performance of, or failure to perform, its obligations under any contract for sale of product, even if Dayton could foresee or has been advised of the possibility of such damages. The Parties expressly agree that these limitations on damages are allocations of risk constituting, in part, the consideration for this contract, and also that such limitations shall survive the determination of any court of competent jurisdiction that any remedy provided in these terms or available at law fails of its essential purpose.